Author reply to Referee comments from **Anonymous Referee # 1** from 21 January 2020 (https://doi.org/10.5194/bg-2019-432-RC1) on:

"Comparison of eddy covariance CO_2 and CH_4 fluxes from mined and recently rewetted sections in a NW German cutover bog" by David Holl et al.

Reviewer comments (RC)
Author comments (AC)
Mentioned line numbers refer to the originally submitted manuscript
Manuscript changes (MC)

This manuscript reports carbon dioxide and methane fluxes for the period June 2012 to May 2014. Using a combination of a single eddy covariance tower, footprint modeling, and manual spatial cover classification using remotely sensed images, the authors distinguish, separately gap-fill, and quantify annual sums for, both actively mined and recently rewetted peat sections. The authors find that rewetting increases methane and decreases carbon dioxide emissions, but those effects manifest themselves much more strongly in the second year after rewetting, indicating lags. Overall the paper is clearly written but could be much shorter. The strongest aspects of the study are the comprehensive scholarship and the clarity of the methods. For example, there is a clear description of eddy covariance data processing for methane, which seems to have been considered with great care, and is an active area of research in the flux community (e.g., European RINGO initiative, perhaps should be linked more specifically). The exploration of gap-filling approaches is also a nice addition, though I think it takes up too much of the paper overall, given that is not the primary focus of the study (not even in the title). There are however some issues with the paper that I think need to be addressed which I outline below.

Major Comments

Soil conditions
In year 2 the authors report a substantial amount of soil data being recorded, including temperature, redox, and water table height. These in turn are included via their variable selection procedure in the predictive models of methane flux. Unfortunately, these data are not presented to the reader at all. This is disappointing as the focus of the paper implied by the title is the difference in fluxes between the two cover types, and soil conditions are likely the mechanism underlying those differences by year 2. I would encourage the authors to explore visualizations of those soil data in the paper, perhaps by substituting it for some of the discussion of either the machine learning or the CO2 discussion.
As mentioned by the referee, our modeling approach does include an identification procedure for likely flux drivers. We also present a short (section 3.1) and extended (Appendix B) discussion on how these drivers can explain flux variability in a mechanistic way. Most likely because our data set was measured over heterogeneous terrain, we did not find a comparably simple flux—driver relation (e. g. with soil temperature or water table) which explained the observed flux variability to a sufficient degree so it could be used to gap-fill our high-frequency data in order to calculate annual flux balances. Due to the complexity of the flux data set, we decided to use a more complex modeling approach. Nevertheless, we agree that it is necessary to depict the site conditions more clearly so a reader can more easily compare to conditions at similar sites and grasp our data set quicker and more comprehensively. We therefore implemented a new modeling approach representing methane flux as a function of soil temperature and water table and explored the results in a new figure and an additional paragraph in section 3.1.

To further investigate the relation between CH_4 flux and the identified likely drivers, we fitted an exponential model of water table and soil temperature (in 40 cm depth) to the CH_4 fluxes from the rewetted section (see Figure XX1). With the exponential dependence of CH_4 flux on soil temperature, a fair amount (R^2 = 0.55) of the flux variability can be explained while the added water table term allows for the optimized temperature-F_{CH4} curve to take two distinct paths above and below an approximate water table threshold of 20 cm below the surface (see Figure XX1, panel A). Half-hourly flux variability is, however, substantial due to the heterogeneity of the site's surface and other confounding factors like for example the above-mentioned air pressure variations and is comparably better explained by our neural network models (see Figure XX1, panel B).

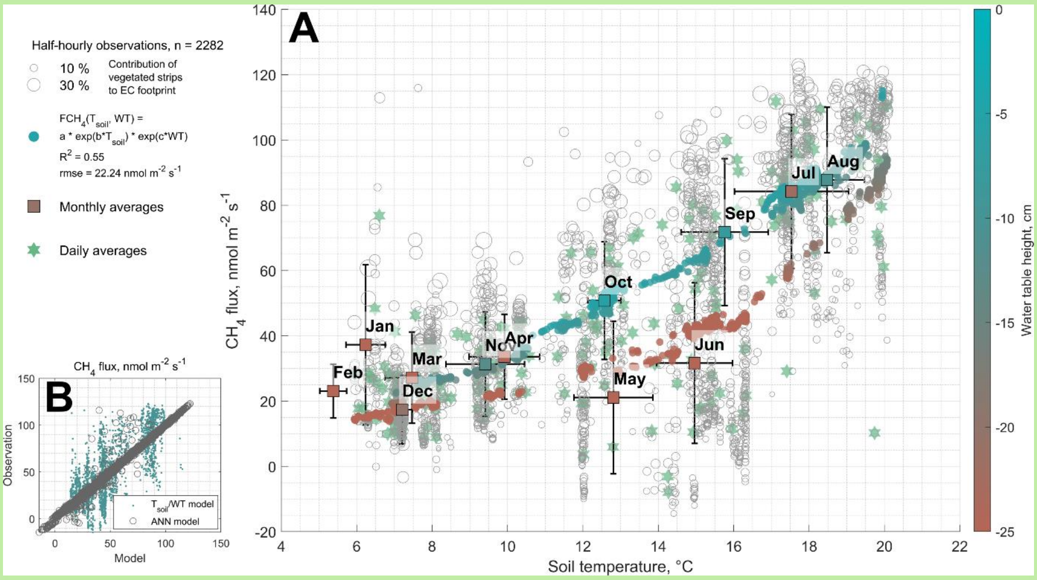

Figure XX1 *Panel A: Observed Half-hourly methane (CH4) fluxes from the rewetted section of Himmelmoor modeled as an exponential function of soil temperature in 40 cm depth and water table (FCH4(Tsoil/WT)). Monthly and daily flux and temperature averages are also given. Panel B: Comparison of a more complex artificial neural network (ANN) model with the exponential model from Panel A. Although methane flux variability can be explained by the exponential model to a reasonable degree, the level of complexity in flux—driver relations appears to be represented considerably better by the ANN.*

Flux Partitioning

Why was the net ecosystem exchange flux partitioning done at the monthly timestep? Can this not be performed at half-hour timesteps in EddyPro? I assume this was done intentionally but the justification is not clear.

No, flux partitioning is not a capability EddyPro provides. We applied our own model (Eq. 1, page 13), and used half-hourly fluxes to optimize the parameters of Eq. 1 (as stated in line 2, page 15). Due to the surface heterogeneity of our site, the independent parameters we chose differ from those used in other common approaches (e.g. Reichstein et al., 2005). We included half-hourly footprint characteristics and radiation but not temperature as drivers of net ecosystem exchange (NEE). Therefore, total ecosystem respiration (TER) in our model is a parameter. To depict the seasonal course of the parameter time series, we optimized one set of parameters for each month of the two-year data set (Fig. 4, page 15). The resolution of the ecosystem respiration time series is therefore limited to monthly steps. In an effort to yield NEE models, which are less likely to be overfitted, we reduced the number of model inputs and parameters and chose monthly, rather than for example daily, flux ensembles for optimization. We were not able to achieve a higher temporal resolution of TER confidently. We could, however, have calculated gross primary production (GPP) for half-hourly intervals using thirty minute radiation measurements and the two parameters Pmax and α (panels C and D in Fig. 4, page 15). Due to the focus of this paper (annual NEE balances and gap-filling), we decided to omit this step at this point. Instead, we compared the determined photosynthesis parameters, which directly relate to plant characteristics, to literature values of plants that also occur at our site in order to examine the credibility of our land use-specific gap-filling models (as stated on page 15, line 1).

Synthesis Literature summaries in the introduction and the discussion need to avoid listing. I am referring to the carbon dioxide flux sections, whereas the methane section is better synthesized (I especially like the comparison to IPCC values). The comparisons made in the results to other studies might be better tabulated. If they are noted in the main text, they should be synthesized better.
We agree, literature synthesis was a bit wordy in the running text. We created three new tables. One for the introduction that summarizes methane gap-filling methods and two in the results section (3.2) where we compare our CO_2 model parameters to literature values. We propose to move the tables to the appendix.

We replaced page 3, line 34 to page 4, line 12 with:
…the relations between environmental drivers and CH4 flux often appear to be more complex than for CO_2. An overview of methods applied in EC literature is given in Table A 1. Basic gap-filling methods include for example interpolation between measured values or the use of an average to replace all gaps. Simple linear models have also proven to be applicable in certain settings. A common approach is to fit Arrhenius-type non-linear functions to the flux as a function of various environmental drivers. However, as stated by Brown et al. (2014), there is evidence that these functional relationships do not necessarily behave monotonically. Artificial neural networks (ANNs) form a category of non-parametric models that have frequently been used to fill gaps in EC CO2 flux time series. Mostly, multilayer perceptrons (MLP) were chosen (Papale and Valentini, 2003; Moffat et al., 2007; Moffat, 2012; Järvi et al., 2012; Pypker et al., 2013; Menzer et al., 2015). Most recent literature on CH_4 flux gap-filling assess MLP models to be the most robust. MLPs are recommended within the processing for the pan-European Integrated Carbon Observation System (ICOS) by Nemitz et al. (2018) and for the new methane component of FLUXNET and the Global Carbon Project's efforts better constrain the global methane budget respectively (Knox et al., 2019).

Appendix A: Gap-filling methods from literature

Table A1. Overview of methods applied in literature to gap-fill eddy covariance methane flux time series.

Method		References
Interpolation		Hanis et al. (2013); Dengel et al. (2011)
Averaging		Hatala et al. (2012); Mikhaylov et al. (2015)
Arrhenius-type non-linear functions	half-hourly	Kroon et al. (2010); Forbrich et al. (2011); Hommeltenberg et al. (2014); Goodrich et al. (2015)
	downsampled	Suyker et al. (1996); Friborg and Christensen (2000); Rinne et al. (2007); Long et al. (2010); Wille et al. (2008); Jackowicz-Korczyński et al. (2010); Parmentier et al. (2011); Brown et al. (2014); Shoemaker et al. (2015); Mikhaylov et al. (2015)
Look-up tables		Pypker et al. (2013); Hommeltenberg et al. (2014); Bhattacharyya et al. (2014)
Mean diurnal variation		Dengel et al. (2011); Jha et al. (2014)
Marginal distribution sampling		Alberto et al. (2014); Shoemaker et al. (2015)
Machine learning	Artificial neural networks	Dengel et al. (2013); Deshmukh et al. (2014); Knox et al. (2015); Goodrich et al. (2015); Nemitz et al. (2018); Knox et al. (2019); Kim et al. (2019)
	Support vector machines	Kim et al. (2019)
	Random forest	Kim et al. (2019)

I replaced page 15, line 1 to page 17, line 9 with:

As a fourth method to evaluate the applicability of our land use-specific flux decomposition, we fitted a combined respiration-photosynthesis model (see Eq. 1) to monthly ensembles of the half-hourly CO_2 SCTS in order to check if the resultant parameters are reasonable in relation to each other and to literature data. In general, the vegetation period, with its productivity maximum between June and July and its cessation between mid-October and November is well depicted in the seasonal course of the model parameters throughout both years. The parameter courses relating to the vegetated strips of the drained and rewetted areas (Figure 4, panels B – D) develop fairly similar. Distinctions between the drained and rewetted areas are more pronounced with respect to CO_2 release from bare peat surfaces (Figure 4, panel A). Ditch-blocking of a rewetted sector close to the EC tower (which therefore made up a large part of the EC footprint) was only performed one year before our measurements started. In summer of 2012 this area therefore was not yet permanently flooded leading to TER_{bare} fluxes exceeding those from the active mining site. From winter 2012/2013 on, inundation of the rewetted bare peat area progressively increased, resulting in lower TER_{bare} fluxes from the rewetted compared to the drained section. Our TER_{bare} fluxes are in concordance with findings from two studies that were also conducted on the active peat extraction area in Himmelmoor with manual chambers; TER data reported from similar peat extraction sites also agree with our results (see Table 3). As model includes the relative contributions of the vegetated strips to the EC footprint we compare the extracted model parameter time series (see Figure 4, panels B – D) with estimates of these plant species-specific values from other studies investigating similar plants and plant communities as found in the vegetated strips in Himmelmoor. Reported averages and ranges agree well with our findings (see Table 4). Additionally, we could distinguish between CO_2 release from decomposing bare peat (TER_{bare}, see Figure 4, panel A and Table 3) and from the vegetated strips (TER_{veg}, see Figure 4, panel B and Table 4) where respiratory CO_2 release also includes autotrophic respiration of plants. In our data set, TER is between twofold and fourfold larger in areas with than without vegetation. TER_{veg} from the rewetted area is mostly larger than from the drained area. Progressive inundation led to a hydrological connection of SC_{veg} and the flooded bare peat areas. An increased input of dead plant material as a result of higher water tables might have promoted heterotrophic respiration. Hampered plant productivity due to flooding is also expressed in lower peak values of P_{max} at the vegetated strips of the rewetted site.

Table 3. Comparison of total ecosystem respiration fluxes from bare peat areas without vegetation (TER_{bare}) between our study (see Figure 4, panel A for full time series) and literature values (closed chamber methods) from the same and similar peat extraction sites.

Reference	Site: Land use	Site: Name, Location	TER_{bare}, µmol m^{-2} s^{-1}
This study	Active mining	Himmelmoor, NW-Germany, 53°N	1.1 ± 0.5 (annual average and standard deviation)
	Ceased mining, rewetted		0.8 ± 0.7 (annual average and standard deviation)
Vanselow-Algan et al. (2015)	Active mining		0.5 ± 0.1 (annual average and uncertainty)
Vybornova et al. (2019)	Active mining		0 to 1 (annual range), 3 (maximum)
	Ceased mining, rewetted		0 to 0.5 (annual range), 1.4 (maximum)
Waddington et al. (2002)	Ceased mining, wet year	Sainte-Marguerite-Marie, SE Canada, 48°N	0.8 (May to August average)
	Ceased mining, dry year		3 (May to August average)
Shurpali et al. (2008)	Active mining	Linnansuo, SE Finland, 62 °N	1.3 (end of August maximum)
			0.2 (mid-November minimum)

Table 4. Total ecosystem respiration (TER_{veg}, µmol m^{-2} s^{-1}), maximum photosynthesis (P_{max}, µmol m^{-2} s^{-1}) and initial quantum yield (α, dimensionless) from the vegetated strips of this study compared to literature values from similar plant species. As the literature record of combined plant and soil respiration measurements of the species that occur at the site of this study is limited, autotrophic respiration respiration (R_a, µmol m^{-2} s^{-1}) estimates of plants from the same genera are also given. Note that R_a values were determined on leaf scale and therefore refer to leaf area. Since shrubs and trees can have a leaf area index larger than 1, fluxes referring to ground surface area could be higher. Model parameter values from this study are given as averages and standard deviation. The latter statistic expresses the value range throughout two annual courses as shown in Figure 4 rather than parameter uncertainty.

Reference	Plant species	TER_{veg}	R_a	P_{max}	α
This study, drained section	*Betula pubescens, Salix spp., Eriophorum vaginatum, E. angustifolium, Molinia caerulea, Calla palustris, Typha latifolia, Carex spp., Juncus effusus, Calamagrostis canescens*	2.5 ± 2.9		14.4 ± 13.8	0.04 ± 0.04
This study, rewetted section	—"—	3.0 ± 2.1		10.5 ± 10.6	0.05 ± 0.03
Vanselow-Algan et al. (2015)	*Molinia caerulea, Betula pubescens, Eriophorum angustifolium*	> 10 (summer)			
Beyer and Höper (2015)	*Molinia caerulea*	≤ 7		15 to 30	
	Eriophorum angustifolium	≤ 5		20 to 70	
Patankar et al. (2013)	*Salix pulchra*		≤ 2		
	Eriophorum vaginatum		≤ 3		
	Carex bigelowi		≤ 1		
Körner (1982)	*Carex curvula*		1		
Murchie and Horton (1997)	*Carex flacca*		1.5		
Kaipiainen (2009)	*Salix dasyclados*		0.8 to 1.2		0.04 to 0.08
Patankar et al. (2013); Gu et al. (2008)	*Betula spp.*		1 to 5	10 to 15	
Lienau (2014)	*Betula pubescens*			32 to 41	
Nygren and Kellomäki (1983)	*Betula pubescens*			4 to 17	
Hoogesteger and Karlsson (1992)	*Betula pubescens*			8	
Chen et al. (2010)	*Typha latifolia*			25	0.02 to 0.07
Ögren (1993)	*Salix spp.*			16 to 29	
Vernay et al. (2016)	*Molinia caerulea*			7 to 15	0.03

Machine Learning In Appendices A and B, the authors outline the machine learning approach used (artificial neural networks). Can the authors justify why they used a single data split as opposed to a k-fold cross validation approach, which tends to give a more stable performance evaluation? Using the alternative year as a “test” set for generalizability is interesting. Can the authors also comment on whether gaps were artificially created during validation. or whether the data splits were performed randomly on all observations?

I assume the referee refers to the division of target data (fluxes) into training and validation sets in the course of network optimization. To my understanding, we actually did use a simple 2-fold cross validation by dividing the data set into two groups. Due to the large number of fluxes (especially in case of methane) that we discarded during quality filtering, a division into more groups would have resulted in a lower number of fluxes per group, impairing network training. As we used ensemble averages of 1000 networks and therefore performed network optimization 1000 times, we also (randomly) divided the target data differently each time and in my opinion sufficiently counteracted effects of overfitting by this proceeding.

Style
I personally enjoyed the descriptive style of the writing, but it is unfortunately much too verbose for a modern readership. I would encourage the authors to mercilessly edit to reduce text. They might be surprised how much shorter the paper is if written in a more declarative style.
Thank you for the feedback. I agree and cut down on verbosity by replacing large parts of running text with tables as suggested in previous comments from Referee #1.

An example:
"We used a factor of 34 to convert FCH4 into CO2e release. This value is given in the Fifth Assessment Report of the Intergovernmental Panel on Climate Change (IPPC AR5, Myhre et al., 2013), refers to a 100-year time horizon and includes climate–carbon feedbacks"
...could be shortened to:
"We used a CH4 global warming potential of 34 kg CO2-eq (IPCC AR5, Myhre et al., 2013), which assumes a 100-year time horizon and includes climate-carbon feedbacks."
Although I understand the referee's general notion, I do not think this is a good example. The edited sentence is shorter mostly because the abbreviation "IPCC AR5" is not explained. In my opinion, also commonly used and widely known abbreviations should be explained when they first occur for consistency.

Or:
"Nevertheless, on an annual basis the periods when the sink character of SCrew prevails do not compensate for CO2 release during periods of reduced plant activity."

"Nevertheless, annually integrated ecosystem respiration outweighs photosynthesis in SCrew."
I agree, sentence replaced.

Minor Comments
Page 2
Line 9: Perhaps "land-use or climate change" rather than "men"
Changed
Line 14: "of carbon dioxide"
Changed
Line 20: "inheres the potentials" is ambiguous phrasing
"Inheres" replaced with "has".
Line 29: perhaps "oxidized" rather than "decomposed"
"decomposed" replaced with "converted to CO_2".
Page 3
Line 3: perhaps "strongly" rather than "gravely"
Changed
Lines 4-20: This is a nice minireview, but could be stronger if structured more systematically, or if the points could be linked more, to sound less like a list.
No change made. The questions are: What is known from literature about the development of methane emissions after peatland rewetting? What is to be expected for a largely vegetation-free site like Himmelmoor? To me the structure is systematic and the points are linked. I am not sure what to change.
Page 7 Line 14: "brown"
Changed
Lines 20-: Can you briefly justify the variable positions of these sensors? How representative is the water-level sensor of the general footprint?
I extended the description of sensor positions:

"A second HMP45 was installed together with a NR01 4-component net radiometer (Hukseflux, Netherlands) 70 m southwest of the EC tower on a tripod at 2~m height. The radiation sensors were not mounted on the EC tower because the field of view of the downward-facing sensors would have covered the peat dam and therefore not be representative for a dominant surface type at the site. These additional HMP45 and NR01 data were logged on a CR-3000 (Campbell Scientific, UK). Another logger of this type was used at the weather station which was taken over from a previous project and for data consistency was left at a position approximately 500~m north of the EC tower.

The water level within the footprint is highly variable as the surface consists of drained and rewetted sections. Our single sensor is representative for the rewetted bare peat strip to the southwest of the EC tower making up a large part of the EC footprint when wind comes from southwesterly directions.

Figure 1: Can you please add some more points for the other sensor installations.

I updated the map with locations of all measurement systems

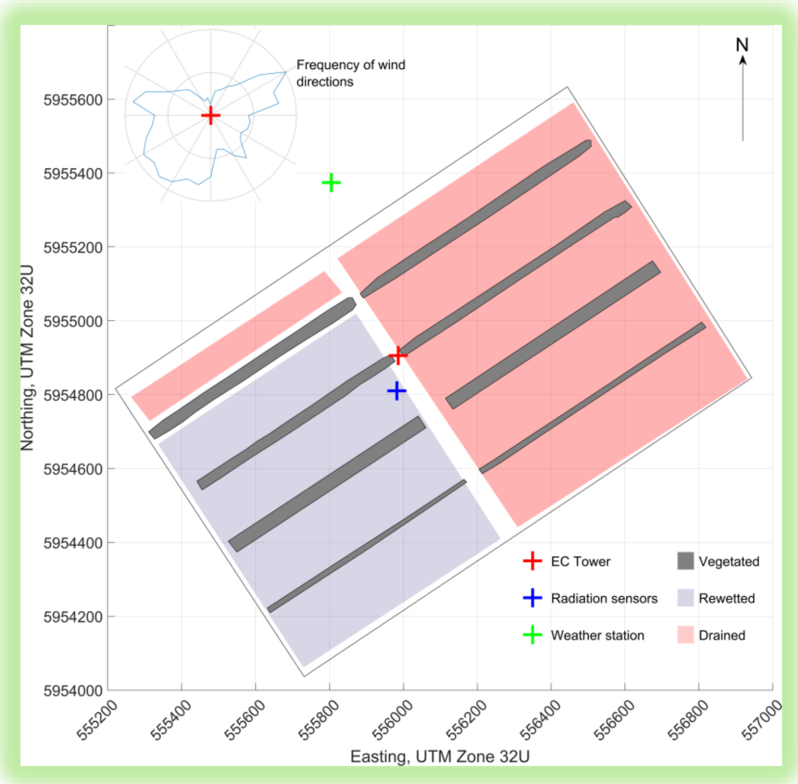

Page 8

Figure 2: This figure can be more useful to visualize how each true calendar year deviates from the long-term average if it just showed the full timeseries in one series (June 2012-May 2014). The problem currently is that it is difficult to visually integrate the deviations from the mean.

Ok. Figure restyled.

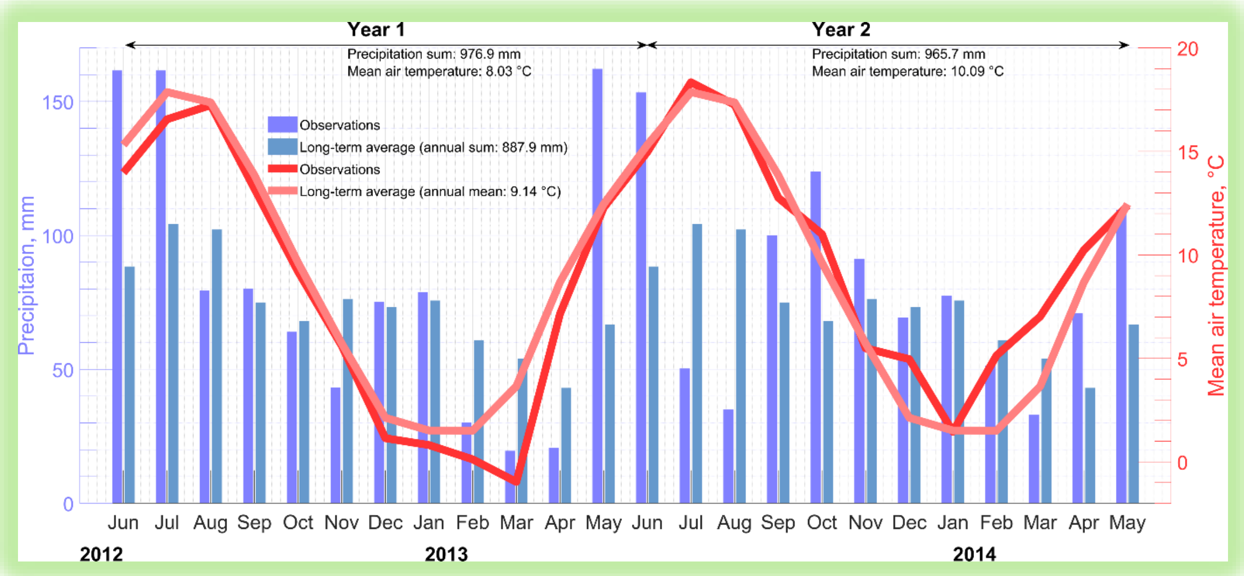

Line 8: Is WPL strictly a correction?

It is true that there is a discussion about this topic as compensation for air density fluctuations can also be seen as part of the eddy covariance method itself and not as a post-processing step and therefore does not qualify as a correction. On the other hand, the term WPL-correction is still widely used in the community, likely for historical reasons. I did not change this terminology.

Page 18 Table: Acres are not SI units. Please report in m2, hectares (ha), or km2

"a^{-1}" stands for "per annum/year". We do report area in m^2. No change made.

Line 33: I think the values in parentheses should be reversed given the order of the sentence.

True, thank you for the hint, order was reversed.

Author reply to Referee comments from **Anonymous Referee # 2** from 23 January 2020 (https://doi.org/10.5194/bg-2019-432-RC2) on:

"Comparison of eddy covariance CO_2 and CH_4 fluxes from mined and recently rewetted sections in a NW German cutover bog" by David Holl et al.

Reviewer comments (RC)
Author comments (AC)
Mentioned line numbers refer to the originally submitted manuscript
Manuscript changes (MC)

General comments

This manuscript tested the use of single EC tower to estimate CO2 and CH4 fluxes from different land surface area (drained and rewetted) in a mined bog in Northwest Germany by partitioning the sources of signals using footprint statistics. It is an interesting paper from both technical perspective and management perspective.

The manuscript in general is well-written. The authors paid special attention to the footprint analysis, which is very good as here we bend the rules for applying eddy covariance technique. And the gap-filling procedure, the model input selection and the comparison of model performance are clearly explained, although it even seems a bit too technical considering the main topic is the comparison of EC CO2 and CH4 fluxes from different surface types of a restored bog. But it is a matter of style.

We see the Referee's point; the model description is a bit lengthy. It would be a possibility to move Appendix A to a supplementary document as it contains only a detailed description of the methods. If I understand Copernicus' rules correctly, all other appendices cannot to moved to the Supplements as they contain results and interpretations. We want to ask the editor for his opinion on moving Appendix A to the supplements. We would argue against removing the algorithm description section entirely as for reproducibility and transparency the methods should be documented somewhere.

One thing not much mentioned in the paper is the information about the processes and controls which I generally have interest in. How did the environmental variables affect the fluxes under different water regime? how important was temperature control, water table and photosynthesis at different time scales in these ecosystems?

The focus of the paper is the impact of land use change on the annual balances of methane and carbon dioxide fluxes. Presumably due to the heterogeneous surface of the site, we did not find simple flux—driver relations. We addressed this complexity by using models that allow for the characterization of discontinuous and non-linear responses of spatially integrated fluxes (as measured with the EC system) to environmental drivers and source area variations. We, however, realize that it is necessary to depict the site conditions more clearly so a reader can more easily compare to conditions at similar sites and grasp our data set quicker and more comprehensively. We therefore implemented a new modeling approach representing methane flux as a function of soil temperature and water table and explored the results in a new figure and an additional paragraph in section 3.1.

To further investigate the relation between CH_4 flux and the identified likely drivers, we fitted an exponential model of water table and soil temperature (in 40 cm depth) to the CH_4 fluxes from the rewetted section (see Figure XX1). With the exponential dependence of CH_4 flux on soil temperature, a fair amount (R^2 = 0.55) of the flux variability can be explained while the added water table term allows for the optimized temperature-F_{CH4} curve to take two distinct paths above and below an approximate water table threshold of 20 cm below the surface (see Figure XX1, panel A). Half-hourly flux variability is, however, substantial due to the heterogeneity of the site's surface and other confounding factors like for example the above-mentioned air pressure variations and is comparably better explained by our neural network models (see Figure XX1, panel B).

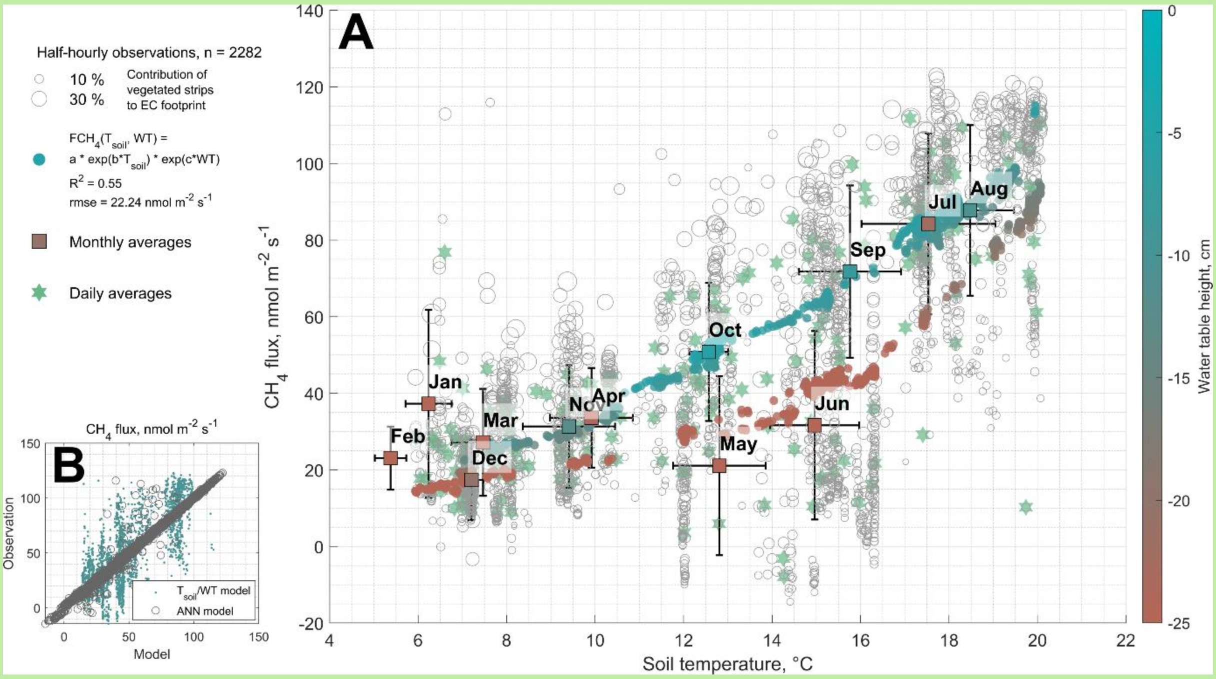

Figure XX1 *Panel A: Half-hourly methane (CH4) flux from the rewetted section of Himmelmoor as an exponential function of soil temperature in 40 cm depth and water table (FCH4(Tsoil/WT)). Monthly and daily flux and temperature averages are also given. Panel B: Comparison of a more complex artificial neural network (ANN) model with the exponential model from Panel A. Although methane flux variability can be explained by the exponential model to a reasonable degree, the level of complexity in flux—driver relations appears to be represented considerably better by the ANN.*

I do like the comparison of TER between bare peat and vegetated strips as shown in fig.4. And I would also like to see similar comparison for CH_4. Vegetated strips are in close proximity of EC tower from both rewetted and drained section. By merely looking at the frequency of wind directions, the most frequent wind direction are apparently from the vegetation stripes. "The vegetated strips in Himmelmoor cover around 10% of the surface and appear to be especially strong sources of CH_4...", as stated in the paper, it further proved the importance of vegetation on CH_4 flux. Thus it would be more interesting and useful to quantify the CH4 flux from vegetation and bare peat separately, rather than solely reporting the annual balance of the mixture.

Agreed, separate methane flux models for the bare and vegetated areas would be desirable. With the limited amount of available data after quality filtering, we were, however, not able to confidently decompose the measured fluxes of the mixtures into time series only referring to the vegetated strips like it was possible in case of carbon dioxide fluxes. For methane, "only" a decomposition into the rewetted and drained section (addressing the main topic of the study, the impact of land use change on GHG balances) was possible for us to accomplish.

We, however, agree that a depiction of the impact of the contribution of the vegetated strips to the EC footprint on methane fluxes should still be added to our manuscript and therefore added new figures. The impact of footprint variability on half-hourly EC flux variability is included in a new Figure XX1 and more specifically addressed in a new Figure XX2. In the latter figure, comparisons of fluxes when the vegetation contribution to the EC footprint was below and above 20 % respectively are shown as boxplots. Systematic distinctions between those two groups (and also the low number of available measurements) are illustrated. Please note the added paragraph shown in response to the referee's comment to Page 20, Line 20 which also refers to the new Figure XX2.

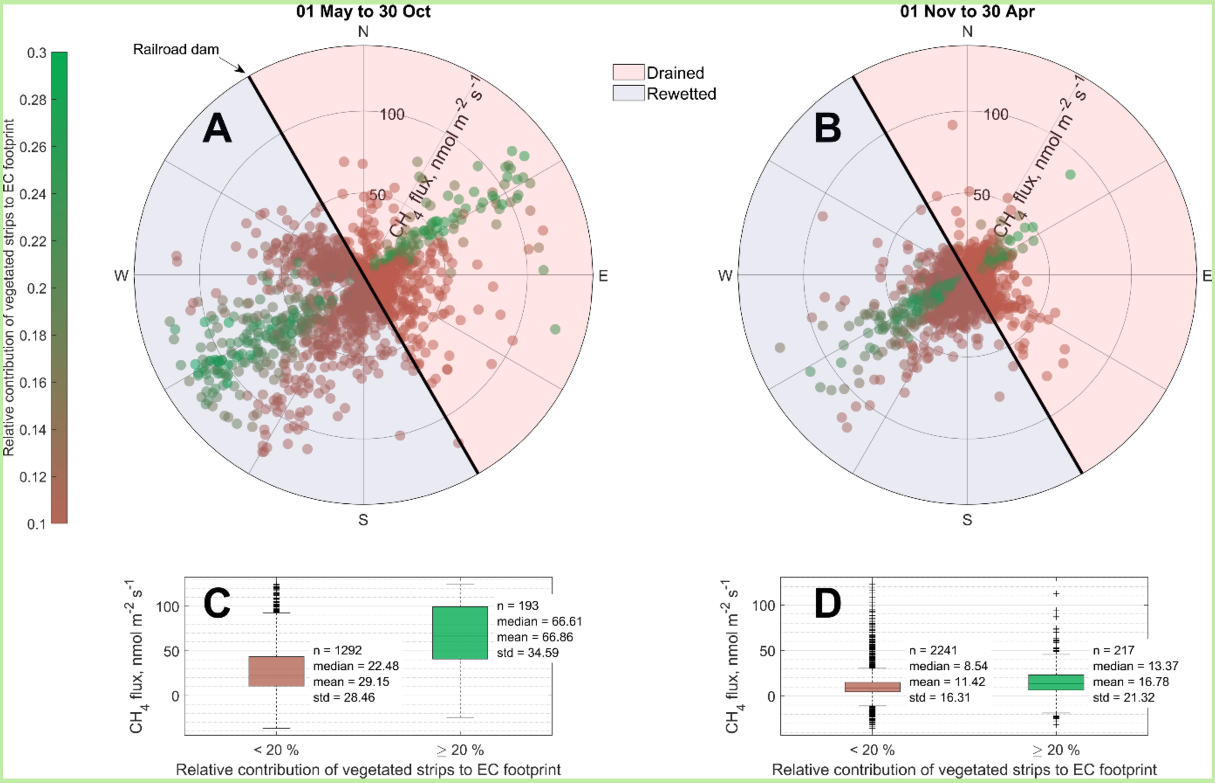

Figure XX2 *Dependence of methane fluxes on wind direction and eddy covariance (EC) source area composition, in particular the contribution of the vegetated strips, in summer (A) and winter (B). Data of both investigated years are shown. The EC tower was placed on a railroad dam dividing the area into an actively (East) and formerly (West) mined section, which had been rewetted prior to measurements. In general, methane emissions from the rewetted section were higher than from the drained section and fluxes when the EC footprint was composed of more than 20 % vegetated areas was significantly (Two-sample Kolmogorow-Smirnow test, $p < 0.01$) higher than from vegetation-free areas, both in summer (C) and winter (D).*

In addition, the section about the vegetation is currently very simple. It would be nice if the authors can provide more information on the vegetation as the EC tower is located just near by. For example , there are tree species like Betula pubescens. How tall are they? Can there be flow distortion since the EC mast is not very high (2m)?

Actually, the EC sensors were mounted at 6 meters height (see page 7, line 20). Tree height in the vegetated strips was up to 2 m. We took differences in roughness length in different wind sectors into account within our footprint model by statistically determining individual roughness length estimates for 2° wind direction bins. We believe that we addressed variations in roughness length sufficiently thorough. We added a sentence after page 9, line 18 for clarity.

Variations in vegetation height and thereby roughness length in different wind sectors were addressed by statistically determining roughness length estimates separately for 2° wind sectors prior to evaluating the footprint model (see Holl2019b for details).

We amended the vegetation description on page 7, line 17 with:

B. pubescens and Salix spp. reached heights of up to 2 m and a combined estimated surface cover within the vegetated strips of up to 10 %.

“In summer of 2012 this area therefore was not yet permanently flooded ...From winter 2012/2013 on, inundation of the rewetted bare peat area progressively increased,...” It would be nice to show the time series of water table level during the study period. How was the dynamics and intensity of the inundation with time?

Unfortunately, water table data are not available for the whole study period, only for the second year (starting in June 2013). We added a new Figure XX1 to illustrate the annual course of water table depth in conjunction with soil temperature and methane fluxes.

I also wonder if the vegetated area was changing during the study period due to the progressive inundation. It was shown by a previous study that the fractal dimension of the vegetation area has the most importance in explaining the variation of fluxes in a restored wetland (Matthes et al., 2014).

Vegetation cover was well established in the vegetated strips (former deep ditches, refilled with peat in the late 1960s) and not the direct result of rewetting. The rewetted former mining areas were largely vegetation-free during our investigation. The contrast between vegetated and unvegetated areas as well as the fraction of vegetated areas in the landscape stayed virtually constant.

The authors have done a nice job reporting the annual greenhouse gas balances and comparing them to other studies. But we should also be careful here, about the reasons behind those numbers. As I can see from the paper, vegetation and progressive inundation have substantial contribution to the results. Imagine if the EC tower is moved somewhere else with higher (or lower) fraction of vegetation in its footprint, or if the measurements are conducted one year before (or later), are we expecting to get similar results from the drained and rewetted sections? Some sensitivity tests would help to show the reliability of results.

Yes, as our data were acquired during a major transition of the site from active peat mining to restoration and I would expect gas flux characteristics to further change in the future. Although, inter-annual variability and systematic shifts in processes cannot be separated precisely with our two-year data set, it also can be seen as a document of shifting conditions and ecosystem response mechanisms. We are confident that the position of the measurement equipment was chosen adequately in order to describe the gas flux dynamics of the site as a whole. The fraction of the vegetated strips within the EC footprint resembles the actual proportion of this surface class within the investigation area. So, yes, moving the tower would potentially change the results. We think our data set is suitable for the purpose of characterizing landscape-scale integrated gas fluxes from the surface class mixture prevalent in Himmelmoor. We added a new Figure XX3 as evidence for this notion.

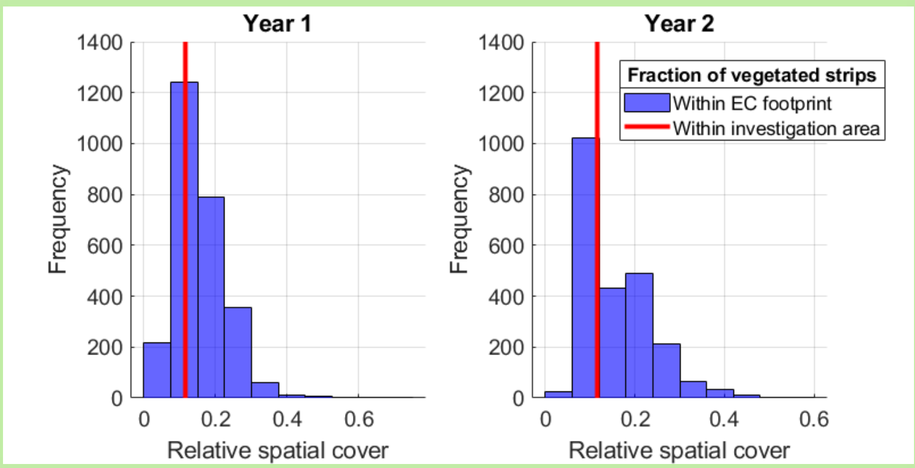

Figure XX3 *Frequency distribution of relative half-hourly contributions of vegetated strips to EC footprint area in both investigated years (Year 1: 01 June 2012 to 31 May 2013; Year 2: 01 June 2013 to 31 May 2014). For comparison, the vegetated strips’ areal fraction within the investigation area is shown, documenting that the measurement system was set up at an adequate position in the landscape in order to represent its spatial proportion of surface classes.*

In the end, I do like to see a bit of advices concerning the management of the peat-extraction fields. For examples, is it advisable to rewet the field in terms of climate impact? What are the pros and cons of having large patches of vegetation during rewetting? Should we aim to regulate the water level during the rewetting?
We added a section discussing the rewetting measures which have been taken at Himmelmoor.

3.4 Implications of rewetting measures for the re-establishment of a mire ecosystem in Himmelmoor

In general, the initialization of peat accumulation by Sphagnum mosses is inevitable (Joosten, 1992; Pfadenhauer and Klötzli,1996; Gaudig, 2002) for the purpose of re-establishing a degraded peatland's natural ecosystem functions. Two (somewhat untypical) features of Himmelmoor need to be considered when evaluating the success of the implemented rewetting measures in terms of mire re-establishment and climate change mitigation: (1) The fact that large vegetation-free areas have been inundated shallowly and (2) that fen-type plants have established at the only vegetated areas which had been taken out of use in the late 1960s. We found peak CH_4 emissions from the vascular plant-dominated areas (see Figure 10) and also attribute this fact causally to the presence of fen-type vegetation. Vascular plants provide an effective transport pathway through their gas-conducting tissue as well as root exudates which form an easily decomposable substrate for soil microbes (Kerdchoechuen, 2005; Neue et al., 1996; Bhullar et al., 2014). Because a water table above the surface instead of close to but below the surface has been established at the bare peat areas, the creation of floating vegetation mats is the only possibility for Sphagnum colonization (Pfadenhauer and Klötzli, 1996). Nevertheless, fast growing vascular plants can support peat moss growth by diminishing wave movement and offering adherence area (Sliva, 1997). Besides the need for a preferably calm water surface, another limiting factor for floating mat growth is the water CO_2 concentration (Gaudig, 2002; Paffen and Roelofs, 1991; Smolders et al., 2001; Lamers, 2001; Lütt, 1992) which can be enhanced by vascular plants by providing oxygen to the rhizosphere fostering soil respiration. It thus seems conceivable that the Sphagnum spp. growth-favoring effects could outweigh the negative ramifications for bog development and climate change mitigation potential that the current plant cover implies. In sections of Himmelmoor with a non-industrial land use history, overgrowth of the grass tussocks, formerly dominating the area, by the bog-type Sphagnum species S. magellanicum and S. papillosum is in progress today (personal observation, 2016). The now prevailing plant species on the extraction site could therefore constitute an intermediate state that can potentially be overcome. The active dispersal of Sphagnum mosses as a management strategy would foster mire re-establishment and possibly lead to drastically diminished CH_4 release as e.g. the study from Järveoja et al. (2016) from an Estonian site where peat mosses dominate after rewetting suggests.

Specific comments

Abstract
Page 1, Line 18: The numbers in CO2 fluxes from rewetted and drained section are wrong. Rewetted section should have lower CO2 emission as stated in the manuscript.
True, numbers were switched around, order was reversed.

Page 1, Line 20: It is not useful to compare the difference in CH4 to the difference in CO2 in an absolute term. Surely CO2 is larger in the magnitude.
We suspect a misunderstanding. In this sentence not absolute CH_4 and CO_2 fluxes are compared but absolute differences in CH_4 fluxes from both land use types.

Introduction
Page 2, Line 27-29: Please provide references.
Still refers to Couwenberg et al. 2010 (see page 2, line24).

Page 3, Line 1: What do you mean by “higher plants”?
We mean “vascular plants” and agree that “higher plants” is ambiguous and therefore replaced this expression.

Material and methods

Page 5, Line 19: So the drained section had also some area rewetted during the study period? Please specify what you meant here.
Ditch blocking was performed on small sections of the drained area after a final harvest in this year (June/July) and therefore after the investigation period of this study. We added a sentence clarifying this fact.
Peat harvesting on the eastern half continued until June 2018, rewetting of smaller sections in this area began, however, already in 2014 (after the investigation period of this study).
Page 7, Line 15: Salix spp..
Extra dot removed
Page 11, Line 1: Maybe replace “and” with “or”
No occurrence of “and” in the mentioned line, no change made.
Page 11,Line 13:“...70 % at all flux gaps that resulted from data division”. What does that mean?
At times when “tower view” fluxes were mostly associated to for example the drained section, the surface class specific time series of the rewetted section have a gap (data division). To later on gap-fill the flux time series, a contribution of the rewetted section of 70 % was prescribed for these gaps.
Page 11, Line 15-17: Why not using median? Maybe a probability density function plot would justify your method for gapfilling CCveg.
We chose the value of the most frequent class because it is closer to the actual fraction of vegetated areas within the investigation area. The new Figure XX3 illustrates this fact.

Results and discussion

Page 14, Line 12-20: Was the ANN model prediction compared with the testing subsets as it should be? As written in Appendix A, “70 % training and 30 % validation data”, it seems there is no testing subset of data.
Yes, that is true. We did not use a testing subset during optimization of the individual networks (1000 per ensemble). Due to rigorous quality filtering and data division (into rewetted and drained), data availability, especially in case of CH_4 fluxes, was limited and we decided to increase the number of training samples to improve training quality at the expense of reserving data points for testing in each individual run. We, however, conducted a similar type of validation (see Figure D3) by driving models that were optimized using Year 1 measurement data as targets with Year 2 environmental data and comparing the results to measured Year 2 gas fluxes. The allocation of testing data is commonly is implemented in ANN optimization in order to generate a data set to later on estimate model quality on data independent from optimization. We believe that we achieved a test of similar meaningfulness by exploiting the fact that we had two independent years of data to work with and could at the same time improve model optimization by increasing the sizes of the training and validation data sets.

Page 20, Line 20: There are many more recent studies on that topic. e.g. “Impact of water table level on annual carbon and greenhouse gas balances of a restored peat extraction area”, Jarveoja et al., 2016, Biogeosciences.
We extended Section 3.3 with a discussion about the recommended publication and others.
..., which is supplied to these areas from the underlying aquifier. Figure XX2 illustrates the dependence of F_{CH4} on the relative contribution of the vegetated strips to the EC footprint. Mean summer fluxes were significantly (Two-sample Kolmogorov-Smirnov test, $p < 0.01$) higher from the vegetated (67 nmol m^{-2} s^{-1}) than from the bare (29 nmol m^{-2} s^{-1}) areas. These results are in line with estimates from Vybornova (2017) who determined a mean annual F_{CH4} of 50 nmol m^{-2} s^{-1} for the same vegetated strips in Himmelmoor with manual chambers. Vybornova et al. (2019) report mean annual F_{CH4} from the bare peat areas of 10

nmol m^{-2} s^{-1}. Further evidence for the decisive role the type of vegetation which is established after rewetting has on the magnitude of CH_4 release is provided by Järveoja et al. (2016). The authors report annual CH_4 budgets of 0.25 and 0.16 g m^{-2} a^{-1} at subsections of their site with relatively high and low water table respectively. The site Järveoja et al. (2016) investigated is the former peat extraction area Tässi in central Estonia (58° N). In contrast to Himmelmoor, restoration measures at this site included the active establishment (dispersal) of peat mosses on a substantial layer (2.5 m) of remnant Sphagnum spp. peat. By the time measurements commenced two years after first restoration efforts were made, Tässi was already dominated by Sphagnum spp. mosses. With a lack of aerenchymatic plants and systematic efforts to re-establish bog vegetation, annual CH_4 release at Tässi is up to 100 times smaller than at Himmelmoor.

Conclusions

Page 21, Line 16-17: "The release of CH4 increases after rewetting and within the present two year data set also over time." This sentence does not read very well.

We agree, section reformulated, see comment below.

Page 21, Line 17-18: This statement does not correspond to the current results. CO_2 decreased from 887 to 567 g m-2 yr-1 while CO_2e of CH_4 increased from 453 to 621 g m-2yr-1 in the rewetted section from year 1 to year 2. Otherwise, comparing the rewetted to the drained section, CO2 dropped from 974 to 567 g m-2 yr-1 and CO_2e of CH_4 increased from 412 to 621 g m-2 yr-1 in year 2. Either way it showed the reduction of CO_2 emission was more prominent than the increase of CH_4 emission during rewetting.

We agree, the sentence is not written very clearly; "on short timescales" is ambiguous. Section replaced with:

CO_2 emissions decreased progressively after rewetting with a reduction of 101 g $m^{-2}a^{-1}$ in Year 1 and of 407 g $m^{-2}a^{-1}$ in Year 2. The release of CH_4-$CO2_e$ increased after rewetting and was constant in both investigated years (209 g $m^{-2}a^{-1}$). The climate impact of elevated CH_4 emissions after rewetting therefore dominated over the effect of decreasing CO_2 release in Year 1, whereas CO_2 emission reduction was nearly twice as high as the CH_4-CO_2e increase in Year 2.

Technical comments

1) Maybe some of the figures D1-4 can be moved to the main text as they validated the modelling and the flux decomposition method.

We propose to move figures D3 and D4 to the results section as they show the most independent and therefore meaningful test of model quality.

2) The results on the cumulative fluxes were repeatedly presented in multiple units (g m-2a-1 in Table 2, mol m-2, CO2-C g m-2 and CH4-C g m-2 in Figure 5). Maybe Table 2 and figure 5 can be combined instead.

The purpose of reporting different units was to facilitate quick comparability to other studies. We agree that spreading the information across Table 2 and Figure 5 is not ideal. We therefore added carbon fluxes to Table 2. Figure 5 was left because there is a reference to the shape of the cumulative curve in the text (Page 18, Line 29).

Table 2. Annual sums of half-hourly carbon dioxide (CO_2) and methane (CH_4) fluxes from the drained and rewetted sections of the peat extraction site in Himmelmoor. CH_4 fluxes are expressed as CO_2 equivalents (CO_2e) using a global warming potential of 34 referring to a 100-year time horizon following Myhre et al. (2013). Year 1: 01 June 2012 to 31 May 2013; Year 2: 01 June 2013 to 31 May 2014

		Cumulative flux, g m^{-2} a^{-1}	
		Surface class *drained*	Surface class *rewetted*
CO_2	Year 1	988 ± 247	887 ± 296
	Year 2	974 ± 292	567 ± 263
CH_4	Year 1	7.2 ± 1.8	13.3 ± 1.9
	Year 2	12.1 ± 1.4	18.3 ± 1.5
CH_4-CO_2e	Year 1	244 ± 61	453 ± 63
	Year 2	412 ± 46	621 ± 51
total CO_2e	Year 1	1232 ± 308	1340 ± 359
	Year 2	1386 ± 338	1188 ± 314
CO_2-C	Year 1	269 ± 67	242 ± 81
	Year 2	266 ± 80	155 ± 72
CH_4-C	Year 1	5.4 ± 1.4	10.0 ± 1.4
	Year 2	9.1 ± 1.1	13.7 ± 1.1

References

Matthes, Jaclyn Hataa and Sturtevant, Cove and Verfaillie, Joseph and Knox, Sara and Baldocchi, Dennis: Parsing the variability in CH4 flux at a spatially heterogeneous wetland: Integrating multiple eddy covariance towers with high-resolution flux footprint analysis, JOURNAL OF GEOPHYSICAL RESEARCH-BIOGEOSCIENCES, 119, 7, 1322-1339, 2014.

Comparison of eddy covariance CO_2 and CH_4 fluxes from mined and recently rewetted sections in a NW German cutover bog

David Holl[1], Eva-Maria Pfeiffer[1], and Lars Kutzbach[1]

[1]Institute of Soil Science, Center for Earth System Research and Sustainability (CEN), Universität Hamburg, Hamburg, Germany

Correspondence: David Holl (david.holl@uni-hamburg.de)

Abstract. With respect to their role in the global carbon cycle, natural peatlands are characterized by their ability to sequester atmospheric carbon. This trait is strongly connected to the water regime of these ecosystems. Large parts of the soil profile in natural peatlands are water-saturated, leading to anoxic conditions and to a diminished decomposition of plant litter. In functioning peatlands, the rate of carbon fixation by plant photosynthesis is larger than the decomposition rate of dead organic material. Over time, the amount of carbon that remains in the soil and is not converted back to carbon dioxide grows. Land use of peatlands often goes along with water level manipulations and thereby with alterations of carbon flux dynamics. In this study, carbon dioxide (CO_2) and methane (CH_4) flux measurements from a bog site in NW Germany that has been heavily degraded by peat mining are presented. Two contrasting types of management have been implemented at the site: (1) drainage during ongoing peat-harvesting on one half of the central bog area and (2) rewetting on the other half that had been taken out of use shortly before measurements commenced. The presented two-year data set was collected with an eddy covariance (EC) system set up on a central railroad dam that divides the two halves of the (former) peat harvesting area. We used footprint analysis to split the obtained CO_2 and CH_4 flux time series into data characterizing the gas exchange dynamics of both contrasting land use types individually. The time series gaps resulting from data division were filled using the response of artificial neural networks (ANNs) to environmental variables, footprint variability and fuzzy transformations of seasonal and diurnal cyclicity. We used the gap-filled gas flux time series from two consecutive years to evaluate the impact of rewetting on the annual vertical carbon balances of the cutover bog. Rewetting had a considerable effect on the annual carbon fluxes and led to increased CH_4 and decreased CO_2 release.

The larger relative difference between cumulative CO_2 fluxes from the rewetted (~~22~~13 ± ~~7~~ 6 mol m^{-2} a^{-1}) and drained (~~13~~22 ± ~~6 mol~~ 7 mol m^{-2} ~~-~~a^{-1}) section occurred in the second observed year when rewetting apparently reduced CO_2 emissions by 40 %. The absolute difference in annual CH_4 flux sums was more similar between both years while the relative difference of CH_4 release between the rewetted (0.83 ± 0.15 mol m^{-2} a^{-1}) and drained (0.45 ± 0.11 mol m^{-2} a^{-1}) section was larger in the first observed year indicating a maximum increase of annual CH_4 release of 84 % caused by rewetting; at this particular site during the study period.

1 Introduction

Peatlands are wetland ecosystems that accumulate peat under water-saturated soil conditions. Peat formation is the result of an imbalance between production and decomposition of organic matter. For a peatland to qualify as a mire, the accumulation of peat has to be ongoing. The term peatland is defined broader and refers to soils that include an at least 30 cm thick peat horizon – with or without ongoing peat accumulation. Concerning long-term carbon sequestration, no other terrestrial ecosystems are as efficient as mires. Although peatlands cover only 3 % (400 million ha) of the Earth's land surface, they store 550 Gt carbon (Yu et al., 2010), which equals the amount of carbon (C) stored in the entire terrestrial biomass and represents twice as much C as sequestered in the Earth's forests respectively. Peatlands are characterized by complex interactions between vegetation, hydrology and peat and are therefore vulnerable to alterations of these factors by ~~men~~ land use or climate change. Traditional land use practices in peatlands are commonly paralleled by interference with the ecosystems' water regimes. Hydrological manipulations can fundamentally modify the carbon flux dynamics of peatlands, regardless if they are undertaken to prepare the area for commercial use (drainage) or to restore a "natural" state of the ecosystem (rewetting). Anthropogenic use of peatlands usually involves their drainage. The stored carbon can then be oxidized, and a C sink is often turned into a C source. It is estimated that at least 3 billion tons (Parish et al., 2008) of carbon dioxide (CO_2) are emitted by degraded peatlands per year globally. This is equivalent to 10 % of the global annual emissions by the combustion of fossil fuels. The rewetting of formerly drained peatlands commonly reduces CO_2 emissions drastically and makes the re-establishment of a CO_2 sink possible on the long run (Couwenberg, 2009; Wilson et al., 2009; Alm et al., 2007; Vanselow-Algan et al., 2015; Beyer and Höper, 2015; Wilson et al., 2016b; Tuittila et al., 1999). Under water-saturated conditions, however, the anaerobic decomposition of organic matter and thereby the production of the greenhouse gas (GHG) methane (CH_4) increases. Land use change of peatlands thus ~~inheres~~ has the potentials to accelerate global warming as well as to mitigate climate change.

For a peatland to act as a CO_2 sink, the water level may fluctuate around the surface only to a minor degree. If it is too low, more plant litter is decomposed aerobically than is being produced. If it is too high, plant production often is inhibited, so that e.g. lakes commonly are carbon sources. At water tables near the surface, CO_2 emissions are low (respectively negative when C is sequestered); with lowering water tables emisions rise. Couwenberg et al. (2010) found a linear correlation between CO_2 flux (F_{CO2}) and water table depth in a meta-analysis of flux data from temperate European peatlands. For sites with mean annual water levels above 40 cm below the surface, CO_2 emissions decrease with rising water tables. CH_4 emissions are also linked to the water table. At levels deeper than 20 cm below the surface, CH_4 emissions are negligible and increase with a rising water table. In case of inundation, diffusive CH_4 release is hampered due to the large difference in gas diffusivity of water and air. Moreover, CH_4 can be ~~decomposed~~ converted to CO_2 on its comparably slow way through the water column if enough dissolved oxygen is present. Two alternative mechanisms for the transport of pedogenic CH_4 to the atmosphere are known. CH_4 release via bubbles can account for a significant portion of the overall CH_4 emissions (Glaser, 2004; Strack et al., 2005; Goodrich et al., 2011). This process is referred to as ebullition and describes the sudden release of gas bubbles that accumulate in the soil pore space until their buoyancy is high enough for them to ascend to the surface. The importance of diffusion and ebullition declines with the presence of vascular plants. The soil and water volume can be bypassed employing plant-mediated transport through the aerenchymae of vascular plants (Whalen, 2005; Bubier, 1995). Moreover, ~~higher~~ vascular plants also provide labile dissolved organic carbon to the rhizosphere. These easily decomposable carbon compounds can act as a substrate for methanogenic microorganisms. CH_4 flux (F_{CH4}) dynamics are therefore ~~gravely~~ strongly impacted by vegetation cover and type.

Wilson et al. (2009) investigated the development of CH_4 emissions and modeled the course of CH_4 emissions for different land use types following peat extraction. The authors conclude, that by long-term inundation of peatlands formerly used for peat harvesting, the creation of a landscape scale methane hotspot is very possible. Nevertheless, the balance of avoided CO_2 emissions by restoration and newly created CH_4 emissions results in a net-reduction of the global warming potential (GWP) at the site Wilson et al. (2009) described. When anaerobic conditions prevail after inundation, CH_4 production is mainly controlled by the availability of fresh organic matter (Couwenberg, 2009; Lai, 2009; Saarnio et al., 2009) as well as soil and water temperature (Schrier-Uijl et al., 2010). Hahn-Schöfl et al. (2010) performed a chamber measurement campaign and incubation experiments on a rewetted former grassland fen in the Peene river valley in NE-Germany. The authors describe the formation of an organic sediment from the rotting former vegetation cover. The CH_4 production potential linked to the anaerobic decomposition of such a substrate is very high. Tiemeyer et al. (2016) investigated GHG release from 48 grassland sites on drained fens and bogs in Germany. They report high CH_4 emissions from relatively nutrient-poor and acidic sites. Incubation experiments from Hahn-Schöfl et al. (2010) show that bare peat is comparatively inactive. This finding is confirmed by Wilson et al. (2016b) for drained as well as rewetted bare peat surfaces in temperate peatlands. In case of a vegetation-free restored peatland site, the risk of CH_4 production depends on which plants are established or colonize the site respectively. Thereby, it is critical how easily decomposable the delivered organic matter is and if plant-mediated methane transport via their aerenchyma (Whalen, 2005) occurs. Furthermore, CH_4 production is negatively correlated with the availability of other electron acceptors like iron or sulfate.

CH_4 is an important GHG and a crucial part of the carbon balance of many (especially wetland) ecosystems. While the earliest landscape scale CH_4 flux measurements date back to the 1990s (Verma et al., 1992; Zahniser et al., 1995; Suyker et al., 1996), considerable advances in laser absorption spectroscopy (LAS) within the last ten years have led to a wide application of fast LAS-based sensors as part of eddy covariance (EC) setups. Intercomparisons of the available sensors are given by Tuzson et al. (2010), Detto et al. (2011), Peltola et al. (2013) and Peltola et al. (2014). Due to its low power consumption and thereby its feasibility for remote sites with limited off-grid energy supply, the Licor LI-7700 open-path sensor (McDermitt et al., 2011) has frequently been used in ecosystem CH_4 flux studies. Because the measurement cell of such a devices is exposed to the atmosphere, it does not require a pump (reducing the sensor's power requirements) but is also subject to adverse conditions like dust or rain, which can deteriorate the acquired data by contaminating the highly reflective mirrors the sensor relies on.

The development of fast sensors provided the possibility to measure long-term landscape scale CH_4 fluxes with the EC technique at high temporal resolution. Ecosystem carbon balances can since be reported more comprehensively. However, to be able to calculate for example annual sums, gaps in the flux time series have to be filled first. Compared to modeling CO_2 fluxes, gap-filling of CH_4 fluxes is more challenging because the relations between environmental drivers and CH_4 flux often appear to be more complex than for CO_2. An overview of methods applied in EC literature is given in supplements table S1.

Basic gap-filling methods include for example interpolation between measured values ~~(Hanis et al., 2013; Dengel et al., 2011)~~ or the use of an average to replace all gaps~~(Hatala et al., 2012; Mikhaylov et al., 2015)~~. Simple linear models have also proven to be applicable in certain settings~~(Alberto et al., 2014; Hanis et al., 2013)~~. A common approach is to fit Arrhenius-type non-linear functions to the flux as a function of various environmental drivers~~, what has been done for half hourly data (Kroon et al., 2010; Forbri~~ ~~as well as for downsampled time series (Suyker et al., 1996; Friborg and Christensen, 2000; Rinne et al., 2007; Long et al., 2010; Wille et a~~ . However, as stated by Brown et al. (2014), there is evidence that these functional relationships do not necessarily behave monotonically.

Artificial neural networks (ANNs) form a category of non-parametric models that have frequently been used to fill gaps in EC CO_2 flux time series. Mostly, multilayer perceptrons (MLP) were chosen (Papale and Valentini, 2003; Moffat et al., 2007; Moffat, 2012; Järvi et al., 2012; Pypker et al., 2013; Menzer et al., 2015)~~while other authors utilized radial basis function (RBF) networks (Schmidt et al., 2008; Kordowski and Kuttler, 2010; Menzer et al., 2015). For~~ . Most recent literature on CH_4 ~~fluxes, MLP models are described by Dengel et al. (2013), Deshmukh et al. (2014), Knox et al. (2015) and Goodrich et al. (2015) as well as a special kind of RBF network, a generalized regression neural network (GRNN) , by Zhu et al. (2013)~~flux gap-filling assess MLP models to be the most robust. MLPs are recommended within the processing for the pan-European Integrated Carbon Observation System (ICOS) by Nemitz et al. (2018) and for the new methane component of FLUXNET and the Global Carbon Project's efforts to better constrain the global methane budget respectively (Knox et al., 2019).

In this study, we compare simple linear and more complex neural network modeling approaches to gap-fill half-hourly EC CH_4 and CO_2 fluxes based on their explanatory power, their number of parameters and their generalization capability. We also give a structured approach to the choice of architectural properties for ANNs. Additionally, we present a new quality filter for CH_4 concentrations measured with LI-7700 (Licor, USA) open-path sensors. By evaluating half-hourly footprint statistics, our data sets from a temperate degraded bog were divided by land use type and gap-filled in order to calculate the annual sums of vertical C exchange between surfaces under contrasting management (drainage and rewetting) and the atmosphere.

Based on two years of CO_2 and CH_4 fluxes, our overriding research questions are: (1) Is gas flux modeling of contrasting surface types within an EC gas flux time series measured over heterogeneous terrain feasible, and (2) what is the climate impact of peatland land use change from drainage to rewetting in the early phase after ditch-blocking following peat mining in a temperate bog?

2 Material and methods

2.1 Site description

2.1.1 Geography and land use history

Himmelmoor is a temperate bog that has been degraded heavily by peat mining. The site is located in NW Germany, around 25 km north-east of Hamburg and 3 km west of Quickborn in Schleswig-Holstein (53° 44'23.3" N, 9°50'55.8" E). The long-term (2000 to 2014) average annual precipitation is 888 mm, measured at a weather station (WMO Station ID: 10146) located

2 km from the peatland center. The mean annual air temperature (2000 – 2014) at this station operated by Deutscher Wetterdienst (DWD) is 9.1 °C. Along with the adjacent grassland-fen of the Bilsbek lowland and the beech-dominated forest stand Kummerfelder Gehege, Himmelmoor forms a nature reserve according to the EU FFH (Flora Fauna Habitat Directive). Federal law of Schleswig-Holstein protects Himmelmoor as a core area of the local biotope network (Zeltner, 2003). By federal legislation enacted in 1973, human intervention in peatland ecosystems is prohibited in the state of Schleswig-Holstein. In case of Himmelmoor, however, unlimited lease agreements from 1920 and 1932 (Kreis Pinneberg, 2004) were in effect. An environment protection law from 1993 dictated the expiration of such agreements until 2003. The mining company and the legislators reached a settlement obligating the company to carry out restoration measures while continuing with peat extraction until 2020. Manual peat extraction, undertaken by the local population over centuries to gain fuel, was limited to the bog's outer margin. Since the mid-19th century, peat-cutting underwent mechanisation and was thereby intensified. Extraction was scaled up in the 1870s, when transport logistics were greatly improved by the construction of a railway track between Quickborn and Altona (today a district of Hamburg). Mining was limitied to peripheral areas until industrial peat extraction began in the 132 ha large (Grube, 2010) central bog area at the beginning of the 20st century (Czerwonka and Czerwonka, 1985). Until 1968, the aim of this operation was the production of peat usable as fuel. Between 1950 and 1968, suitable material was mined from positions deep in the peat profile. These deep ditches were refilled annually with dug-out peat and still exist in this refilled state today. Locally, these strips are called *Pütten*. Today, fen-type vegetation is covering these strips, which are between 600 m and 700 m long in ENE-WSW direction and 20 m to 50 m wide in NNW-SSE direction. In the late 1960s, the mining company began to target a different, surface-near type of peat to yield a substrate for horticulture. The extraction site is divided into two halves by a NNW-SSE running railroad dam. Areas on the western half have been stepwise taken out of operation by the local peat plant operator since 2008. The eastern part was still being harvested during the measurement period (1 June 2012 to 31 May 2014), whereas most of the western section was already rewetted, apart from a 90 m wide strip in the northwest (see Figure 1). These areas of opposing water regimes and land use will be referred to as surface class *drained* (SC_{dra}) and surface class *rewetted* (SC_{rew}) respectively throughout this text. Peat harvesting on the eastern half continued until June 2018, rewetting of smaller sections in this area began, however, already in ~~2014.~~ 2014 (after the investigation period of this study). Peat extraction is now ceased. Ditches were blocked, and new peat dams were built to rewet the extraction site, leaving large, shallowly inundated areas underlain by bare peat.

2.1.2 Peat formation and stratigraphy

The bog developed in a river valley, which was preformed as a glacial meltwater valley during the Weichselian glaciation in the depressed fringe of a salt dome. Peatland formation from a standing water body began 10.020 ± 100 years BP (Pfeiffer, 1997). Following the deposition of organic lake sediments, a *Phragmites-Carex* fen and a subsequent birch forest formed. Around 8000 years BP, a rising groundwater level led to the extinction of the forest vegetation, to the spread of *Sphagnum spp.* peat mosses and eventually to the development of a bog. Organic-rich silt constitutes the peatland's foundation but is not evenly distributed across the whole area. In the northern part, this layer is at its thickest (up to 2 m). There, the base of the peatland is at its deepest (around 7 m a.s.l.). The formation of the peatland most likely began at this location (Grube et al., 2010). Bog-

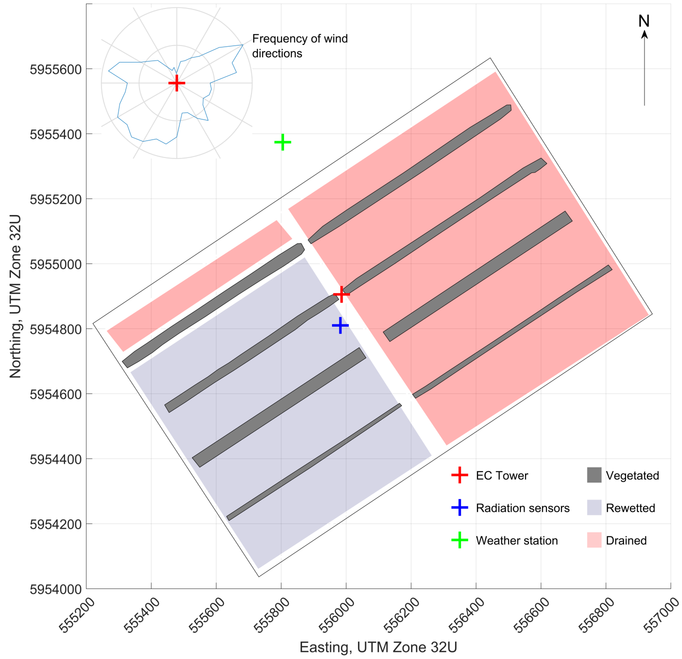

Figure 1. Distribution of surface classes *rewetted*, *drained* and *vegetated* in Himmelmoor during the measurement period between 1 June 2012 and 31 May 2014. The map section shows the central extraction area with the EC tower located on the central railroad dam. Grid spacing is 200 m, coordinates refer to UTM zone 32U. The polar histogram in the top left corner displays two years of half-hourly wind direction measurements at the EC tower location binned in 2° classes.

type peat consisting mostly of *Sphagnum* remnants is (in its original stratigraphic position) today only present in the northern marginal area, locally called *Knust*, with a thickness of 3.8 m (Grube et al., 2010). Bog peat was completely removed from the central extraction area where fen-type peat is present area-wide with a maximum thickness of 2.2 m. Pfeiffer (1997) divides these peat deposits in 30 – 45 cm *Eriophorum-Betula* peat over 45 – 85 cm birch forest peat over *Phragmites-Carex* peat. Soil properties were altered severely by peat decomposition and subsidence during decades of drainage and peat extraction. Drainage led to compaction and settlement of the peat profile of about 40 % of its original depth. The peatland's ability to self-regulate the water table for optimal peat forming and carbon sequestering conditions is thereby lost. The performed ditch-blocking leads to a strongly oscillating water table over the course of the year in the early years of rewetting (< 5 years, own observations made between 2011 and 2018). Himmelmoor drains into the two local creeks Bilsbek and Pinnau. The peatland mainly receives water from precipitation. Additional minerotrophic water inflow takes place through the *Pütten*, which are distributed regularly across the central bog area. These ditches reach below the peat base and penetrate the mineral ground. They were later refilled with peat but still provide a connection to the aquifer beneath, from which minerotrophic groundwater is supplied.

2.1.3 Vegetation

The central, former extraction area is largely vegetation-free. *Sphagnum spp.* peat mosses occur in ditches and along the shores of some rewetted, inundated polders of the former mining area. *Betula pubescens*, *Molinia caerulea*, *Eriophorum angustifolium*, *E. vaginatum*, *Erica tetralix* and ~~brwon~~ brown mosses (*Odontoschisma spp.*, *Cephalozia spp.*) occur in often isolated patches on drier areas. Fen-type vegetation is common at the *Pütten*. *Betula pubescens*, *Salix spp.* ~~.~~ (presumably *Salix aurita* and *Salix caprea*), *Eriophorum vaginatum*, *Betula pubescens*, *Molinia caerulea*, *Eriophorum angustifolium*, *Calla palustris*, *Typha latifolia*, *Carex spp.*, *Juncus effusus* and *Calamagrostis canescens* occur there. *B. pubescens* and *Salix spp.* reached heights of up to 2 m and a combined estimated surface cover within the vegetated strips of up to 10 %.

2.2 Instrumentation

Eddy covariance CH_4 fluxes were measured using an open-path gas analyzer (LI-7700; Licor, USA) and a 3-D sonic anemometer (R3; Gill, UK) mounted on a tower at 6 m height. Water vapour and CO_2 concentrations were determined with an enclosed-path sensor (LI-7200; Licor, USA). Data were recorded on a LI-7550 (Licor, USA) logger at 20 Hz. Additionally, a HMP45 (Vaisala, Finland) temperature and relative humidity probe was mounted on the EC tower and logged with the same device. A second HMP45 was installed together with a NR01 4-component net radiometer (Hukseflux, Netherlands) 70 m southwest of the EC tower on a tripod at 2 m height. The radiation sensors were not mounted on the EC tower because the field of view of the downward-facing sensors would have covered the peat dam and therefore not be representative for a dominant surface type at the site. These data were logged on a CR-3000 (Campbell Scientific, UK). Another logger of this type was used at the weather station which was taken over from a previous project and left at a position approximately 500 m ~~northeast~~ north of the EC tower for data consistency. The sensors there included a third HMP45 and a tipping bucket rain gauge (R.M. Young, USA). Per depth, redox potentials were determined with three parallel fibreglass probes with platinum sensor tips and recorded on a Hypnos II logger (MVH Consult, Netherlands). The redox probes were installed in a vegetated strip approximately 100 meters west of the EC tower. Water level was measured and logged with a hydrostatic pressure transducer (Mini-Diver; Schlumberger Water Services, USA) around 150 m west-southwest of the EC tower. Rain and long-term temperature data as presented in Figure 2 was taken from a nearby station operated by DWD (WMO-Station ID 10146), which is located east-southeast from the EC tower at approximately 2 km distance. Two years of turbulent flux data were available for analysis from Himmelmoor. The EC setup did not change during that time. The first year from 1 June 2012 to 31 May 2013 is from hereon called Year 1, the second year from 1 June 2013 to 31 May 2014 is called Year 2.

2.3 Flux calculation and qualitiy filtering

Turbulent fluxes were computed by applying the EC approach (as for example described in more detail by Aubinet et al., 2012) using the software EddyPro 5.2.1 (Licor, USA). Raw data processing included (1) an angle of attack correction, i. e. compensation for flow distortion induced by the anemometer frame (Nakai et al., 2006), (2) coordinate rotation to align the anemometer x-axis to the current mean streamlines (Kaimal and Finnigan, 1994, double rotation), (3) linear detrending

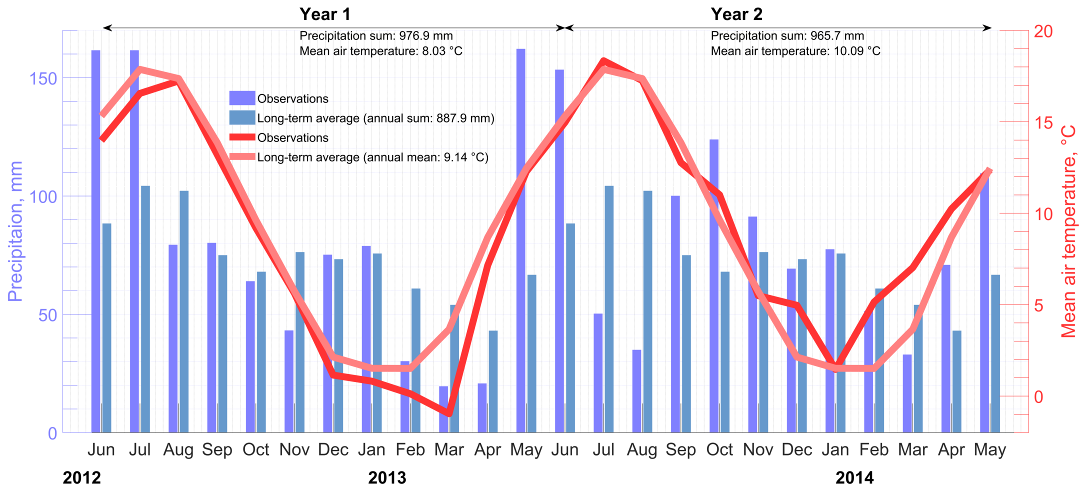

Figure 2. Climate diagram of the two investigated years from 1 June 2012 to 31 May 2013 (Year 1) and form 1 June 2013 to 31 May 2014 (Year 2) as measured in Himmelmoor and a 14 year average of a nearby DWD station (WMO-Station ID 10146).

(Gash and Culf, 1996), (4) time lags compensation, (5) spectral corrections (see below for details) and (6) WPL-correction to compensate for air density fluctuations due to thermal expansion and water dilution (Burba et al., 2012). High frequency loss due to path averaging, signal attenuation and finite time response of the instruments was accounted for following Fratini et al. (2012). Low frequency loss due to finite averaging time and linear raw data detrending was corrected for according to Moncrieff et al. (2004). More details on the single flux calculation steps are given in Holl et al. (2019a).

Thirty minute fluxes were screened for quality according to the following scheme. To check whether general assumptions necessary for the application of the EC method were met, atmospheric stability and developed turbulence were analyzed as described by Mauder and Foken (2004). By this step, fluxes were classified into three groups: MF0, MF1 and MF2, with MF0 denoting data of highest and MF2 of lowest quality. Due to potentially faulty WPL correction, CH_4 and CO_2 fluxes of half-hours when sensible or latent heat flux were flagged with MF2 were discarded. Certain quality flags that were derived from raw data statistics as described by Vickers and Mahrt (1997) were evaluated. If skewness or kurtosis of vertical wind or sonic temperature were assigned a hard flag (skewness outside [-2,2], kurtosis outside [1,8]) or if CH_4 or CO_2 concentration statistics were rated with a soft flag (skewness outside [-1,1], kurtosis outside [2,5]), trace gas fluxes where discarded. Furthermore, half-hourly fluxes were rejected if the respective 20 Hz concentration time series failed the amplitude resolution test (Vickers and Mahrt, 1997).

Additionally, diagnostic values from the LI-7700 and LI-7200 gas analyzers were used for quality screening. LI-7200 data was omitted when the signal strength indication (AGC) lay above 63. Due to a change in the signal quality definition along with a software upgrade, this rule was modified to discarding data below a value of 75 for data acquired when the sensor was running on firmware version 6.6 and above. With respect to the LI-7700, the sensor's relative signal strenth indication (RSSI) and the heater diagnostics were evaluated. The bottom and top mirror of the gas analyzer's measurement cell can be

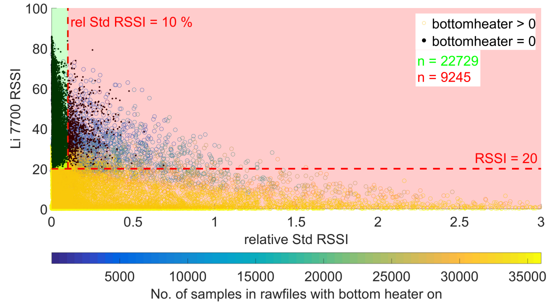

Figure 3. Illustration of the empirically derived threshold for the new LI-7700 open path methane analyzer quality filter. This check evaluates raw 20 Hz RSSI statistics to remove erroneous half-hourly methane fluxes. The filter is designed to capture concentration time series that were deteriorated by switching events in a LI-7700 mirror heater. Black data points denote half-hour intervals, during which the heater of the bottom mirror was switched off entirely. Colored points represents half hour intervals, during which switching events (maximum: 36000) in the 20 Hz time series occured.

heated to counter condensation and frost on the mirrors. The LI-7700 instrument software allows for user-defined thresholds that control the power-on of the heaters. For the bottom heater, a RSSI threshold $\mathrm{RSSI_{th}}$, below which the heater is turned on can be adjusted. For the top heater, an ambient temperature offset threshold $\mathrm{T_{a,\,offset}}$ can be defined. This mirror is heated to keep its temperature about $\mathrm{T_{a,\,offset}}$ above ambient temperature. In the present case, $\mathrm{RSSI_{th}}$ was set to 20 and $\mathrm{T_{a,\,offset}}$ to 1 °C. The number of samples within one half hour, for which a heater is switched on, is recorded. Accordingly, these diagnostics (bottom heater on: $\mathrm{BH_{\,on}}$; top heater on: $\mathrm{TH_{\,on}}$) take maximum values of 36000 if a heater is switched on for an entire half hour. Heater diagnostics were investigated closely due to the observation that within an averaging interval, high variation in RSSI was often accompanied by switching events in the 20 Hz heater time series, i.e. if $\mathrm{BH_{on}}$ or $\mathrm{TH_{\,on}}$ were neither 0 nor 36000. Moreover, methane concentrations had the tendency to covary with RSSI values if the latter showed large changes, what renders calculated fluxes not trustworthy. In general, the top heater was switched on most of the time whereas switching events in the $\mathrm{BH_{\,on}}$ time series were more common, which is why we mainly focused on the bottom heater diagnostics for the analysis of this phenomenon. Figure 3 shows the relationship between half-hourly averaged RSSI values, the corresponding relative standard deviation of 20 Hz RSSI ($\mathrm{RSSI_{relStd}}$) values and $\mathrm{BH_{on}}$. From this graph, we empirically derived a $\mathrm{RSSI_{relStd}}$ threshold of 10 % , above which the respective flux records were neglected. Additionally, methane fluxes were discarded if the mean RSSI of the respective averaging interval was below 20.

The next quality screening step addressed the filtering of fluxes related to undesired source areas. We first classified the surface using georeferenced orthoimages of the area. As the surface types we aimed to discriminate were quite large and easily distinguishable on the images, we could draw polygons around the different classes and get the coordinates of their corners. This step was implemented through the Matlab 8.4 Mapping and Image Processing Toolboxes. We defined the surface classes *drained* (SC_{dra}), *rewetted* (SC_{rew}) and *vegetated* (SC_{veg}), the latter of which is contained in the other two surface types as formerly deep, now refilled and vegetated ditches (*Pütten*). Calculating a 2-D footprint function after Kormann and Meixner (2001) with 1 $\mathrm{m^2}$ resolution (see Holl et al., 2019b, for details on footprint model implementation) and summing up the contribution values of all pixels within each of the three surface types, yielded half-hourly class contribution fractions of the different classes to the EC signal (CC_{rew}; CC_{dra}; CC_{veg}). Variations in vegetation height and thereby roughness length in different wind sectors were addressed by statistically determining roughness length estimates separately for 2 °wind sectors prior to evaluating the footprint model (see Holl et al., 2019b, for details). Gas fluxes of half hour intervals when the EC footprint was composed of the railroad dam and areas outside the mining site by more than 70 % were discarded. Fluxes were then filtered for absolute limits. CH_4 data outside [-100 1000] nmol m^{-2} s^{-1} and CO_2 data outside [-10 10] µmol m^{-2} s^{-1} were neglected. In case of the CH_4 flux time series, outlier removal was addressed furthermore by assessing the frequency distribution of the remaining MF0 data. Values smaller than the bin center of the 1st (BC_1) or larger than the 99th percentile's bin center (BC_{99}) were omitted. As a last step, CH_4 fluxes with random uncertainties calculated with EddyPro after Finkelstein and Sims (2001) larger than 400 nmol m^{-2} s^{-1} were filtered out.

Overall, a large amount of data were removed throughout the course of quality filtering. Of the original 19665 F_{CH4} records 28 % of quality classes MF0 and MF1 were left after filtering. Most fluxes (35 %) were removed because they failed the skewness/kurtosis test. In case of CO_2 fluxes, 51 % MF0 and MF1 records of the original 31271 fluxes remained after filtering. The largest amount of data (15 %) were removed because either H or LE of the same half hourly interval were flagged with MF2.

2.4 Flux modeling

We applied a two-step gap-filling process to CO_2 and CH_4 fluxes separately for each of the two available years. We first filled gaps resulting from quality filtering of the measured EC gas fluxes, which represent approximations of the landscape-scale fluxes integrated over the whole ecosystem and thus include areas of contrasting land use types (tower view time series, TVTS). In order to quantify the impact of rewetting on the vertical annual C balances of the peat extraction areas in Himmelmoor, we used EC footprint variables to select fluxes when the EC source area was mainly composed of drained or rewetted surfaces respectively. In particular, we created these surface class time series (SCTS) by selecting all flux values for the class contributions CC_{dra} and CC_{rew} above a threshold of 70 %. As this data division necessarily resulted in further gaps in the SCTS, we used new sets of models to fill those gaps. We used multilinear regressions (MLRs) and artificial neural networks (ANNs), in particular multilayer perceptrons (MLPs), to model gas fluxes as a response to measured environmental and EC footprint variables as well as to generated fuzzy logic representations of diurnal and seasonal periodicity. Additionally, we used a model input selection scheme in an effort to exclude redundant and irrelevant variables from the model input matrix. A description of model input selection and model setup is given in ~~Appendix A~~the supplements to this manuscript. Details on data set division by surface class contribution, gap-filling and flux decomposition ~~using a mechanistic approach~~ are given here.

Apart from the class contribution variables, the inputs presented to the selection scheme were the same for TVTS and SCTS modeling. To gap-fill a SCTS, the contributions of the respective opposite surface classes were omitted from the input space. To model the time series representing the rewetted area for instance, CC_{dra} and $CC_{veg,dra}$ (see Table A1) were removed from the input matrix. Also, the surface class of interest was set to the threshold value of 70 % at all flux gaps that resulted from data division. We used this threshold value instead of 100 % class contribution to avoid extrapolating outside the scope of the training data sets, as the EC footprint was virtually never composed of one surface class only. The measured contributions of the vegetated strips were binned in ten classes and the bin-center of the most frequent class was used to fill gaps in the respective CC_{veg} time series. We used the selected variables as inputs for MLRs and MLP ensembles with 1000 networks each. To optimize the model parameters, we used only observed data of quality class 0 as targets. Based on the better performance of MLPs compared to MLRs (see section 3.2), we decided to use MLP models for TVTS as well as SCTS gap-filling. To express model uncertainty, we used the standard deviations of the 1000 single MLPs making up each model ensemble for each half hour. We confirmed normal distribution of the 1000 model fluxes for each half hour by applying a Kolmogorov-Smirnov test at all time steps. To calculate surface class specific annual sums, we included measurement data of quality class 1 back into the SCTS. All quality class 1 values that corresponded to CC_{dra} or CC_{rew} ranging above 70 % were used to replace the modeled SCTS data for the respective time steps. We filled remaining gaps in the gas flux time series, when no environmental data was available, with a mean diurnal variation (MDV) method (see Falge et al., 2001). If this algorithm encounters a gap, it searches for available values of the same variable in adjacent days at the same hour of day and uses the mean of the found records to fill the gap. At first, a window of $\pm$ 1 day around the gap is screened. If not at least one data point is found, the search range is increased in steps of one day until the gap can be filled. We calculated two annual sums for all four SCTS (two gases and two land use types) from the gap-filled time series. We calculated uncertainty estimates of the annual sums by taking the root of the sum of squared half-hourly uncertainties. For measurements we used the random uncertainty estimate following Finkelstein and Sims (2001), for data modeled with an MLP ensemble the ensemble standard deviation and for data modeled with the MDV method the standard deviation of averaging samples.

In case of the F_{CO2} SCTS, we used a deterministic modeling approach to further decompose the net flux into components related to respiration and photosynthesis. As large parts of Himmelmoor are vegetation-free, we included the class contribution of the vegetated strips (*Pütten*, SC_{veg}) to the EC footprint to scale the model terms relating to the respective surface classes (as e.g. in Rößger et al., 2019; Forbrich et al., 2011) in the following way:

$$NEE(CC_{veg}, PAR) = (1 - CC_{veg}) \times TER_{bare} + CC_{veg} \times TER_{veg} - CC_{veg} \times \frac{P_{max} \times \alpha \times PAR}{P_{max} + \alpha \times PAR} \tag{1}$$

where CC_{veg} is the class contribution of the vegetated strips, PAR is photosynthetically active radiation (µmol m^{-2} s^{-1}), TER_{veg} and TER_{bare} are ecosystem respirations (µmol m^{-2} s^{-1}) of the vegetated strips and the areas covered by bare peat respectively, P_{max} is the maximum photosynthetic rate (µmol m^{-2} s^{-1}), and α is the initial quantum yield. Prior to fitting, CC_{veg} and CC_{bare} were rescaled to sum up to 1 so that

$$1 - CC_{veg} = CC_{bare}. \tag{2}$$

The last term of Eq. 1 consists of a rectangular hyperbolic Michaelis-Menten type function to simulate plant photosynthesis (Thornley, 1998; Zheng et al., 2012). This type of light saturation curve has proven to be feasible for modeling plant carbon dioxide fixation driven by radiation. In order for the model to express net CO_2 flux, two ecosystem respiration terms were added to the formula; the combined plant and soil respiration TER_{veg} scaled by CC_{veg} and the microbial respiration TER_{bare} taking place in the vegetation-free areas scaled with CC_{bare}. This function was fitted to monthly ensembles of all CO_2 SCTS, yielding

Table 1. ~~Model inputs used for methane and carbon dioxide flux gap-filling sorted by type. (x: available, -: not available)~~

~~*Type*~~	~~*Name*~~	~~*Unit*~~	~~*Quantity symbol*~~	~~*available in...*~~	
				~~*Year 1*~~	~~*Year 2*~~
~~**Biomet**~~	~~Global radiation~~	~~$W\ m^{-2}$~~	~~R_g~~	~~x~~	~~x~~
	~~Air temperature~~	~~°C~~	~~T_{air}~~	~~x~~	~~x~~
	~~Outgoing longwave radiation~~	~~$W\ m^{-2}$~~	~~Lw_{out}~~	~~x~~	~~x~~
	~~Photosynthetically active radiation~~	~~$\mu mol\ m^{-2}\ s^{-1}$~~	~~PAR~~	~~x~~	~~x~~
	~~Air pressure~~	~~kPa~~	~~p_{air}~~	~~x~~	~~x~~
	~~Rate of change in air pressure~~	~~kPa/1800 s~~	~~$slope_{Pair}$~~	~~x~~	~~x~~
	~~Water vapour pressure deficit~~	~~Pa~~	~~VPD~~	~~x~~	~~x~~
	~~Soil redox potential in 2 cm depth~~	~~mV~~	~~$Redox_2$~~	~~-~~	~~x~~
	~~Soil redox potential in 5 cm depth~~	~~mV~~	~~$Redox_5$~~	~~-~~	~~x~~
	~~Soil redox potential in 10 cm depth~~	~~mV~~	~~$Redox_{10}$~~	~~-~~	~~x~~
	~~Soil redox potential in 20 cm depth~~	~~mV~~	~~$Redox_{20}$~~	~~-~~	~~x~~
	~~Soil temperature in 2 cm depth~~	~~°C~~	~~T_{Soil2}~~	~~-~~	~~x~~
	~~Soil temperature in 5 cm depth~~	~~°C~~	~~T_{Soil5}~~	~~-~~	~~x~~
	~~Soil temperature in 10 cm depth~~	~~°C~~	~~T_{Soil10}~~	~~-~~	~~x~~
	~~Soil temperature in 20 cm depth~~	~~°C~~	~~T_{Soil20}~~	~~-~~	~~x~~
	~~Soil temperature in 40 cm depth~~	~~°C~~	~~T_{Soil40}~~	~~-~~	~~x~~
	~~Water table below surface~~	~~cm~~	~~WT~~	~~-~~	~~x~~
~~**Fuzzy**~~	~~Morning~~	~~n.a.~~	~~$fuzzy_{mo}$~~	~~x~~	~~x~~
	~~Afternoon~~	~~n.a.~~	~~$fuzzy_{af}$~~	~~x~~	~~x~~
	~~Evening~~	~~n.a.~~	~~$fuzzy_{ev}$~~	~~x~~	~~x~~
	~~Night~~	~~n.a.~~	~~$fuzzy_{ni}$~~	~~x~~	~~x~~
	~~Summer~~	~~n.a.~~	~~$fuzzy_{su}$~~	~~x~~	~~x~~
	~~Winter~~	~~n.a.~~	~~$fuzzy_{wi}$~~	~~x~~	~~x~~
~~**Footprint**~~	~~Class contribution of rewetted area~~	~~n.a.~~	~~CC_{rew}~~	~~x~~	~~x~~
	~~Class contribution of drained area~~	~~n.a.~~	~~CC_{dra}~~	~~x~~	~~x~~
	~~Class contribution of vegetated area within rewetted part~~	~~n.a.~~	~~$CC_{veg,\ rew}$~~	~~x~~	~~x~~
	~~Class contribution of vegetated area within drained part~~	~~n.a.~~	~~$CC_{veg,\ dra}$~~	~~x~~	~~x~~

time series of the four model parameters for the drained and rewetted areas for two years. The included scaling of the model terms with the surface class contributions facilitates comparability of the parameter time series among each other and with literature values describing the light response of similar plant communities as found in the vegetated strips of Himmelmoor.

3 Results and discussion

3.1 Model input selection and flux–driver relations

~~Results~~ Detailed results of our model input selection scheme ~~(see Appendix A)~~ are given in ~~Appendix B~~the supplements to this article. A summarized description ~~of its outcome~~ follows here. Three categories of potential model inputs were presented to the selection scheme: Thirty minute time series of meteorological and soil (Biomet) variables, fuzzy variables representing diurnal and seasonal cycles (following Papale and Valentini, 2003) and footprint variables in the form of surface class contribution estimates. Table A1 gives an overview of the available variables. Note that in Year 1 no soil properties were recorded.

In case of CO_2 flux modeling, all input matrices contain measures for the main driver of photosynthesis which is radiation. PAR and R_g were selected for both land use types in Year 1 and the time-lagged version of PAR for both land use types in Year 2. More emphasis on the impact of plant activity on CO_2 fluxes is put by the inclusion of the footprint contribution of the vegetated strips for both years and land use types. A response of CO_2 release to respiration is indicated by the selection of peat temperatures, redox potentials and water table height in Year 2 and Lw_{out} in Year 1. T_{air} was selected for all land use types and years and includes both seasonal and diurnal frequency content like the slowly and fast changing fuzzy variables which belong to all final input spaces as well.

In case of CH_4 flux modeling, the selection scheme focused on the footprint contribution of the vegetated strips, VPD and peat temperatures in both years and for both land use types. In Year 1, soil temperatures were indirectly addressed by the inclusion of Lw_{out} (being a measure of surface temperature) and $fuzzy_{su}$ which is correlated strongly to T_{Soil40} (Pearson's correlation coefficient r = 0.9). Diurnal and seasonal cycles were weighted highly by the inclusion of higher frequency fuzzy variables, VPD and T_{air} in both years. In Year 1, p_{air} was included for the rewetted section, stressing the higher likelihood of ebullition events taking place at these inundated areas, which could be facilitated by air pressure variations. The selection of redox potential and water table height time series in Year 2 gives further confidence that our scheme is able to identify physically meaningful driving variables as soil redox conditions are known to be a major limiting factor for methane production in soils.

~~In case of CO_2 flux modeling, all input matrices contain measures for the main driver of photosynthesis which is radiation. PAR and R_g were selected for both land use types in Year 1 and the time-lagged version of PAR for both land use types in Year 2. More emphasis on the impact of plant activity on CO_2 fluxes is put by the inclusion of the footprint contribution of the vegetated strips for both years and land use types. A response of CO_2 release to respiration isindicated by the selection of peat temperatures, redox potentials and water table height in Year 2 and Lw_{out} in Year 1. T_{air} was selected for all land use types and years and includes both seasonal and diurnal frequency content like the slowly and fast changing fuzzy variables which belong to all final input spaces as well~~To further investigate the relation between CH_4 flux and likely drivers as identified by our model input selection scheme, we fitted an exponential model of water table and soil temperature (in 40 cm depth) to the CH_4 fluxes

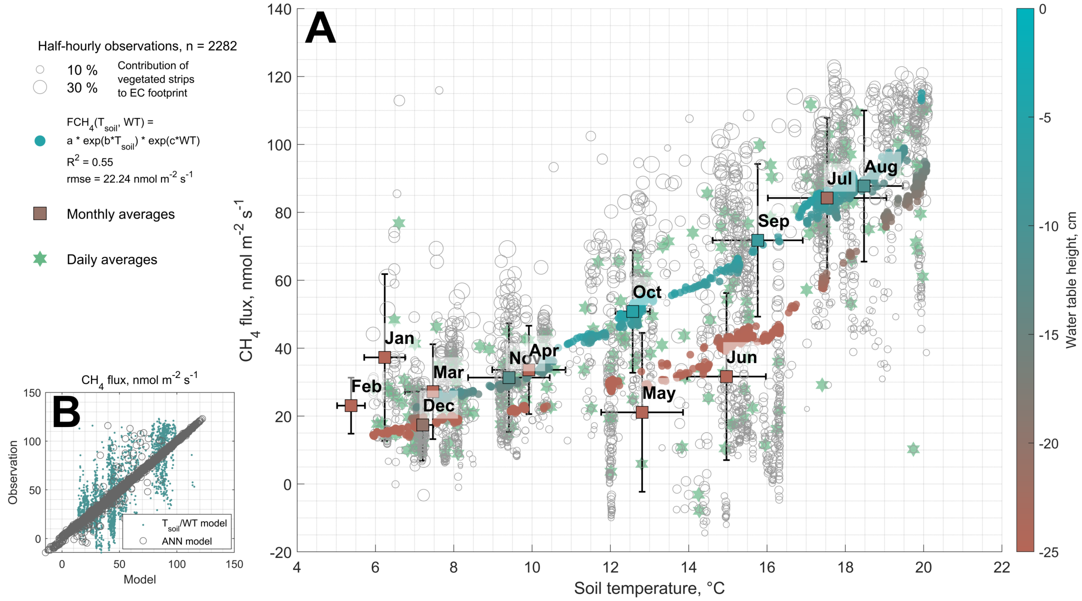

Figure 4. Panel A: Observed half-hourly methane fluxes (F_{CH4}) from the rewetted section of Himmelmoor modeled as an exponential function $F_{CH4}(T_{soil},WT)$ of soil temperature in 40 cm depth (T_{soil}) and water table (WT). Monthly and daily flux and temperature averages are also given. Panel B: Comparison of a more complex artificial neural network (ANN) model with the exponential model from Panel A. Although methane flux variability can be explained by the exponential model to a reasonable degree, the level of complexity in flux—driver relations appears to be represented considerably better by the ANN.

from the rewetted section (see Figure 4). With the exponential dependence of F_{CH4} on soil temperature, a fair amount (R^2 = 0.55) of the flux variability can be explained while the added water table term allows for the optimized temperature-F_{CH4} curve to take two distinct paths above and below an approximate water table threshold of 20 cm below the surface (see Figure 4 panel A). Half-hourly flux variability is, however, substantial due to the heterogeneity of the site's surface and other confounding factors like the above-mentioned air pressure variations and is comparably better explained by our neural network models (see Figure 4 panel B).

3.2 Model performance

In order to (I) evaluate the general feasibility of our flux decomposition and modeling method and to (II) compare the performance of MLP and MLR models, we used four approaches. We first compared statistics of MLP and MLR surface class-specific flux models with observed data, which we separated beforehand using an EC footprint model into fluxes relating to either one of the two main surface classes SC_{dra} and SC_{rew}. Results are shown in Figures B1 and B2 in the appendix. In all eight cases (two years, two gases, two surface classes), MLPs outperform MLR models with respect to coefficients of determination (R^2), Akaike information criterion (AIC) values and root mean squared errors (RMSEs). While MLRs often perform well, there is a tendency for them to overestimate highest and underestimate lowest fluxes in case of CH_4 flux modeling leading to S-shaped point clouds around the 1:1 line in the scatter plots given in Figure B1. In case of CO_2 models, this tendency of MLRs appears to be less pronounced, whereas there is one case (Year 1, SC_{dra}; see Figure B1) where the MLR model explains only 32 % of the measurement data's variability and is therefore evaluated as inept for gap-filling of at least this data set. As a way to evaluate the generalization capability of both model types independently from data used for model optimization, we secondly drove the models which were optimized using Year 1 observations with Year 2 environmental data and compared the results to Year 2 measurements (see Figure B3). Results highlight the applicability of both model types for gas flux time series extrapolation while MLPs again perform superior compared to MLRs in all cases. As expressed in the lower AIC values throughout, the higher model complexity of the MLPs appears to be justified, and the better goodness of fit measures do not seem to be the result of a too tight approximation of the training data. We attribute this result partly to our efforts to reduce the number of hidden layer nodes and the number of independent input variables (i.e. dimensionality reduction of the model input matrices). As a third way to compare model performance as well as to evaluate our method of decomposing gas flux time series obtained with a single EC tower over heterogeneous terrain into surface class-specific time series, we recombined these SCTS by scaling them with their respective contribution to the EC footprint. We calculated the sum of both scaled half-hourly SCTS and compared them to the TVTS measured over heterogeneous terrain at the EC tower. These fluxes include values with mixed surface class contributions also below the threshold of 70 %, which was used to extract target data for SCTS model optimization. Results are shown in Figure B4 ~~in the appendix~~ and again illustrate the better performance of MLPs compared to MLRs. More importantly, the outcome of this circular rescaling experiment demonstrates that after multiple model layers the original measurement data relating to a heterogeneous surface could still be recovered to a reasonable degree.

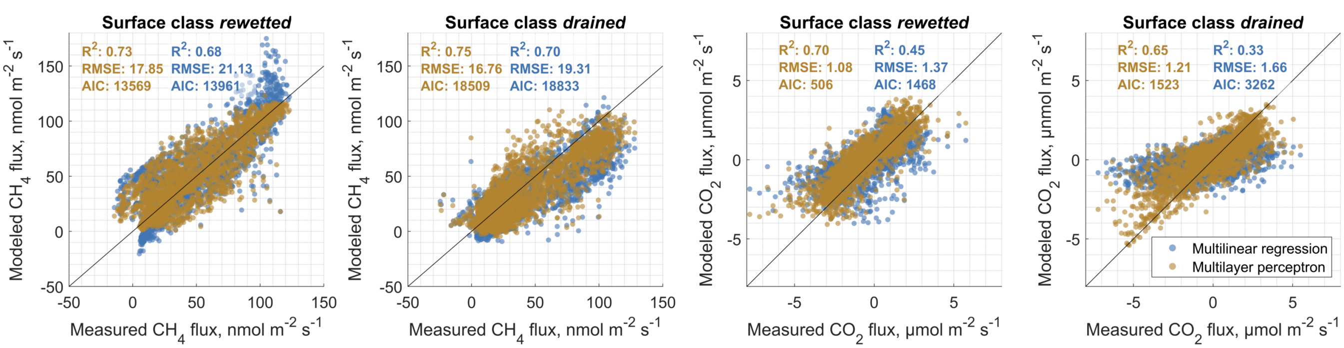

Figure 5. Comparative validation of surface class-specific multilinear regression and artificial neural network (in particular multilayer perceptron) carbon dioxide (CO_2) and methane (CH_4) flux models. For this depiction, we drove models that were optimized using Year 1 measurement data as targets with Year 2 environmental data and compared the results to measured Year 2 gas fluxes. This type of comparison enables an evaluation of the developed models with observed data which is completely independent from model optimization. Therefore, good agreement cannot be attributed to models which are overfit to the provided target data. The results of this investigation substantiate the notion that multilayer perceptrons provide more reliable estimates of gas fluxes as they are superior to multilinear models with respect to the coefficient of determination (R^2), the Akaike information criterion (AIC) and the root mean squared error (RMSE) in all cases.

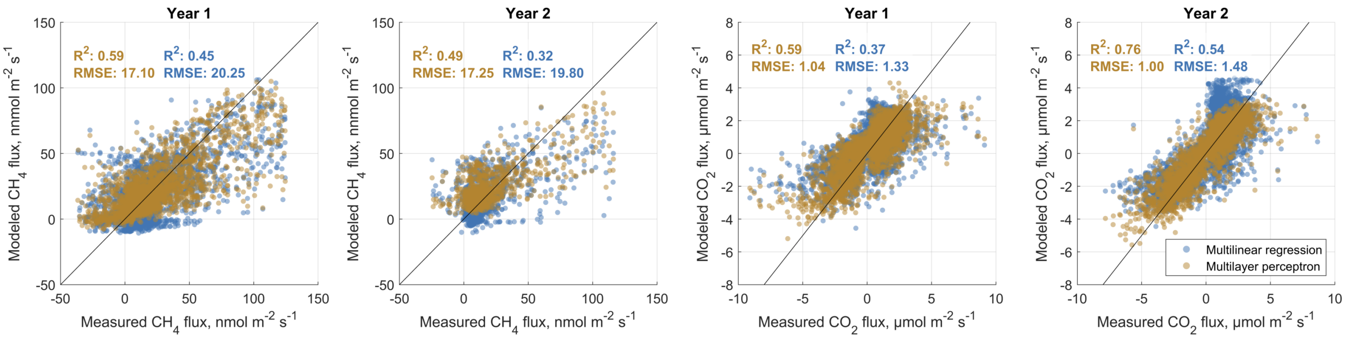

Figure 6. Comparative validation of multilinear regression and artificial neural network (in particular multilayer perceptron) carbon dioxide (CO_2) and methane (CH_4) flux models. For this analysis, both surface class-specific flux models were combined using the footprint contribution of the respective classes yielding an estimate of the landscape-integrated signal recorded at the eddy covariance tower. These derived 'tower view' gas flux time series are compared to the actually observed data at the eddy covariance tower. In all cases, the multilayer perceptron models' performances surpass the attainment of multilinear regression models with respect to the coefficient of determination (R^2) and the root mean squared error (RMSE). Results also highlight the general feasibility of our approach to decompose an eddy covariance (EC) time series recorded over heterogeneous terrain into contributions of differently functioning landscape units within the EC footprint area.

As a fourth method to evaluate the applicability of our land use-specific flux decomposition, we fitted a combined respiration-photosynthesis model (see Eq. 1) to monthly ensembles of the half-hourly CO_2 SCTS in order to check if the resultant parameters are reasonable in relation to each other and to literature data. In general, the vegetation period, with its productivity maximum between June and July and its cessation between mid-October and November is well depicted in the seasonal course of the model parameters throughout both years. The parameter courses relating to the vegetated strips of the drained and rewetted areas (Figure 7, panels B – D) develop fairly similar. Distinctions between the drained and rewetted areas are more pronounced with respect to CO_2 release from bare peat surfaces (Figure 7, panel A). Ditch-blocking of a rewetted sector close to the EC tower (which therefore made up a large part of the EC footprint) was only performed one year before our measurements started. In summer of 2012 this area therefore was not yet permanently flooded leading to TER_{bare} fluxes exceeding those from the active mining site. From winter 2012/2013 on, inundation of the rewetted bare peat area progressively increased, resulting in lower TER_{bare} fluxes from the rewetted compared to the drained section.

Our TER_{bare} fluxes are in concordance with findings from two studies that were also conducted on the active peat extraction area in Himmelmoor with manual chambers.~~ Vanselow-Algan et al. (2015) report mean annual CO_2 emissions from the active mining site of 0.53 ± 0.05 mol m^{-2} s^{-1} with summertime maxima between around 2 and 4 mol m^{-2} s^{-1}. Vybornova et al. (2019) determined similar mean mid-day fluxes using opaque chambers. For the drained bare peat areas of the extraction site, the latter authors report average fluxes between 0 and 1 mol m^{-2} s^{-1} throughout the year and a maximum of 3 mol m^{-2} s^{-1} at a single replicate plot in late August. Vybornova et al. (2019) furthermore measured CO_2 release from a rewetted and shallowly inundated bare peat area with opaque floating chambers. The reported mid-day fluxes are generally lower (between 0 and~~

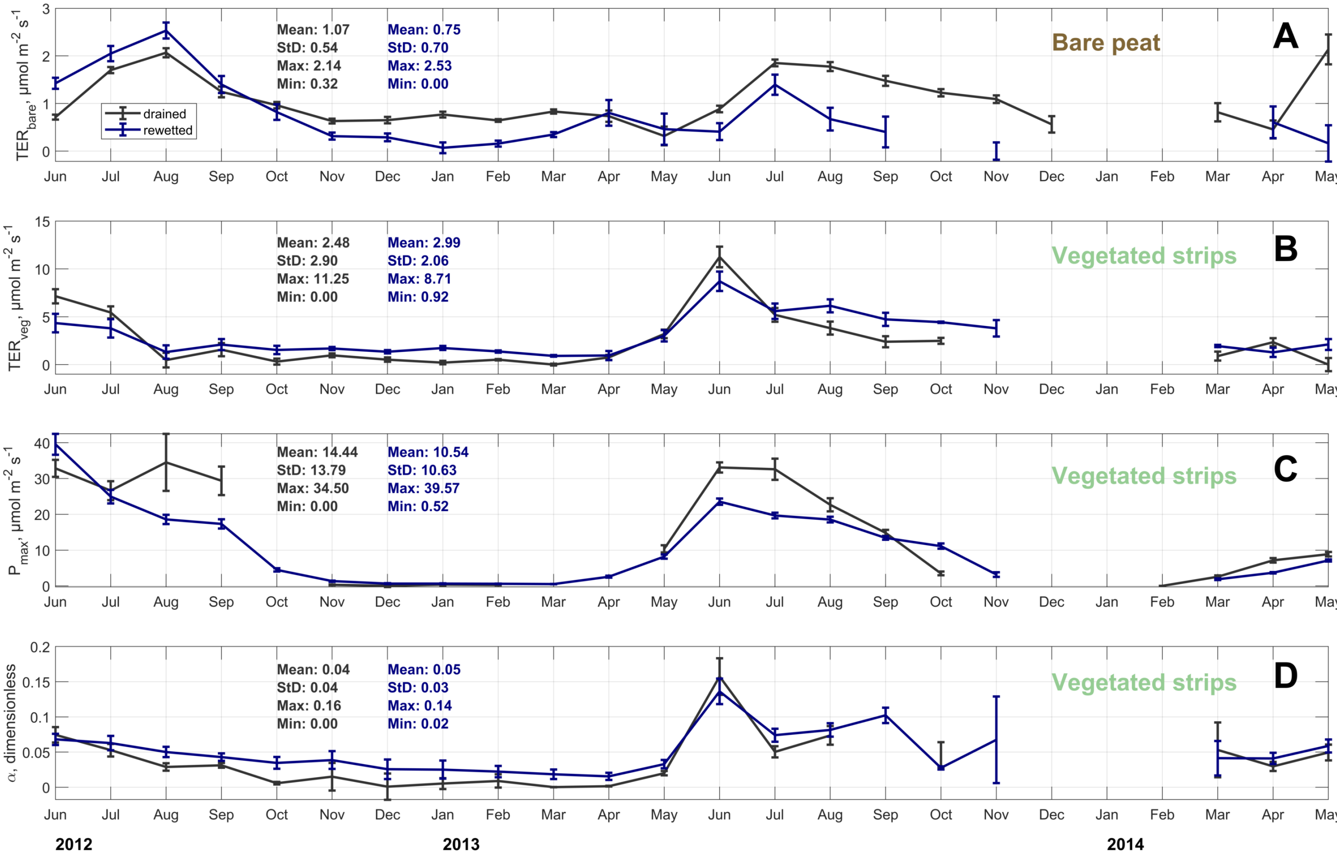

Figure 7. Time series of monthly carbon dioxide flux model parameters (ses Eq. 1). Total ecosystem respiration (TER) series are given for the bare (A) and vegetated (B) sections of Himmelmoor. Photosynthesis parameters maximum photosynthesis P_{max} (C) and initial quantum yield α (D) were only determined for areas with vegetation. All parameter time series are given for the rewetted and drained sections of Himmelmoor.

~~0.5 mol m^{-2} s^{-1}, summer maximum 1.4 mol m^{-2} s^{-1}) than from the drained extraction site confirming our results. The values of the two mentioned manual chamber flux studies from Himmelmoor are well within range of the seasonal course of TER$_{bare}$ as it displays for the bare peat areas of SC$_{dra}$ (1.1 ± 0.5 mol m^{-2} s^{-1}) and SC$_{rew}$ (0.8 ± 0.7 mol m^{-2} s^{-1}) alike (see Figure 7, panel A). TER~~ ; TER data reported from similar peat extraction sites also agree with our results ~~. Waddington et al. (2002) determined TER fluxes from a bog in Qu´ebec (48 N), Canada, which had been cutover two and three years before dark chamber gas flux measurements. May to August TER averages ranged from 0.8 mol m^{-2} s^{-1} in a relatively wet to 3 mol m^{-2} s^{-1} in a comparably dry observed year. Shurpali et al. (2008) measured TER at an active peat mining site in eastern Finland (62 N) and determined vegetation period maximum fluxes of 1.3 mol m^{-2} s^{-1} at the end of August and minima in mid-November of 0.2 mol m^{-2} s^{-1}~~(see Table C2).

~~Our combined respiration photosynthesis model (see Eq. 1)~~ As our model includes the relative contributions of the vegetated strips to the EC footprint~~. Using this method enabled us to compare~~ , we compared the extracted model parameter time series (see Figure 7, panels B ~~to D) , which can be directly related to plant characteristics,~~ – D) with estimates of these plant species-specific values ~~which have been determined in other studies for~~ from other studies investigating similar plants and plant communities as found in the vegetated strips in Himmelmoor. Reported averages and ranges agree well with our findings (see Table C1). Additionally, we could distinguish between CO_2 release from decomposing bare peat (TER_{bare}, see Figure 7, panel A and Table C2) and from the vegetated strips (TER_{veg}, see Figure 7, panel B and Table C1) where respiratory CO_2 release also includes autotrophic respiration of plants. In our data set, TER is between twofold and fourfold larger in areas with ~~(Figure 7, panel B) than without (Figure 7, panel A)~~ than without vegetation. TER_{veg} from the rewetted area is mostly larger than from the drained area. Progressive inundation led to a hydrological connection of SC_{veg} and the flooded bare peat areas. An increased input of dead plant material as a result of higher water tables might have promoted heterotrophic respiration. Hampered plant productivity due to flooding is also expressed in lower peak values of P_{max} at the vegetated strips of the rewetted site.

~~Below, we compare our TER_{veg} time series, with literature data from similar plant communities. Using data from chamber measurements, Vanselow-Algan et al. (2015) partitioned NEE from different vegetation communities at the outer edge of Himmelmoor. These areas were restored three decades ago after being degraded by small-scale manual peat-cutting. Although the plants dominating the vegetated strips of the mining site were not examined by Vanselow-Algan et al. (2015), some of the species investigated by the authors also frequently occur in SC_{veg} being the subject of the present study. The 'purple moor grass' microform in Vanselow-Algan et al. (2015) for example is dominated by *Molinia caerulea*; *Betula pubescens* and *Eriophorum angustifolium* also occur. In summer, TER fluxes form this site were estimated to range above 10 mol m^{-2} s^{-1} being in the same range like our summer TER peaks from the vegetated strips. Beyer and Höper (2015) report results from a former north German peat extraction site that was rewetted 30 years prior to their chamber measurement campaign. TER estimates from these authors are available for a site dominated by *Molinia caerulea* (up to 7 mol m^{-2} s^{-1} in August) and by *Eriophorum angustifolium* (up to 5 mol m^{-2} s^{-1} in late July). A substantial portion of the SC_{veg} is covered by *Betula pubescens*, *Salix spp.*, *Eriophorum vaginatum*, *Eriophorum angustifolium*, *Typha latifolia*, *Molinia caerulea*, *Carex spp.*, *Juncus effusus* and *Calamagrostis canescens*. Further combined plant and soil respiration measurements of the species found in SC_{veg} are not present in literature. Nevertheless, properties of plants from the same genera are known. Most reported fluxes, however, describe autotrophic respiration as they were determined on leaf scale and therefore refer to leaf area. Since shrubs and trees can have a leaf area index larger than 1, fluxes refreed to ground surface area could be higher. Measurements of *Betula spp.* dark respiration are given by Patankar et al. (2013) and Gu et al. (2008) (between 1 and 5 mol m^{-2} s^{-1}). Patankar et al. (2013) also assessed autotrophic respiration of *Salix pulchra* (up to 2 mol m^{-2} s^{-1}), *Eriophorum vaginatum* (up to 3 mol m^{-2} s^{-1}), and *Carex bigelowi* (up to 1 mol m^{-2} s^{-1}). Other *Carex* species are in the same range as shown by Körner (1982) (*Carex curvula* 1 mol m^{-2} s^{-1}) and Murchie and Horton (1997) (*Carex flacca* 1.5 mol m^{-2} s^{-1}). *Salix* summer dark respiration has as well been investigated by Kaipiainen (2009) with *Salix dasyclados* (between 0.8 and 1.2 mol m^{-2} s^{-1}).~~

~~Regarding the photosynthesis parameters P_{max} and α in the second model term of Eq. 1, more literature values are available for comparison . Chamber gas exchange studies of a single birch (*Betula pubescens*) in Himmelmoor during three summer months in 2014 by Lienau (2014) resulted in P_{max} values between 32 and 41 mol m^{-2} s^{-1}. More P_{max} estimates from the same tree species have been reported by Nygren and Kellomäki (1983) (4 to 17 mol m^{-2} s^{-1}) and Hoogesteger and Karlsson (1992) . In the latter study, PAR was limited to 800 mol m^{-2} s^{-1}, P_{max} was assessed to be 8 mol m^{-2} s^{-1}. Other evaluations of *Betula spp.* maximum photosynthesis range between 10 and 15 mol m^{-2} s^{-1} (Patankar et al., 2013; Gu et al., 2008). With P_{max} values commonly around 25 but also above 30 mol m^{-2} s^{-1} (Chen et al., 2010), *Typha latifolia* is photosynthically more active which is also the case for *Salix spp.* ranging between 16 and 29 mol m^{-2} s^{-1} (Ögren, 1993). Lab-experiments from Vernay et al. (2016) provide P_{max} estimates of *Molinia caerulea* (7 to 15 mol m^{-2} s^{-1}). For *Juncus effusus* only net photosynthesis values of 6 to 11 mol m^{-2} s^{-1} (Mann and Wetzel, 1999) have been reported so far. From the North German site investigated by Beyer and Höper (2015) , comparably high P_{max} estimates are reported for *Molinia caerulea* that commonly range between 15 and 30 mol m^{-2} s^{-1} but also reach values up to 60 mol m^{-2} s^{-1} in June. The P_{max} parameters given by these authors for *Eriopohorum angustifolium* are also rather large (up to 70, often around 20 mol m^{-2} s^{-1}). Inititial quantum yield estimates of plants also common in in the vegetated strips in Himmelmoor range between 0.02 and 0.08 (Vernay et al., 2016; Nygren and Kellomäki, 1983; Murchie and Horton, 1997; Kaipiai .~~

In comparison to small-scale measurements from the same and similar sites, we could confirm the credibility of our mechanistic modeling approach for which we used relative class contributions of contrasting surface types to scale single model terms. Moreover, the previously performed division of the TVTS into SCTS apparently yields reasonable flux estimates that can be interpreted in a mechanistic way, increasing our confidence in the applied flux decomposition method.

3.3 Annual greenhouse gas balances

We used the eight (two gases, two land use types, two years) surface-class specific flux time series, which we gap-filled with MLP ensembles, to calculate annual CO_2 and CH_4 balances for the rewetted and drained sections of Himmelmoor.

The results are expressed as molar and mass fluxes (Figure 8) and as release of CO_2 equivalents (CO_2e, see Table 2). We used a factor of 34 to convert F_{CH4} into CO_2e release. This value is given in the Fifth Assessment Report of the Intergovernmental Panel on Climate Change (IPPC AR5, Myhre et al., 2013), refers to a 100-year time horizon and includes climate–carbon feedbacks. The impact of rewetting on the development of vertical carbon release is documented with the shown results. Overall, both the rewetted and the mined sections of Himmelmoor were considerable sources of GHGs in both years. Annual F_{CO2} from the restored site undercuts the cumulative CO_2 emissions from the drained part of Himmelmoor in both years while this difference increases with time. Annual CH_4 release from the wetter surfaces exceeds the cumulative F_{CH4} from the drained mining site in both years while both fluxes rise from Year 1 to Year 2.

In Year 1, F_{CO2} from the rewetted area was already cumulatively lower than from the mining site (20 ± 7 vs. 22 ± 6 mol m^{-2} a^{-1}) while the margins of uncertainty largely overlap. In Year 2, the annual CO_2 balance from the rewetted site dropped by 35 % increasing the difference to the cumulative mining site flux, which did not change from Year 1 to Year 2, to over 40 % (13 ± 6 vs. 22 ± 7 mol m^{-2} a^{-1}). Margins of uncertainty still overlap in Year 2 but less widely. At the end and the beginning of Year 2

Table 2. Annual sums of half-hourly carbon dioxide (CO_2) and methane (CH_4) fluxes from the drained and rewetted sections of the peat extraction site in Himmelmoor. CH_4 fluxes are expressed as CO_2 equivalents (CO_2e) using a global warming potential of 34 referring to a 100-year time horizon following Myhre et al. (2013). Year 1: 01 June 2012 to 31 May 2013; Year 2: 01 June 2013 to 31 May 2014

		Cumulative flux, g m^{-2} a^{-1}	
		Surface class *drained*	Surface class *rewetted*
CO_2	Year 1	988 ± 247	887 ± 296
	Year 2	974 ± 292	567 ± 263
CH_4	Year 1	7.2 ± 1.8	13.3 ± 1.9
	Year 2	12.1 ± 1.4	18.3 ± 1.5
CH_4-CO_2e	Year 1	244 ± 61	453 ± 63
	Year 2	412 ± 46	621 ± 51
total CO_2e	Year 1	1232 ± 308	1340 ± 359
	Year 2	1386 ± 338	1188 ± 314
CO_2-C	Year 1	269 ± 67	242 ± 81
	Year 2	266 ± 80	155 ± 72
CH_4-C	Year 1	5.4 ± 1.4	10.0 ± 1.4
	Year 2	9.1 ± 1.1	13.7 ± 1.1

(i.e. in summer), the cumulative F_{CO2} curve from SC_{rew} ceases to slope upwards. By reaching these vertexes, the points in time when the rewetted area briefly turns from a CO_2 source into a sink are indicated. Nevertheless, ~~on an annual basis the periods when the sink character of~~ annually integrated ecosystem respiration outweighs photosynthesis in SC_{rew} ~~prevails do not compensate for CO_2 release during periods of reduced plant activity~~.

CH_4 fluxes from both surface classes rise from Year 1 to Year 2 while the absolute differences between both land use types stays rather constant. The cumulative CH_4 flux from SC_{rew} is nearly 90 % higher than from SC_{dra} in Year 1 (0.45 ± 0.11 vs. 0.83 ± 0.12 mol m^{-2}) and 50 % higher in Year 2 (0.76 ± 0.08 vs. 1.14 ± 0.09 mol m^{-2}). Compared to the molar F_{CO2} sums of both surface classes, cumulative molar CH_4 release is a factor of around 30 smaller in Year 1 and about 20 times smaller in Year 2. The development of both molar GHG emissions over time documents the rising importance of CH_4 emissions in the course of rewetting. Transforming the molar cumulative sums into sums of CO_2e allows for comparability between the two GHG fluxes with respect to their climate impact. Overall, the rewetted section of Himmelmoor is a larger CO_2e source in the first observed Year, while the drained section emits more CO_2e in Year 2. CO_2e fluxes at the drained site increase from Year 1 to Year 2, whereas they decline from Year 1 to Year 2 at the rewetted site. The sum of cumulative F_{CO2} and F_{CH4} released from SC_{dra} are dominated by F_{CO2} in both years. For SC_{rew}, CH_4-CO_2e emission sums are much smaller than the release of CO_2 in Year 1, whereas CH_4-CO_2e fluxes dominate the GWP balance in the second observed year. Although the cumulative CH_4-CO_2e fluxes also increases from Year 1 to Year 2, they mainly dominate the SC_{rew} GWP sum due to a large drop in F_{CO2} from Year 1 to Year 2.

The annual CO_2 emissions from the drained parts of 988 ± 247 g m^{-2} a^{-1} and 974 ± 292 g m^{-2} a^{-1} are higher but in the same range as previously inferred from chamber data acquired at the mining site in Himmelmoor by Vanselow-Algan et al. (2015) (730 ± 67 g m^{-2} a^{-1}) and Vybornova et al. (2019) (740 ± 270 g m^{-2} a^{-1}). Moreover, our results are in line with the emission factors given in the Wetlands Supplement to the 2006 IPCC Guidlines for National Greenhouse Gas Inventories (Hiraishi et al., 2014) for which Wilson et al. (2016a) published an update. Both publications give an average CO_2 release of 1027 g m^{-2} a^{-1} for boreal and temperate peatlands drained for peat extraction. While boreal extraction sites generally appear to emit less CO_2 as reported in a meta-study by Maljanen et al. (2010) (697 ± 263 g m^{-2} a^{-1}), Drösler et al. (2008) who analyzed 11 drained peat extraction sites in Europe also report CO_2 release of up to 1300 g m^{-2}a^{-1}. Interesting to note is that in the National Inventory Report Germany submitted under the United Nations Framework Convention on Climate Change in April of 2019, CO_2 release from drained peat extraction areas are accounted for with a comparably small factor of 587 g m^{-2} a^{-1}. Taking into account, the amount of carbon removed from Himmelmoor by peat extraction (11000 ± 1000 g m^{-2} a^{-1}), CO_2 emissions account for less than one tenth of the total carbon loss per year. This value from Vanselow-Algan et al. (2015) is, however, expressed as CO_2 and assumes the instant decomposition of the material after removal. Restored cutover bogs commonly are CO_2 sinks when active peat extraction has been ceased for several decades (Tuittila et al., 1999; Wilson et al., 2016b; Beyer and Höper, 2015). However, shortly after ditch-blocking, the rewetted section of Himmelmoor still was a considerable CO_2 source (887 ± 296 g m^{-2} a^{-1} and 567 ± 263 g m^{-2} a^{-1}). During regular visits to the area between 2011 and 2019, we observed that the amplitude of seasonal water table oscillations in a rewetted, formerly mined strip (polder) would decrease with the time passed after ditch-blocking. We assume that anoxic conditions did not prevail throughout the year in all polders as already discussed above with respect to TER_{bare} fluxes from these sites. Additionally, ditch-blocking in Himmelmoor went along with the construction of dams encompassing the newly rewetted polders. Vybornova et al. (2019) showed that shortly after raising these dams they can be large sources of CO_2 with fluxes up to four times larger than from bare peat areas which are drained for ongoing mining.

The CH_4 flux sums of 13.3 ± 1.8 g m^{-2} a^{-1} and 18.3 ± 1.5 g m^{-2} a^{-1} from the rewetted sections of Himmelmoor are confirmed by findings from Beyer and Höper (2015) who report CH_4 balances between 16.2 ± 2.2 g m^{-2} a^{-1} and 24.2 ± 5.0 g m^{-2} a^{-1} from inundated cutover bogs in northern Germany. Wilson et al. (2016b) report annual CH_4 emission sums of 12.0 ± 2.6 g m^{-2} a^{-1} from an Irish Atlantic blanket bog that had been rewetted 14 years prior to the investigation. Results from a boreal peat extraction site, 20 years after mining had been ceased, are given by Tuittila et al. (2000). Although only the growing season has been covered by these authors, the cumulative seasonal F_{CH4} of 1.27 g m^{-2} a^{-1} suggests that CH_4 release from boreal peatlands is much lower compared to temperate sites. This circumstance has also been noted by Tiemeyer et al. (2016), who furthermore conclude that IPCC estimates for CH_4 release from rewetted bogs, as they are primarily based on data from boreal peatlands, are not representative for temperate regions. In the above mentioned meta-study of Wilson et al. (2016a), temperate and boreal rewetted peat extraction sites are reported with average emissions of 12.3 g m^{-2} a^{-1}. Annual CH_4 release from the drained sections of Himmelmoor (7.2 ± 1.8 g m^{-2} a^{-1} and 12.1 ± 1.3 g m^{-2} a^{-1}) are lower than from the rewetted parts but high compared to IPCC emission factors. Wilson et al. (2016a) give an average release of 3.3 g m^{-2} a^{-1} for drained peat mining sites including a 5 % surface cover of ditches to which the authors assign high CH_4 fluxes, as given in Hiraishi et al. (2014) with 10

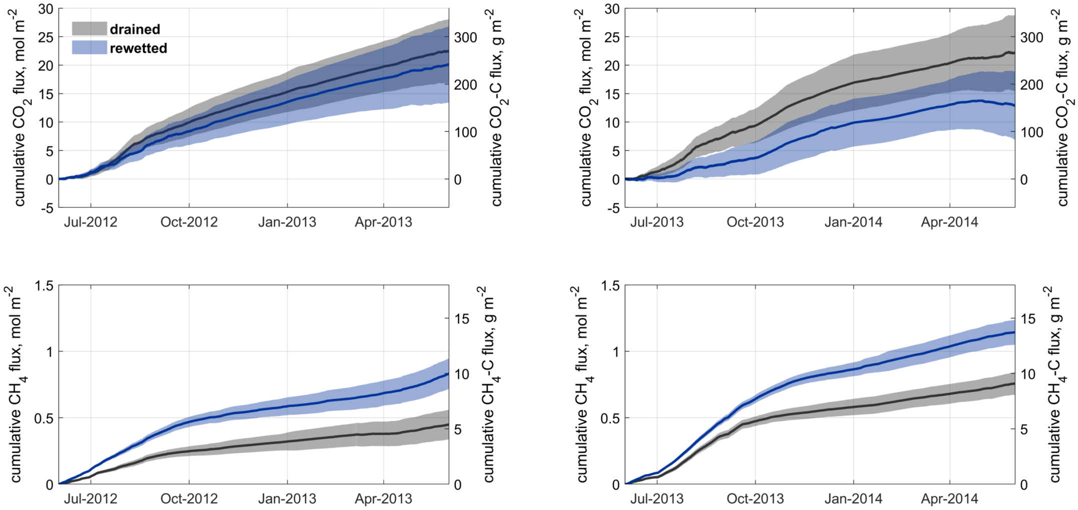

Figure 8. Cumulative carbon dioxide (CO_2) and methane CH_4 fluxes from the drained and rewetted sections of the peat extraction sites in Himmelmoor for both investigated years. Shaded areas represent model uncertainty estimates derived from the standard deviation of artificial neural net ensembles as well as measurement uncertainty estimates. Values are depicted as molar and carbon (C) fluxes.

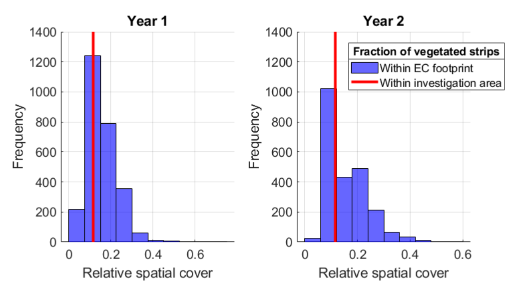

Figure 9. Frequency distribution of relative half-hourly contributions of vegetated strips to EC footprint area in both investigated years (Year 1: 01 June 2012 to 31 May 2013; Year 2: 01 June 2013 to 31 May 2014). For comparison, the vegetated strips' areal fraction within the investigation area is shown, documenting that the measurement system was set up at an adequate position in the landscape in order to represent its spatial proportion of surface classes.

to 98 g m^{-2} a^{-1}. The vegetated strips in Himmelmoor cover around 10 % of the surface ~~and appear to be~~ (see Figure 9) and are especially strong sources of CH_4 what we attribute to the high density of vascular, aerenchymatic plants in combination with a supply of nutrient-rich, minerogenic water, which is supplied to these areas from the underlying aquifer. Figure 10 illustrates the dependence of F_{CH4} on the relative contribution of the vegetated strips to the EC footprint. Mean summer fluxes were significantly (Two-sample Kolmogorov-Smirnov test, $p < 0.01$) higher from the vegetated (67 nmol m^{-2} s^{-1}) than from the bare (29 nmol m^{-2} s^{-1}) areas. These results are in line with estimates from Vybornova (2017) who determined a mean annual F_{CH4} of 50 nmol m^{-2} s^{-1} for the same vegetated strips in Himmelmoor with manual chambers. Vybornova et al. (2019) report mean

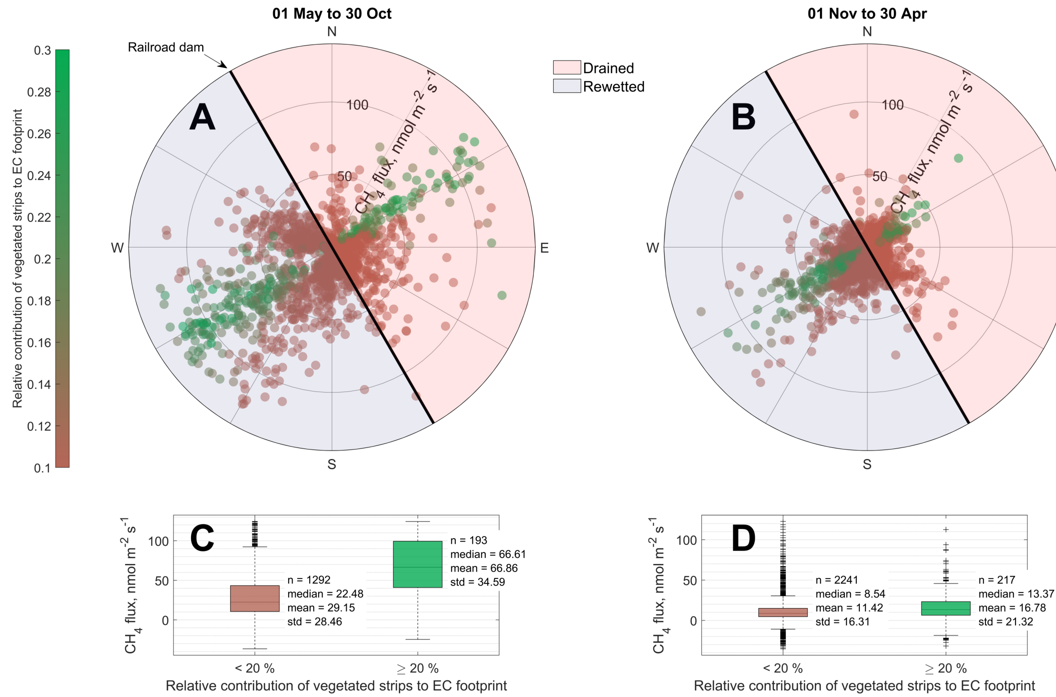

Figure 10. Dependence of methane fluxes on wind direction and eddy covariance (EC) source area composition, in particular the contribution of the vegetated strips, in summer (A) and winter (B). Data of both investigated years are shown. The EC tower was placed on a railroad dam dividing the area into an actively (East) and formerly (West) mined section, which had been rewetted prior to measurements. In general, methane emissions from the rewetted section were higher than from the drained section and fluxes when the EC footprint was composed of more than 20 % vegetated areas was significantly (Two-sample Kolmogorov-Smirnov test, $p < 0.01$) higher than from vegetation-free areas, both in summer (C) and winter (D).

annual F_{CH4} from the bare peat areas of 10 nmol m^{-2} s^{-1}. Further evidence for the decisive role the type of vegetation which is established after rewetting has on the magnitude of CH_4 release is provided by Järveoja et al. (2016). The authors report annual CH_4 budgets of 0.25 and 0.16 g m^{-2} a^{-1} at subsections of their site with relatively high and low water table respectively. The site Järveoja et al. (2016) investigated is the former peat extraction area Tässi in central Estonia (58 °N). In contrast to Himmelmoor, restoration measures at this site included the active establishment (dispersal) of peat mosses on a substantial layer (2.5 m) of remnant *Sphagnum spp.* peat. By the time measurements commenced two years after first restoration efforts were made, Tässi was already dominated by *Sphagnum spp.* mosses. With a lack of aerenchymatic plants and systematic efforts to re-establish bog vegetation, annual CH_4 release at Tässi is up to 100 times smaller than at Himmelmoor.

3.4 Implications of rewetting measures for the re-establishment of a mire ecosystem in Himmelmoor

In general, the initialization of peat accumulation by *Sphagnum* mosses is inevitable (Joosten, 1992; Pfadenhauer and Klötzli, 1996; Gaudig for the purpose of re-establishing a degraded peatland's natural ecosystem functions. Two (somewhat untypical) features of

Himmelmoor need to be considered when evaluating the success of the implemented rewetting measures in terms of mire re-establishment and climate change mitigation: (1) The fact that large vegetation-free areas have been inundated shallowly and (2) that fen-type plants have established at the only vegetated areas which had been taken out of use in the late 1960s. We found peak CH_4 emissions from the vascular plant-dominated areas (see Figure 10) and also attribute this fact causally to the presence of fen-type vegetation. Vascular plants provide an effective transport pathway through their gas-conducting tissue as well as root exudates which form an easily decomposable substrate for soil microbes (Kerdchoechuen, 2005; Neue et al., 1996; Bhullar et al., 2014) . Because a water table above the surface instead of close to but below the surface has been established at the bare peat areas, the creation of floating vegetation mats is the only possibility for *Sphagnum* colonization (Pfadenhauer and Klötzli, 1996) . Nevertheless, fast growing vascular plants can support peat moss growth by diminishing wave movement and offering adherence area (Sliva, 1997). Besides the need for a preferably calm water surface, another limiting factor for floating mat growth is the water CO_2 concentration (Gaudig, 2002; Paffen and Roelofs, 1991; Smolders et al., 2001; Lamers, 2001; Lütt, 1992) which can be enhanced by vascular plants by providing oxygen to the rhizosphere fostering soil respiration. It thus seems conceivable that the *Sphagnum spp.* growth-favoring effects could outweigh the negative ramifications for bog development and climate change mitigation potential that the current plant cover implies. In sections of Himmelmoor with a non-industrial land use history, overgrowth of the grass tussocks, formerly dominating the area, by the bog-type *Sphagnum* species *S. magellanicum* and *S. papillosum* is in progress today (personal observation, 2016). The now prevailing plant species on the extraction site could therefore constitute an intermediate state that can potentially be overcome. The active dispersal of *Sphagnum* mosses as a management strategy would foster mire re-establishment and possibly lead to drastically diminished CH_4 release as e. g. the study from Järveoja et al. (2016) from an Estonian site where peat mosses dominate after rewetting suggests.

4 Conclusions

As a methodological challenge, we addressed the feasibility of a single EC tower for the estimation of gas flux time series from two surface classes within the EC footprint. Due to the specific setup with (1) the tower position on the border between the surface classes and (2) an adequate measurement height of the EC system, we could attribute fluxes to individual surface classes. This subdivision of EC time series was possible owing to the scale (hundreds of meters) on which surface patterning exists in Himmelmoor. Additionally, the contrast in gas flux dynamics between the different surface classes allowed for a better discriminability between EC fluxes associated to the individual surface types. In situations where flux contrasts are less pronounced and surface classes are more interlaced this method might not be applicable. To be able to estimate gas flux time series of subsections within the EC footprint, rigorous filtering of the original time series is inevitable. Consequently, a considerable amount of measurement data is omitted leading to a relatively high amount of time series gaps. To fill these gaps, we tested multilinear models and artificial neural networks (ANNs) and found that ANNs consistently performed superior. We attribute this fact partly to our data-driven model input selection gravely reducing the number of model parameters. Secondly, we programmatically reduced the number of ANN hidden layer neurons, and thereby furthermore lowered the number of model parameters. Apart from the reduction of the model input space dimensionality, our input selection method also outlined physically sound explanatory frameworks for flux–driver connections. Although it cannot ultimately be appraised if the relevant flux drivers have been captured by our routine, the selection results point to the method's ability to discriminate between weaker and stronger flux–driver relations, which do not necessarily have to be linear. We therefore conclude that when applying empirical models to gap-fill trace gas flux time series, a method for the selection of input variables that takes into account the sensitivity of gas fluxes to model input variability can improve model predictions considerably. When ANNs are used in particular, efforts should be made to set them up in the least convoluted way a sufficient approximation of the target data allows for.

With the estimates of surface class-specific GHG fluxes from two consecutive years, we could address the impact rewetting had on the GHG balance of the peat mining site. Six years after the first polders in Himmelmoor had been rewetted, the area was still a clear GHG source. The two investigated land use types (drainage and rewetting) show distinct CO_2 and CH_4 flux features. CO_2 emissions ~~decrease~~ decreased progressively after rewetting ~~.~~ with a reduction of 101 g m^{-2} a^{-1} in Year 1 and of 407 g m^{-2} a^{-1} in Year 2. The release of CH_4~~increases~~ -CO_2e increased after rewetting and ~~within the present two year data set also over time. On short timescales, the~~ was constant in both investigated years (209 g m^{-2} a^{-1}). The climate impact of elevated CH_4 emissions ~~appears to dominate~~ after rewetting therefore dominated over the effect of decreasing CO_2 release ~~.~~ in Year 1, whereas CO_2 emission reduction was nearly twice as high as the CH_4-CO_2e increase in Year 2. It is conceivable that Himmelmoor can be transformed into a carbon-accumulating peatland. However, this process will probably take decades to centuries and will take place only when sustained management of the area is employed.

Appendix A: ~~Model setup and input selection scheme~~

~~This section describes the selection of model inputs (see Table A1) using our scoring table approach. Also, the method we used to select properties for the multilayer perceptron (MLP) neural networks is outlined. The MLPs were set up with one hidden layer, tan-sigmoid activation functions, a single output layer node with a linear transfer function and Levenberg-Marquardt backpropagation as supervised learning method. See Papale and Valentini (2003), Dengel et al. (2013), Sarle (1994) for details on MLP architecture. The input data was divided randomly in 70 % training and 30 % validation data. Inputs were re-scaled before training to range between -1 and 1. Training data were used to optimize the network weights and biases for low MSE. Validation data served as inputs independent from training data to check the generalization capability of the model. The model performance in relation to the validation data was used to avoid overfitting by terminating the learning process if for six consecutive iterations the MSE of the validation data did not decrease (early stopping). Instead of using the response of a single MLP, we calculated the ensemble average of multiple networks starting with varying initial weights and different sets of training and validation data each. This method is frequently described in neural network literature (Naftaly et al., 1997; Perrone and Cooper, 1993; V as one type of so called committee machines. To avoid unnecessarily complex network architecture and thereby a higher amount of model parameters we inspected the model performance of committee machines with 100 MLPs each for different numbers of hidden layer nodes (#HLN) between 1 and 20.~~

~~We expected to find a #HLN optimum at the AIC minimum. However, for different gases and data sets, we encountered two functional forms a relation like this would commonly assume. A parabola-like curve with a clear minimum and an asymptotic function of the form~~ $AIC(\#HLN) = \#HLN^{-1} + a$. ~~We fitted parabolas to the according data sets and assumed the function vertex as #HLN optimum. In the other cases, we fitted reciprocal functions and differentiated the results. We rounded the first derivatives to the nearest multiple of 10 in case of~~ CH_4 ~~and to 100 in case of~~ CO_2 ~~flux modeling. We then defined the #HLN optimum to be at the position where the rounded derivative turns zero for the first time. We performed #HLN optimization in each case before applying MLPs for input sensitivity analysis or gap-filling~~

~~We applied a selection procedure aiming for the identification of redundant as well as irrelevant model inputs. This scheme evaluates the outcome of stepwise MLRs in combination with the analysis of the response of MLPs to differently manipulated versions of the input space. We used methods addressing predictive and causal importance as defined by Sarle (1997). In short, predictive importance measures are those that check the change of model performance when an input is omitted, whereas causal importance measures evaluate the change of a performance function when inputs are manipulated. The latter can be realized by degrading the variability of an input for example by replacing it partly with its average (as in Schmidt et al., 2008; Hunter et al., 2000) . Three categories of potential model inputs were presented to the selection scheme. Thirty minute time series of meteorological and soil (Biomet) variables, fuzzy variables representing diurnal and seasonal cycles (following Papale and Valentini, 2003) and footprint variables in the form of surface class contribution estimates. Table A1 gives an overview of the available variables. Note that in Year 1 no soil properties were recorded. We derived a second set of Biomet variables by estimating the time lag between each Biomet variable and the gas flux time series and subsequently shifting each Biomet time series by the calculated~~

~~time lag. We used the lag time within a one-day window for which the absolute cross-correlation between Biomet and gas flux time series was maximized (Kettunen et al., 1996) to shift the respective Biomet time series.~~

~~Three data sets were used for sensitivity analysis: Only the original Biomet data, only the lagged data and both. All data sets were extended by fuzzy and footprint data. We applied four methods to estimate the relevance of the individual inputs and combined them via a scoring table. If an input was selected by one method, one point was assigned to it. Inputs with more points were regarded as more important.~~

~~As previously applied by Dengel et al. (2013) for EC flux gap-filling, we used the outcome of a stepwise multilinear regression (MLR) with bidirectional elimination to identify important model inputs. Independent variables that remained in the final model received one point in our scoring table. The calculations were made using the Matlab 8.4 Statistics and Machine Learning Toolbox following Draper and Smith (1998). At each step the p-values of an F-statistic of models with or without each input were evaluated by comparing them with an enter condition $p_{enter} = 0.05$ and an exit condition $p_{remove} = 0.1$. If inputs currently not in the model had p-values below p_{enter}, the one with the lowest value was included into the model until the next step (forward selection). If inputs currently in the model had p-values above p_{remove}, the one with the highest value was removed from the model (backward elimination). These steps were repeated until the model could not be improved further by a single step. The initial model contained no inputs.~~

~~Following Schmidt et al. (2008), we calculated two similar measures of causal importance from the output of MLP ensembles. The variability of each input variable was manipulated by replacing 50 % and 100 % with its median, while all remaining variables in the input matrix were left unchanged. A MLP ensemble was first trained with the original data and then simulated with the artificial input matrix. The relation of the resultant mean squared errors (MSEs) was calculated and called relative error (RE). This process was repeated 1000 times for all input variables to obtain diverse results for different data divisions. The resulting values for RE were binned into six classes with centers at 0.8, 0.9, 1.0, 1.1, 1.2 and 1.3. If the latter was the bin with the most counts, one point was assigned to this input variable in the scoring table, meaning that the manipulation of this input vector resulted in a deterioration of the respective MSE of more than 25 % in most cases. This method yielded two measures of causal importance for each input variable, RE_{50} and RE_{100}, referring to the two percentages of data being manipulated.~~

~~We furthermore analyzed the weights resulting from MLP optimization based on the algorithm of Garson (1991) as presented in Olden and Jackson (2002). This method interprets the weights of a neural network similar to the coefficients of a linear model. Before calculating the relative importance (RI) of an input, the products of the weights that connect this input with each hidden neuron and the output layer is determined and normalized by the sum of weight products feeding also into the same hidden unit. These so called neuron contributions are summed up and normalized by the sum of all neuron contributions resulting in the RIs of all inputs. We calculated the mean, median and maximum RIs of 1000 MLP runs for all input variables. We then compiled three lists in which we sorted the inputs in descending order with respect to the determined statistics. The lengths of those lists were afterwards shortened to equal the number of variables that were included in the MLR model that was derived before – only variables with the highest RI statistics stayed in the lists. All inputs that occurred at least in two of three lists received one point in the scoring table, which was completed with this step. We then summed up the scores for all input variables and calculated two score thresholds above which an input was to be selected. One threshold was derived for~~

~~the original and the lagged Biomet variables, one for fuzzy and footprint data. We proceeded like this owing to the structure of the three input data sets. Each Biomet variable occurred in two of three data sets, each fuzzy and footprint variable was part of all data sets, making it more likely for them to reach a high score. We calculated the mean score of the respective variable category and used the next larger integer as a score threshold. The inputs that were selected via the scoring table were fed into a final stepwise MLR removing further apparently irrelevant model inputs. In the last step of the input selection algorithm we checked if both a variable and its lagged derivative remained in the input matrix. If so, the scores of those two variables were compared, and only the higher scoring variable stayed in the input matrix. In case there was no score difference, the lagged derivative was removed from the input space, whose reduction was hereby finished.~~

Appendix B: ~~Model input selection results~~

~~To gain first insight into the relations between input variables and landscape-scale gas fluxes (tower view time series, TVTS) as well as between the input variables among each other, scatter plots were inspected and Pearson's correlation coefficient (r) was determined for each pair. See Table A1 for definitions of the quantity symbols used hereafter. Three Biomet time series correlate with r values of 0.4 or higher with CH_4 flux in both years: Lw_{out}, T_{air} and R_g. In Year 1, this list is extended by VPD and PAR while the highest linear relation exists with CC_{rew} (0.5) and $CC_{veg, rew}$ (0.6). In Year 2, additional connections with r values of 0.4 or higher include soil temperatures T_{Soil20}, T_{Soil2} and T_{Soil40}. Footprint variables were not as closely related as in Year 1. Nevertheless, $CC_{veg, rew}$ yields again the highest correlation among the footprint variables. Compared to F_{CH4}, linear relations between model input variables and CO_2 flux are more clear as the only strong connections exist with PAR and R_g (both r = 0.5 in Year 1 and r = 0.6 in Year 2). Regarding linear dependencies between Biomet variables, R_g and PAR (r > 0.9 both years), T_{air} and VPD (r = 0.7 in both years) as well as T_{air} and Lw_{out} (r > 0.9 both years) were highly correlated. In Year 2, soil temperatures were closely connected among each other (r > 0.9) and with T_{air} (r > 0.7). Water table depth was correlated negatively with all redox measurements at different positions in the soil profile, with the largest absolute r of -0.7 for the relation with $Redox_{20}$. WT was also correlated with T_{Soil20} (r = 0.3). The seasonality embedded in soil temperature measurements was reflected by high correlation coefficients with the two low-frequency fuzzy variables fuzzy variable summer ($fuzzy_{su}$) and fuzzy variable winter ($fuzzy_{wi}$). The deeper in the soil profile the temperature measurements were taken, the less amplitude response they show to diurnal variations and the less noisy the relation to the fuzzy data appears to be.~~

~~Correlation analysis emphasizes the (not surprising) fact that collinearity does exist in the model input space. In order to avoid overfitting and thereby to increase the predictive power of the applied models, we reduced the input matrices which drive these models using our scoring table approach. Results of this input variables selection are detailed in tables B1 to B4 in the appendix. As a measure to ascertain collinearity reduction, we calculated the condition numbers (Belsley et al., 2005) of the input matrices at successive stages of the selection process as well as for the complete original and time-lagged input series (see figures C1 and C2). Within all 12 data sets, the condition numbers dropped throughout the selection process by at least one order of magnitude denoting a consistent removal of collinear variables from the input space. In all cases, between 30 % and 40 % of the variables presented to the selection scheme were included in the final model input matrices.~~

~~In the following section, detailed results of our model input selection scheme are shown. The four tables cover two gases and two years. Within each table, results for the two land use types (surface class *drained*, SC_{dra} and surface class *rewetted*, SC_{rew}) are shown. See Table A1 for declarations of the used quantity symbols. Only variables reaching a score above the respective score threshold (cf. Appendix A) are included. Variables which were selected in the last step of the scheme and used for gas flux modeling are printed in bold face.~~

Table B1. ~~Result of the model input selection scheme for Year 1 CO_2 fluxes. Score threshold for Biomet variables: SC_{dra} (6), SC_{rew} (6). Score threshold for Fuzzy and Footprint variables: SC_{dra} (9), SC_{rew} (10)~~

	~~Surface class *drained*~~		~~Surface class *rewetted*~~	
	~~Variable~~	~~Score~~	~~Variable~~	~~Score~~
~~**Biomet**~~	~~**Lw_{out}**~~	8	~~**Lw_{out}**~~	~~8~~
	~~**T_{air}**~~	~~8~~	~~**T_{air}**~~	~~8~~
	~~R_g~~	~~7~~	~~**R_g**~~	~~8~~
	~~**PAR**~~	~~7~~	~~Lw_{out}, lagged~~	~~8~~
	~~Lw_{out}, lagged~~	~~7~~	~~PAR~~	~~7~~
	~~R_g, lagged~~	~~7~~	~~VPD, lagged~~	~~6~~
	~~T_{air}, lagged~~	~~7~~	~~T_{air}, lagged~~	~~6~~
~~**Fuzzy & Footprint**~~	~~**$CC_{veg, dra}$**~~	~~12~~	~~**$CC_{veg, rew}$**~~	~~12~~
	~~**$fuzzy_{su}$**~~	~~12~~	~~**$fuzzy_{wi}$**~~	~~12~~
	~~**$fuzzy_{wi}$**~~	~~12~~	~~**$fuzzy_{af}$**~~	~~11~~
	~~**$fuzzy_{af}$**~~	~~9~~	~~**$fuzzy_{ni}$**~~	~~11~~
	~~**$fuzzy_{ev}$**~~	~~9~~	~~**$fuzzy_{mo}$**~~	~~10~~

Table B2. ~~Result of the model input selection scheme for Year 2 CO_2 fluxes. Score threshold for Biomet variables: SC_{dra} (6), SC_{rew} (6). Score threshold for Fuzzy & Footprint variables: SC_{dra} (9), SC_{rew} (9)~~

	~~Drained~~		~~Rewetted~~	
	~~Variable~~	~~Score~~	~~Variable~~	~~Score~~
~~**Biomet**~~	~~**T_{air}**~~	~~8~~	~~**T_{air}**~~	~~8~~
	~~**PAR, lagged**~~	~~8~~	~~**T_{Soil2}**~~	~~8~~
	~~T_{Soil2}~~	~~7~~	~~**T_{Soil5}**~~	~~8~~
	~~**$Redox_5$**~~	~~7~~	~~**T_{Soil10}**~~	~~8~~
	~~T_{air}, lagged~~	~~7~~	~~**PAR, lagged**~~	~~8~~
	~~**T_{Soil20}, lagged**~~	~~7~~	~~**T_{Soil40}**~~	~~7~~
	~~**$Redox_2$, lagged**~~	~~7~~	~~T_{Soil40}, lagged~~	~~7~~
	~~T_{Soil5}~~	~~6~~	~~T_{Soil2}, lagged~~	~~7~~
	~~T_{Soil10}~~	~~6~~	~~T_{Soil5}, lagged~~	~~7~~
	~~$Redox_{10}$~~	~~6~~	~~T_{Soil10}, lagged~~	~~7~~
	~~$Redox_{20}$~~	~~6~~	~~**T_{Soil20}, lagged**~~	~~7~~
	~~**WT, lagged**~~	~~6~~	~~T_{Soil20}~~	~~6~~
	~~T_{Soil2}, lagged~~	~~6~~	~~**$Redox_2$**~~	~~6~~
	~~**T_{Soil10}, lagged**~~	~~6~~	~~**$Redox_{10}$**~~	~~6~~
	~~$Redox_5$, lagged~~	~~6~~	~~T_{air}, lagged~~	~~6~~
	~~**$Redox_{10}$, lagged**~~	~~6~~	~~$Redox_{20}$, lagged~~	~~6~~
	~~$Redox_{20}$, lagged~~	~~6~~		
~~**Fuzzy & Footprint**~~	~~**$CC_{veg, dra}$**~~	~~12~~	~~**$fuzzy_{su}$**~~	~~11~~
	~~**$fuzzy_{wi}$**~~	~~9~~	~~**$fuzzy_{wi}$**~~	~~11~~
	~~**$fuzzy_{af}$**~~	~~9~~	~~**$CC_{veg, rew}$**~~	~~9~~
	~~**$fuzzy_{ev}$**~~	~~9~~	~~**$fuzzy_{af}$**~~	~~9~~
	~~**$fuzzy_{ni}$**~~	~~9~~	~~**$fuzzy_{ev}$**~~	~~9~~
	~~**$fuzzy_{su}$**~~	~~9~~	~~**$fuzzy_{ni}$**~~	~~9~~

Table B3. ~~Result of the model input selection scheme for Year 1 CH_4 fluxes. Score threshold for Biomet variables: SC_{dra} (6), SC_{rew} (6). Score threshold for Fuzzy & Footprint variables: SC_{dra} (8), SC_{rew} (8)~~

	~~Drained~~		~~Rewetted~~	
	~~Variable~~	~~Score~~	~~Variable~~	~~Score~~
~~**Biomet**~~	~~**VPD**~~	~~8~~	~~**VPD**~~	~~8~~
	~~**T_{air}, lagged**~~	~~8~~	~~Lw_{out}, lagged~~	~~8~~
	~~**Lw_{out}**~~	~~7~~	~~T_{air}, lagged~~	~~8~~
	~~T_{air}~~	~~7~~	~~**Lw_{out}**~~	~~7~~
	~~VPD, lagged~~	~~7~~	~~**p_{air}**~~	~~7~~
	~~Lw_{out}, lagged~~	~~6~~	~~**T_{air}**~~	~~7~~
~~**Fuzzy & Footprint**~~	~~**$CC_{veg, dra}$**~~	~~12~~	~~**$CC_{veg, rew}$**~~	~~12~~
	~~**$fuzzy_{su}$**~~	~~12~~	~~**$fuzzy_{su}$**~~	~~12~~
	~~**$fuzzy_{af}$**~~	~~10~~	~~**$fuzzy_{af}$**~~	~~11~~
	~~$fuzzy_{mo}$~~	~~8~~	~~**$fuzzy_{mo}$**~~	~~8~~
	~~**$fuzzy_{wi}$**~~	~~8~~		

Table B4. ~~Result of the model input selection scheme for Year 2 CH_4 fluxes. Score threshold for Biomet variables: SC_{dra} (6), SC_{rew} (7). Score threshold for Fuzzy & Footprint variables: SC_{dra} (8), SC_{rew} (9)~~

	~~Drained~~		~~Rewetted~~	
	~~Variable~~	~~Score~~	~~Variable~~	~~Score~~
~~**Biomet**~~	~~**VPD**~~	~~8~~	~~**VPD**~~	~~8~~
	~~**T_{Soil40}**~~	~~8~~	~~WT~~	~~8~~
	~~**T_{Soil5}**~~	~~8~~	~~**T_{Soil5}**~~	~~8~~
	~~$Redox_{10}$~~	~~8~~	~~**T_{Soil20}**~~	~~8~~
	~~T_{Soil40}, lagged~~	~~8~~	~~**$Redox_{10}$**~~	~~8~~
	~~T_{Soil10}, lagged~~	~~8~~	~~**$Redox_{20}$**~~	~~8~~
	~~**$Redox_5$, lagged**~~	~~8~~	~~WT, lagged~~	~~8~~
	~~**Lw_{out}**~~	~~7~~	~~**$Redox_2$, lagged**~~	~~8~~
	~~T_{Soil2}~~	~~7~~	~~**T_{Soil40}**~~	~~7~~
	~~**T_{Soil10}**~~	~~7~~	~~T_{Soil2}~~	~~7~~
	~~**$Redox_2$**~~	~~7~~	~~T_{Soil40},lagged~~	~~7~~
	~~**T_{Soil2}, lagged**~~	~~7~~	~~**T_{Soil2},lagged**~~	~~7~~
	~~T_{Soil5}, lagged~~	~~7~~	~~T_{Soil5}, lagged~~	~~7~~
	~~T_{Soil20}, lagged~~	~~7~~	~~T_{Soil5},lagged~~	~~7~~
	~~$Redox_2$, lagged~~	~~7~~	~~$Redox_{20}$, lagged~~	~~7~~
	~~$Redox_{10}$, lagged~~	~~7~~		
	~~T_{air}, lagged~~	~~6~~		
	~~**T_{Soil20}**~~	~~6~~		
	~~**$Redox_{20}$**~~	~~6~~		
	~~VPD, lagged~~	~~6~~		
	~~**WT, lagged**~~	~~6~~		
	~~$Redox_{20}$, lagged~~	~~6~~		
~~**Fuzzy & Footprint**~~	~~**$CC_{veg, dra}$**~~	~~12~~	~~**$CC_{veg, rew}$**~~	~~12~~
	~~**$fuzzy_{su}$**~~	~~10~~	~~**$fuzzy_{wi}$**~~	~~12~~
	~~**$fuzzy_{mo}$**~~	~~9~~	~~**$fuzzy_{mo}$**~~	~~9~~
	~~**$fuzzy_{af}$**~~	~~8~~	~~**$fuzzy_{su}$**~~	~~9~~

Appendix C: ~~Effect of dimension reduction of model input space on matrix condition~~

~~In this section, matrix condition numbers of the differently manipulated versions of input variable combinations that were fed into the input selection scheme (first three groups from the left in the plots below) and condition numbers of matrices at the two final stages of the selection scheme (last two groups from the left in the plots below) are given. Lower condition numbers denote a smaller degree of linear dependencies within different variables in a matrix. See Appendix A for details on the input selection method. Three data sets were modeled for each gas flux time series per year: The originally measured EC fluxes (tower view) representing landscape-scale integrated fluxes and the extracted time series, using EC footprint modeling, which relate to areas under different land use (drainage and rewetting) are shown.~~

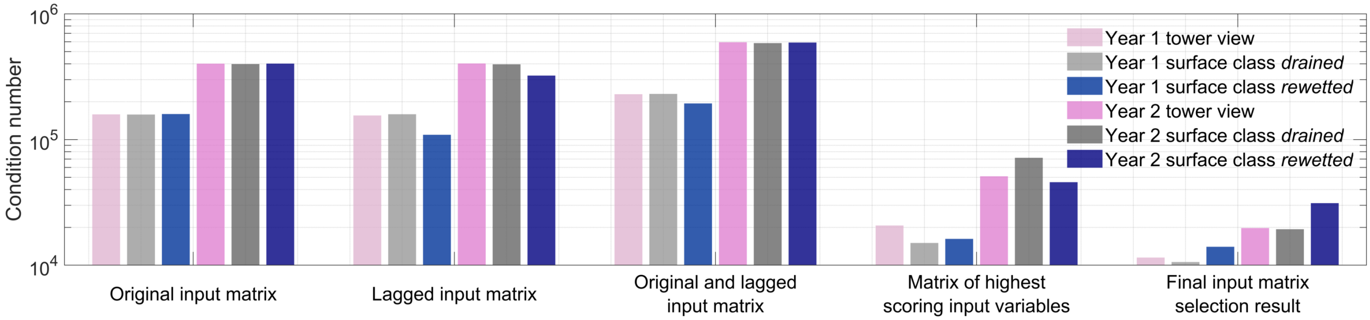

Figure C1. ~~Matrix condition numbers of input combinations which were fed into the CH_4 flux model input selection scheme (first three groups from the left) and condition numbers of matrices at the two final stages of the selection scheme (last two groups from the left).~~

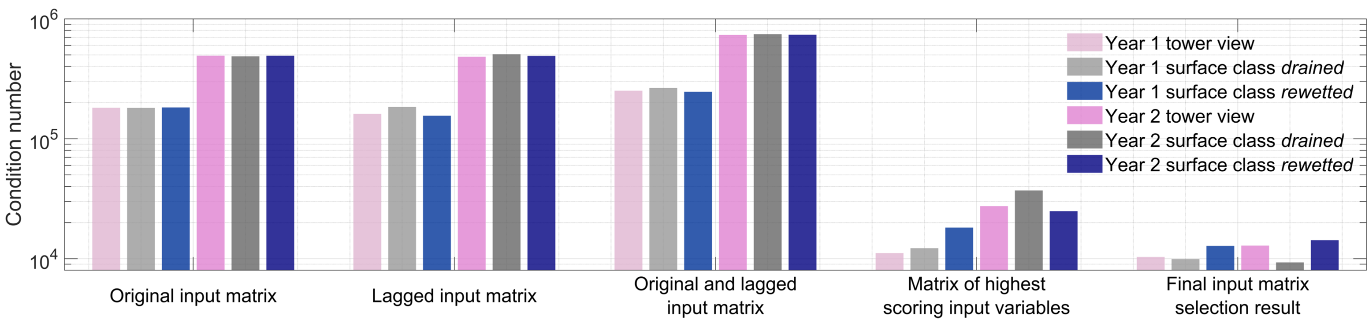

Figure C2. ~~Matrix condition numbers of input combinations which were fed into the CO_2 flux model input selection scheme (first three groups from the left) and condition numbers of matrices at the two final stages of the selection scheme (last two groups from the left).~~

Appendix A: Model input variables

Table A1. Model inputs used for methane and carbon dioxide flux gap-filling sorted by type. (x: available, -: not available)

Type	*Name*	*Unit*	*Quantity symbol*	*available in...*	
				Year 1	*Year 2*
Biomet	Global radiation	$W\ m^{-2}$	R_g	x	x
	Air temperature	°C	T_{air}	x	x
	Outgoing longwave radiation	$W\ m^{-2}$	Lw_{out}	x	x
	Photosynthetically active radiation	$\mu mol\ m^{-2}\ s^{-1}$	PAR	x	x
	Air pressure	kPa	p_{air}	x	x
	Rate of change in air pressure	kPa/1800 s	$slope_{Pair}$	x	x
	Water vapour pressure deficit	Pa	VPD	x	x
	Soil redox potential in 2 cm depth	mV	$Redox_2$	-	x
	Soil redox potential in 5 cm depth	mV	$Redox_5$	-	x
	Soil redox potential in 10 cm depth	mV	$Redox_{10}$	-	x
	Soil redox potential in 20 cm depth	mV	$Redox_{20}$	-	x
	Soil temperature in 2 cm depth	°C	T_{Soil2}	-	x
	Soil temperature in 5 cm depth	°C	T_{Soil5}	-	x
	Soil temperature in 10 cm depth	°C	T_{Soil10}	-	x
	Soil temperature in 20 cm depth	°C	T_{Soil20}	-	x
	Soil temperature in 40 cm depth	°C	T_{Soil40}	-	x
	Water table below surface	cm	WT	-	x
Fuzzy	Morning	n.a.	$fuzzy_{mo}$	x	x
	Afternoon	n.a.	$fuzzy_{af}$	x	x
	Evening	n.a.	$fuzzy_{ev}$	x	x
	Night	n.a.	$fuzzy_{ni}$	x	x
	Summer	n.a.	$fuzzy_{su}$	x	x
	Winter	n.a.	$fuzzy_{wi}$	x	x
Footprint	Class contribution of rewetted area	n.a.	CC_{rew}	x	x
	Class contribution of drained area	n.a.	CC_{dra}	x	x
	Class contribution of vegetated area within rewetted part	n.a.	$CC_{veg,\ rew}$	x	x
	Class contribution of vegetated area within drained part	n.a.	$CC_{veg,\ dra}$	x	x

Appendix B: Comparative validation of multilayer perceptron and multilinear regression models

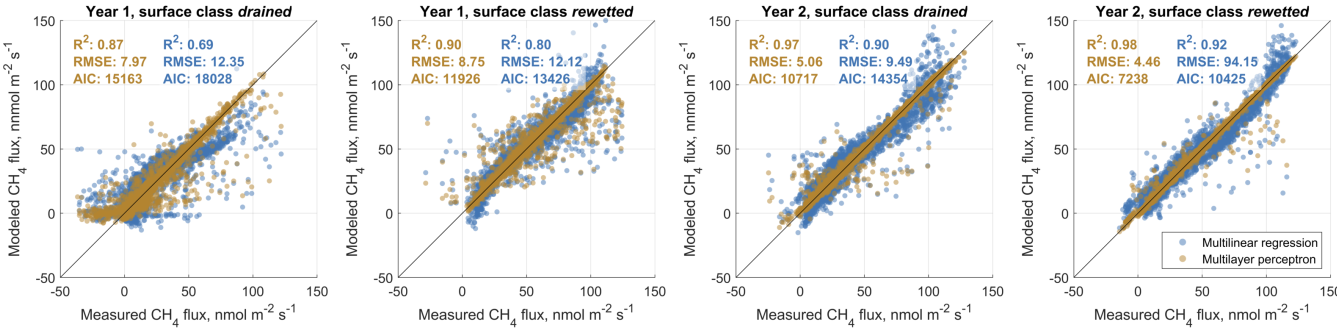

Figure B1. Comparative validation of surface class-specific multilinear regression and artificial neural network (in particular multilayer perceptron) methane (CH_4) flux models for both investigated years. Multilayer perceptrons appear to be superior with respect to the coefficient of determination (R^2), the Akaike information criterion (AIC) and the root mean squared error (RMSE) in all cases. Moreover, multilinear regression models tend to be S-shaped and therefore overestimate high and low measured fluxes.

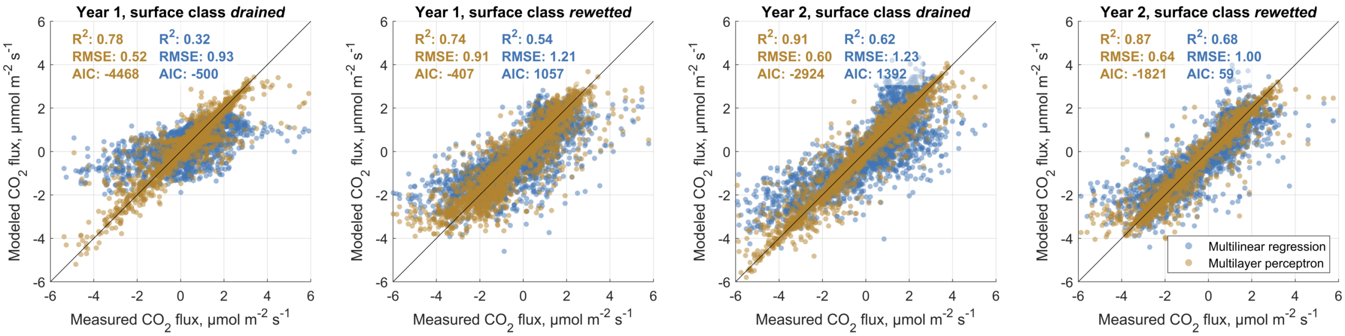

Figure B2. Comparative validation of surface class-specific multilinear regression and artificial neural network (in particular multilayer perceptron) carbon dioxide (CO_2) flux models for both investigated years. Multilayer perceptrons appear to be superior with respect to the coefficient of determination (R^2), the Akaike information criterion (AIC) and the root mean squared error (RMSE) in all cases.

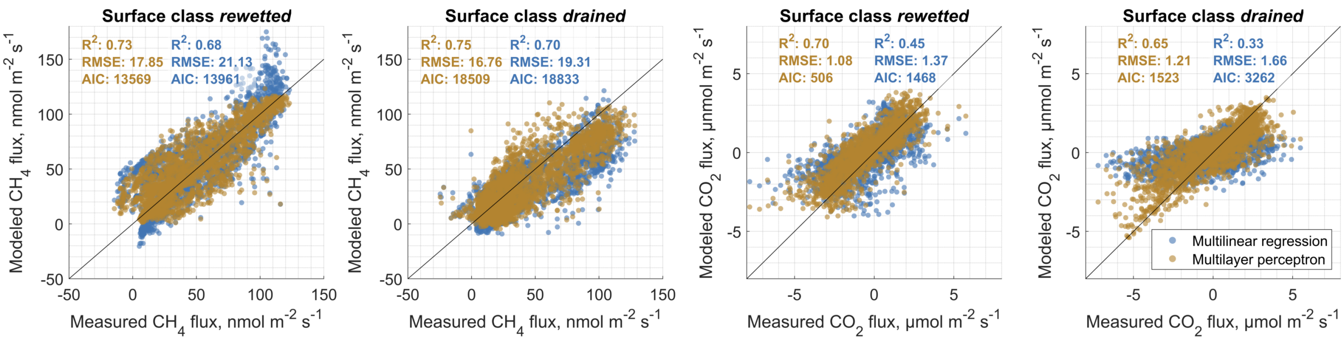

Figure B3. ~~Comparative validation of surface class-specific multilinear regression and artificial neural network (in particular multilayer perceptron) carbon dioxide (CO_2) and methane (CH_4) flux models. For this depiction, we drove models that were optimized using Year 1 measurement data as targets with Year 2 environmental data and compared the results to measured Year 2 gas fluxes. This type of comparison enables an evaluation of the developed models with observed data which is completely independent from model optimization. Therefore, good agreement cannot be attributed to models which are overfit to the provided target data. The results of this investigation substantiate the notion that multilayer perceptrons provide more reliable estimates of gas fluxes as they are superior to multilinear models with respect to the coefficient of determination (R^2), the Akaike information criterion (AIC) and the root mean squared error (RMSE) in all cases.~~

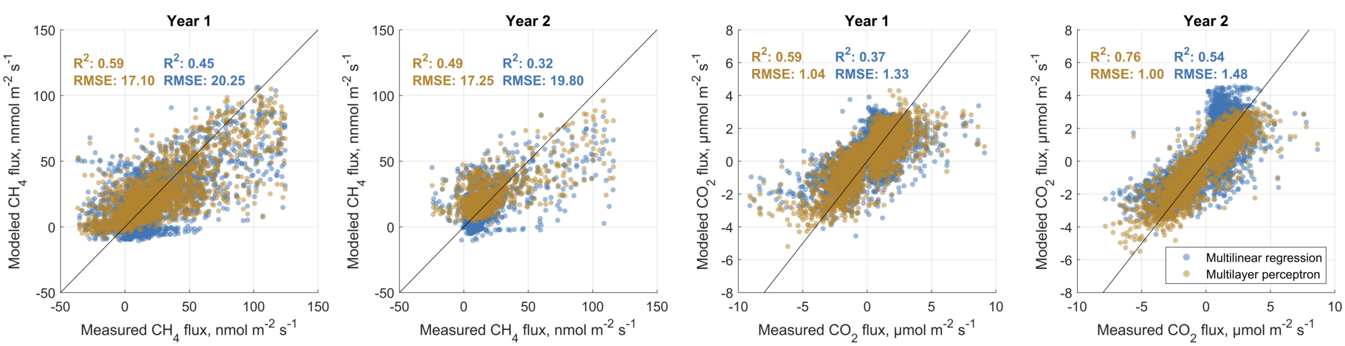

Figure B4. ~~Comparative validation of multilinear regression and artificial neural network (in particular multilayer perceptron) carbon dioxide (CO_2) and methane (CH_4) flux models. For this analysis, both surface class-specific flux models were combined using the footprint contribution of the respective classes yielding an estimate of the landscape-integrated signal recorded at the eddy covariance tower. These derived 'tower view' gas flux time series are compared to the actually observed data at the eddy covariance tower. In all cases, the multilayer perceptron models' performances surpass the attainment of multilinear regression models with respect to the coefficient of determination (R^2) and the root mean squared error (RMSE). Results also highlight the general feasibility of our approach to decompose an eddy covariance (EC) time series recorded over heterogeneous terrain into contributions of differently functioning landscape units within the EC footprint area.~~

Appendix C: Comparison of NEE model parameters with literature values

Table C1. Total ecosystem respiration (TER_{veg}, µmol m^{-2} s^{-1}), maximum photosynthesis (P_{max}, µmol m^{-2} s^{-1}) and initial quantum yield (α, dimensionless) from the vegetated strips of this study compared to literature values from similar plant species. As the literature record of combined plant and soil respiration measurements of the species that occur at the site of this study is limited, autotrophic respiration respiration (R_a, µmol m^{-2} s^{-1}) estimates of plants from the same genera are also given. Note that R_a values were determined on leaf scale and therefore refer to leaf area. Since shrubs and trees can have a leaf area index larger than 1, fluxes referring to ground surface area could be higher. Model parameter values from this study are given as averages and standard deviation. The latter statistic expresses the value range throughout two annual courses as shown in Figure 7 rather than parameter uncertainty.

Reference	Plant species	TER_{veg}	R_a	P_{max}	α
This study, drained section	*Betula pubescens, Salix spp., Eriophorum vaginatum, E. angustifolium, Molinia caerulea, Calla palustris, Typha latifolia, Carex spp., Juncus effusus, Calamagrostis canescens*	2.5 ± 2.9		14.4 ± 13.8	0.04 ± 0.04
This study, rewetted section	—"—	3.0 ± 2.1		10.5 ± 10.6	0.05 ± 0.03
Vanselow-Algan et al. (2015)	*Molinia caerulea, Betula pubescens, Eriophorum angustifolium*	> 10 (summer)			
Beyer and Höper (2015)	*Molinia caerulea*	≤ 7		15 to 30	
	Eriophorum angustifolium	≤ 5		20 to 70	
Patankar et al. (2013)	*Salix pulchra*		≤ 2		
	Eriophorum vaginatum		≤ 3		
	Carex bigelowi		≤ 1		
Körner (1982)	*Carex curvula*		1		
Murchie and Horton (1997)	*Carex flacca*		1.5		
Kaipiainen (2009)	*Salix dasyclados*		0.8 to 1.2		0.04 to 0.08
Patankar et al. (2013); Gu et al. (2008)	*Betula spp.*		1 to 5	10 to 15	
Lienau (2014)	*Betula pubescens*			32 to 41	
Nygren and Kellomäki (1983)	*Betula pubescens*			4 to 17	
Hoogesteger and Karlsson (1992)	*Betula pubescens*			8	
Chen et al. (2010)	*Typha latifolia*			25	0.02 to 0.07
Ögren (1993)	*Salix spp.*			16 to 29	
Vernay et al. (2016)	*Molinia caerulea*			7 to 15	0.03

Table C2. Comparison of total ecosystem respiration fluxes from bare peat areas without vegetation (TER_{bare}) between our study (see Figure 7, panel A for full time series) and literature values (closed chamber methods) from the same and similar peat extraction sites.

Reference	Site		TER_{bare}, µmol m^{-2} s^{-1}
	Land use	Name, Location	
This study	Active mining	Himmelmoor, NW-Germany, 53°N	1.1 ± 0.5 (annual average and standard deviation)
	Ceased mining, rewetted		0.8 ± 0.7 (annual average and standard deviation)
Vanselow-Algan et al. (2015)	Active mining		0.5 ± 0.1 (annual average and uncertainty)
Vybornova et al. (2019)	Active mining		0 to 1 (annual range), 3 (maximum)
	Ceased mining, rewetted		0 to 0.5 (annual range), 1.4 (maximum)
Waddington et al. (2002)	Ceased mining, wet year	Sainte-Marguerite-Marie, SE Canada, 48°N	0.8 (May to August average)
	Ceased mining, dry year		3 (May to August average)
Shurpali et al. (2008)	Active mining	Linnansuo, SE Finland, 62 °N	1.3 (end of August maximum)
			0.2 (mid-November minimum)

Author contributions. LK and EMP conceptualized and administered the planning of the research activity and acquired the funds for it. DH and LK conducted the field work. DH conducted literature research, analyzed the data, created visualizations and wrote the original draft. LK, EMP and DH reviewed and edited the original draft.

Competing interests. No competing interests are present

Acknowledgements. None of the research projects carried out in Himmelmoor would have been possible without the fantastic, continuous support of the peat plant operators. We want to thank the manager of the peat plant, Klaus-Dieter Czerwonka, his wife Monika, their son Hans and Hans Müller for their always reliable, hands-on approach to the diverse challenges that come with the installation and operation of measurement equipment in hard to access areas. For the technical planning and setting up of the measurement equipment we cordially thank Peter Schreiber and Christian Wille. For supporting the fieldwork in Himmelmoor, we thank Norman Rüggen, Ben Runkle, Olga Vybornova, Adrian Heger, Tim Pfau, Tom Huber, Ben Kreitner, Laure Hoeppli, Anastasia Tatarinova, Zoé Rehder and Oliver Kaufmann. We thank Peter Klink for helping with literature research. This work was supported through the Cluster of Excellence CliSAP (EXC177), Universität Hamburg, funded through the German Research Foundation (DFG).

References

Alberto, M. C. R., Wassmann, R., Buresh, R. J., Quilty, J. R., Correa, T. Q., Sandro, J. M., and Centeno, C. A. R.: Measuring methane flux from irrigated rice fields by eddy covariance method using open-path gas analyzer, Field Crops Research, 160, 12 – 21, https://doi.org/10.1016/j.fcr.2014.02.008, 2014.

Alm, J., Shurpali, N. J., Minkkinen, K., Aro, L., Hytoenen, J., Laurila, T., Lohila, A., Maljanen, M., Martikainen, P. J., and Maekiranta, P.: Emission factors and their uncertainty for the exchange of CO_2, CH_4 and N_2O in Finnish managed peatlands, Boreal Environment Research, 12, 191 – 209, 2007.

Aubinet, M., Vesala, T., and Papale, D.: Eddy covariance: a practical guide to measurement and data analysis, Springer, Dordrecht, 2012.

Belsley, D. A., Kuh, E., and Welsch, R. E.: Detecting and Assessing Collinearity, chap. 3, pp. 85–191, John Wiley & Sons, Ltd, https://doi.org/10.1002/0471725153.ch3, 2005.

Beyer, C. and Höper, H.: Greenhouse gas exchange of rewetted bog peat extraction sites and a Sphagnum cultivation site in northwest Germany, Biogeosciences, 12, 2101–2117, 2015.

Bhullar, G. S., Edwards, P. J., and Olde Venterink, H.: Influence of Different Plant Species on Methane Emissions from Soil in a Restored Swiss Wetland, PLOS ONE, 9, 1–5, 2014.

Brown, M. G., Humphreys, E. R., Moore, T. R., Roulet, N. T., and Lafleur, P. M.: Evidence for a nonmonotonic relationship between ecosystem-scale peatland methane emissions and water table depth, Journal of Geophysical Research - Biogeosciences, 119, 826 – 835, https://doi.org/10.1002/2013JG002576, 2014.

Bubier, J. L.: The relationship of vegetation to methane emission and hydrochemical gradients in northern peatlands, Journal of Ecology, 83, 403–420, 1995.

Burba, G., Schmidt, A., Scott, R. L., Nakai, T., Kathilankal, J., Fratini, G., Hanson, C., Law, B., Mcdermitt, D. K., Eckles, R., Furtaw, M., and Velgersdyk, M.: Calculating CO_2 and H_2O eddy covariance fluxes from an enclosed gas analyzer using an instantaneous mixing ratio, Global Change Biology, 18, 385 – 399, https://doi.org/10.1111/j.1365-2486.2011.02536.x, 2012.

Chen, H., Zamorano, M. F., and Ivanoff, D.: Effect of flooding depth on growth, biomass, photosynthesis, and chlorophyll fluorescence of Typha domingensis, Wetlands, 30, 957–965, 2010.

Couwenberg, J.: Emission factors for managed peat soils (organic soils, histosols) An analysis of IPCC default values, Wetlands International, Ede, 2009.

Couwenberg, J., Dommain, R., and Joosten, H.: Greenhouse gas fluxes from tropical peatlands in south-east Asia, Global Change Biology, 16, 1715 – 1732, https://doi.org/10.1111/j.1365-2486.2009.02016.x, 2010.

Czerwonka, K.-D. and Czerwonka, M.: Das Himmelmoor - Dokumentationen, Berichte, Kommentare, Geschichten, self-published, Quickborn, 1985.

Dengel, S., Levy, P. E., Grace, J., Jones, S. K., and Skiba, U. M.: Methane emissions from sheep pasture, measured with an open-path eddy covariance system, Global Change Biology, 17, 3524 – 3533, https://doi.org/10.1111/j.1365-2486.2011.02466.x, 2011.

Dengel, S., Zona, D., Sachs, T., Aurela, M., Jammet, M., Parmentier, F. J. W., Oechel, W., and Vesala, T.: Testing the applicability of neural networks as a gap-filling method using CH_4 flux data from high latitude wetlands, Biogeosciences, 10, 8185 – 8200, https://doi.org/10.5194/bg-10-8185-2013, 2013.

Deshmukh, C., Serça, D., Delon, C., Tardif, R., Demarty, M., Jarnot, C., Meyerfeld, Y., Chanudet, V., Guédant, P., Rode, W., Descloux, S., and Guérin, F.: Physical controls on CH_4 emissions from a newly flooded subtropical freshwater hydroelectric reservoir: Nam Theun 2, Biogeosciences, 11, 4251–4269, 2014.

Detto, M., Verfaillie, J., Anderson, F., Xu, L., and Baldocchi, D.: Comparing laser-based open- and closed-path gas analyzers to measure methane fluxes using the eddy covariance method, Agricultural and Forest Meteorology, 151, 1312 – 1324, https://doi.org/10.1016/j.agrformet.2011.05.014, 2011.

Draper, N. R. and Smith, H.: Applied Regression Analysis, John Wiley and Sons, New York, 3rd edn., https://doi.org/10.1198/tech.2005.s303, 1998.

Drösler, M., Freibauer, A., Christensen, T. R., and Friborg, T.: Observations and status of peatland greenhouse gas emissions in Europe, in: The continental-scale greenhouse gas balance of Europe, pp. 243–261, Springer, New York, 2008.

Falge, E., Baldocchi, D., Olson, R., Anthoni, P., Aubinet, M., Bernhofer, C., Burba, G., Ceulemans, R., Clement, R., Dolman, H., Granier, A., Gross, P., Grünwald, T., Hollinger, D., Jensen, N.-O., Katul, G., Keronen, P., Kowalski, A., Lai, C. T., Law, B. E., Meyers, T., Moncrieff, J., Moors, E., Munger, J., Pilegaard, K., Rannik, Ü., Rebmann, C., Suyker, A., Tenhunen, J., Tu, K., Verma, S., Vesala, T., Wilson, K., and Wofsy, S.: Gap filling strategies for defensible annual sums of net ecosystem exchange, Agricultural and Forest Meteorology, 107, 43 – 69, https://doi.org/10.1016/S0168-1923(00)00225-2, 2001.

Finkelstein, P. L. and Sims, P. F.: Sampling error in eddy correlation flux measurements, Journal of Geophysical Research, 106, 3503, https://doi.org/10.1029/2000JD900731, 2001.

Forbrich, I., Kutzbach, L., Wille, C., Becker, T., Wu, J., and Wilmking, M.: Cross-evaluation of measurements of peatland methane emissions on microform and ecosystem scales using high-resolution landcover classification and source weight modelling, Agricultural and Forest Meteorology, 151, 864 – 874, https://doi.org/10.1016/j.agrformet.2011.02.006, 2011.

Fratini, G., Ibrom, A., Arriga, N., Burba, G., and Papale, D.: Relative humidity effects on water vapour fluxes measured with closed-path eddy-covariance systems with short sampling lines, Agricultural and Forest Meteorology, 165, 53 – 63, https://doi.org/10.1016/j.agrformet.2012.05.018, 2012.

Friborg, T. and Christensen, T.: Trace gas exchange in a high-arctic valley 2 . Landscape CH 4 fluxes measured and modeled using eddy correlation have measurements, Global Biogeochemical Cycles, 14, 715 – 723, 2000.

Garson, G. D.: Interpreting Neural-network Connection Weights, AI Expert, 6, 46 – 51, 1991.

Gash, J. H. C. and Culf, a. D.: Applying a linear detrend to eddy correlation data in realtime, Boundary-Layer Meteorology, 79, 301 – 306, https://doi.org/10.1007/BF00119443, 1996.

Gaudig, G.: The research project: "Peat mosses (Sphagnum) as a renewable resource: establishment of peat mosses - optimising growth conditions, Telma, 32, 227 – 242, 2002.

Glaser, P. H.: Surface deformations as indicators of deep ebullition fluxes in a large northern peatland, Global Biogeochemical Cycles, 18, n/a – n/a, https://doi.org/10.1029/2003GB002069, 2004.

Goodrich, J., Campbell, D., Roulet, N., Clearwater, M., and Schipper, L.: Overriding control of methane flux temporal variability by water table dynamics in a Southern Hemisphere, raised bog, Journal of Geophysical Research: Biogeosciences, 120, 819 – 831, 2015.

Goodrich, J. P., Varner, R. K., Frolking, S., Duncan, B. N., and Crill, P. M.: High-frequency measurements of methane ebullition over a growing season at a temperate peatland site, Geophysical Research Letters, 38, https://doi.org/10.1029/2011GL046915, 2011.

Grube, A., Fuest, T., and Menzel, P.: Geology of the Himmelmoor(bog) near Quickborn, Telma, 40, 19 – 32, 2010.

Gu, M., Robbins, J. A., Rom, C. R., and Choi, H. S.: Photosynthesis of birch genotypes (Betula L.) under varied irradiance and CO_2 concentration, HortScience, 43, 314–319, 2008.

Hahn-Schöfl, M., Zak, D., Minke, M., Gelbrecht, J., Augustin, J., and Freibauer, a.: Organic sediment formed during inundation of a degraded fen grassland emits large fluxes of CH_4 and CO_2, Biogeosciences Discussions, 7, 9273 – 9303, https://doi.org/10.5194/bgd-7-9273-2010, 2010.

Hanis, K. L., Tenuta, M., Amiro, B. D., and Papakyriakou, T. N.: Seasonal dynamics of methane emissions from a subarctic fen in the Hudson Bay Lowlands, Biogeosciences, 10, 4465 – 4479, https://doi.org/10.5194/bg-10-4465-2013, 2013.

Hashem, S.: Optimal Linear Combinations of Neural Networks., Neural networks : the official journal of the International Neural Network Society, 10, 599 – 614, https://doi.org/10.1016/S0893-6080(96)00098-6, 1997.

Hatala, J. a., Detto, M., and Baldocchi, D. D.: Gross ecosystem photosynthesis causes a diurnal pattern in methane emission from rice, Geophysical Research Letters, 39, 1 – 5, https://doi.org/10.1029/2012GL051303, 2012.

Haykin, S.: Neural Networks: a comprehensive foundation, Prentice Hall, Upper Saddle River, 1999.

Hiraishi, T., Krug, T., Tanabe, K., Srivastava, N., Baasansuren, J., Fukuda, M., and Troxler, T.: 2013 supplement to the 2006 IPCC Guidelines for National Greenhouse Gas Inventories: Wetlands, IPCC, Switzerland, 2014.

Holl, D., Pancotto, V., Heger, A., Camargo, S. J., and Kutzbach, L.: Cushion bogs are stronger carbon dioxide net sinks than moss-dominated bogs as revealed by eddy covariance measurements on Tierra del Fuego, Argentina, Biogeosciences Discussions, 2019, 1–36, https://doi.org/10.5194/bg-2019-156, https://www.biogeosciences-discuss.net/bg-2019-156/, 2019a.

Holl, D., Wille, C., Sachs, T., Schreiber, P., Runkle, B. R. K., Beckebanze, L., Langer, M., Boike, J., Pfeiffer, E.-M., Fedorova, I., Bolshianov, D. Y., Grigoriev, M. N., and Kutzbach, L.: A long-term (2002 to 2017) record of closed-path and open-path eddy covariance CO_2 net ecosystem exchange fluxes from the Siberian Arctic, Earth System Science Data, 11, 221–240, https://doi.org/10.5194/essd-11-221-2019, https://www.earth-syst-sci-data.net/11/221/2019/, 2019b.

Hommeltenberg, J., Mauder, M., Drösler, M., Heidbach, K., Werle, P., and Schmid, H. P.: Ecosystem scale methane fluxes in a natural temperate bog-pine forest in southern Germany, Agricultural and Forest Meteorology, 198, 273 – 284, 2014.

Hoogesteger, J. and Karlsson, P.: Effects of defoliation on radial stem growth and photosynthesis in the mountain birch (Betula pubescens ssp. tortuosa), Functional Ecology, pp. 317–323, 1992.

Hunter, A., Kennedy, L., Henry, J., and Ferguson, I.: Application of neural networks and sensitivity analysis to improved prediction of trauma survival, Computer Methods and Programs in Biomedicine, 62, 11 – 19, 2000.

Jackowicz-Korczyński, M., Christensen, T. R., Bäckstrand, K., Crill, P., Friborg, T., Mastepanov, M., and Ström, L.: Annual cycle of methane emission from a subarctic peatland, Journal of Geophysical Research, 115, 1 – 10, https://doi.org/10.1029/2008JG000913, 2010.

Järveoja, J., Peichl, M., Maddison, M., Soosaar, K., Vellak, K., Karofeld, E., Teemusk, A., and Mander, U.: Impact of water table level on annual carbon and greenhouse gas balances of a restored peat extraction area, Biogeosciences, 13, 2637–2651, https://doi.org/10.5194/bg-13-2637-2016, 2016.

Järvi, L., Nordbo, A., Junninen, H., Riikonen, A., Moilanen, J., Nikinmaa, E., and Vesala, T.: Seasonal and annual variation of carbon dioxide surface fluxes in Helsinki, Finland, in 2006–2010, Atmospheric Chemistry and Physics, 12, 8475 – 8489, https://doi.org/10.5194/acp-12-8475-2012, 2012.

Joosten, H.: Bog regeneration in the Netherlands: A review, in: Peatland Ecosystems and Man: An Impact Assessment, edited by Bragg, O. M., Department of Biological Sciences, University of Dundee, Dundee, 1992.

Kaimal, J. and Finnigan, J.: Atmospheric Boundary Layer Flows: Their structure and measurements, Oxford University Press, Oxford, 1994.

Kaipiainen, E. L.: Parameters of photosynthesis light curve in Salix dasyclados and their changes during the growth season, Russian Journal of Plant Physiology, 56, 445–453, 2009.

Kerdchoechuen, O.: Methane emission in four rice varieties as related to sugars and organic acids of roots and root exudates and biomass yield, Agriculture, Ecosystems & Environment, 108, 155 – 163, 2005.

Kettunen, A., Kaitala, V., Alm, J., Silvola, J., Nykänen, H., and Martikainen, P. J.: Cross-correlation analysis of the dynamics of methane emissions from a boreal peatland, Global Biogeochemical Cycles, 10, 457–471, https://doi.org/10.1029/96GB01609, 1996.

Knox, S. H., Sturtevant, C., Matthes, J. H., Koteen, L., Verfaillie, J., and Baldocchi, D.: Agricultural peatland restoration: effects of land-use change on greenhouse gas (CO_2 and CH_4) fluxes in the Sacramento-San Joaquin Delta, Global Change Biology, 21, 750 – 765, https://doi.org/10.1111/gcb.12745, 2015.

Knox, S. H., Jackson, R. B., Poulter, B., McNicol, G., Fluet-Chouinard, E., Zhang, Z., Hugelius, G., Bousquet, P., Canadell, J. G., Saunois, M., Papale, D., Chu, H., Keenan, T. F., Baldocchi, D., Torn, M. S., Mammarella, I., Trotta, C., Aurela, M., Bohrer, G., Campbell, D. I., Cescatti, A., Chamberlain, S., Chen, J., Chen, W., Dengel, S., Desai, A. R., Euskirchen, E., Friborg, T., Gasbarra, D., Goded, I., Goeckede, M., Heimann, M., Helbig, M., Hirano, T., Hollinger, D. Y., Iwata, H., Kang, M., Klatt, J., Krauss, K. W., Kutzbach, L., Lohila, A., Mitra, B., Morin, T. H., Nilsson, M. B., Niu, S., Noormets, A., Oechel, W. C., Peichl, M., Peltola, O., Reba, M. L., Richardson, A. D., Runkle, B. R. K., Ryu, Y., Sachs, T., Schäfer, K. V. R., Schmid, H. P., Shurpali, N., Sonnentag, O., Tang, A. C. I., Ueyama, M., Vargas, R., Vesala, T., Ward, E. J., Windham-Myers, L., Wohlfahrt, G., and Zona, D.: FLUXNET-CH4 Synthesis Activity: Objectives, Observations, and Future Directions, Bulletin of the American Meteorological Society, 100, 2607–2632, https://doi.org/10.1175/BAMS-D-18-0268.1, 2019.

Kordowski, K. and Kuttler, W.: Carbon dioxide fluxes over an urban park area, Atmospheric Environment, 44, 2722 – 2730, https://doi.org/10.1016/j.atmosenv.2010.04.039, 2010.

Kormann, R. and Meixner, F. X.: An analytical footprint model for non-neutral stratification, Boundary-Layer Meteorology, 99, 207 – 224, https://doi.org/10.1023/A:1018991015119, 2001.

Körner, C.: CO_2 exchange in the alpine sedge Carex curvula as influenced by canopy structure, light and temperature, Oecologia, 53, 98–104, 1982.

Kroon, P. S., Schrier-Uijl, a. P., Hensen, a., Veenendaal, E. M., and Jonker, H. J. J.: Annual balances of CH4 and N2O from a managed fen meadow using eddy covariance flux measurements, European Journal of Soil Science, 61, 773 – 784, https://doi.org/10.1111/j.1365-2389.2010.01273.x, 2010.

Lai, D. Y. F.: Methane Dynamics in Northern Peatlands: A Review, Pedosphere, 19, 409 – 421, https://doi.org/10.1016/S1002-0160(09)00003-4, 2009.

Lamers, L.: Tackling Biochemical Questions in Peatlands, Ph.D. thesis, Katholieke Universiteit Nijmegen, 2001.

Lienau, D.: Untersuchung der diurnalen Variabilität der Photosyntheseraten der Moorbirke im Himmelmoor, Master's thesis, Universität Hamburg, Hamburg, 2014.

Long, K., Flanagan, L. B., and Cai, T.: Diurnal and seasonal variation in methane emissions in a northern Canadian peatland measured by eddy covariance, Global Change Biology, 16, 2420 – 2435, https://doi.org/10.1111/j.1365-2486.2009.02083.x, 2010.

Lütt, S.: Produktionsbiologische Untersuchungen zur Sukzession der Torfstichvegetation in Schleswig-Holstein, Arbeitsgemeinschaft Geobotanik in Schleswig-Holstein und Hamburg, Kiel, 1992.

Maljanen, M., Sigurdsson, B. D., Guðmundsson, J., Óskarsson, H., Huttunen, J. T., and Martikainen, P. J.: Greenhouse gas balances of managed peatlands in the Nordic countries – present knowledge and gaps, Biogeosciences, 7, 2711–2738, https://doi.org/10.5194/bg-7-2711-2010, https://www.biogeosciences.net/7/2711/2010/, 2010.

Mann, C. J. and Wetzel, R. G.: Photosynthesis and stomatal conductance of Juncus effusus in a temperate wetland ecosystem, Aquatic Botany, 63, 127–144, 1999.

Mauder, M. and Foken, T.: Documentation and instruction manual of the eddy covariance software package TK2, Univ, Arbeitsergebnisse, Universität Bayreuth, Abt. Mikrometeorologie, 26, 45, 2004.

Kreis Pinneberg: Natur kehrt zurück ins Himmelmoor, URL: https://www.kreis-pinneberg.de/Ver%C3%B6ffentlichungen/Pressemitteilungen/Natur+kehrt+zur%C3%BCck+ins+Himmelmoor.html, 2004.

McDermitt, D., Burba, G., Xu, L., Anderson, T., Komissarov, a., Riensche, B., Schedlbauer, J., Starr, G., Zona, D., Oechel, W., Oberbauer, S., and Hastings, S.: A new low-power, open-path instrument for measuring methane flux by eddy covariance, Applied Physics B: Lasers and Optics, 102, 391 – 405, https://doi.org/10.1007/s00340-010-4307-0, 2011.

Menzer, O., Meiring, W., Kyriakidis, P. C., and McFadden, J. P.: Annual sums of carbon dioxide exchange over a heterogeneous urban landscape through machine learning based gap-filling, Atmospheric Environment, 101, 312 – 327, https://doi.org/10.1016/j.atmosenv.2014.11.006, 2015.

Mikhaylov, O. A., Miglovets, M. N., and Zagirova, S. V.: Vertical methane fluxes in mesooligotrophic boreal peatland in European Northeast Russia, Contemporary Problems of Ecology, 8, 368 – 375, https://doi.org/10.1134/S1995425515030099, 2015.

Moffat, A. M.: A new methodology to interpret high resolution measurements of net carbon fluxes between terrestrial ecosystems and the atmosphere, Ph.D. thesis, Friedrich-Schiller-Universität Jena, 2012.

Moffat, A. M., Papale, D., Reichstein, M., Hollinger, D. Y., Richardson, A. D., Barr, A. G., Beckstein, C., Braswell, B. H., Churkina, G., Desai, A. R., Falge, E., Gove, J. H., Heimann, M., Hui, D., Jarvis, A. J., Kattge, J., Noormets, A., and Stauch, V. J.: Comprehensive comparison of gap-filling techniques for eddy covariance net carbon fluxes, Agricultural and Forest Meteorology, 147, 209 – 232, https://doi.org/10.1016/j.agrformet.2007.08.011, 2007.

Moncrieff, J., Clement, R., Finnigan, J., and Meyers, T.: Averaging, detrending, and filtering of eddy covariance time series, Handbook of Micrometeorology, pp. 7 – 31, https://doi.org/10.1007/1-4020-2265-4_2, 2004.

Murchie, E. H. and Horton, P.: Acclimation of photosynthesis to irradiance and spectral quality in British plant species: chlorophyll content, photosynthetic capacity and habitat preference, Plant, Cell and Environment, 20, 438–448, 1997.

Myhre, G., Shindell, D., Bréon, F.-M., Collins, W., Fuglestvedt, J., Huang, J., Koch, D., Lamarque, J.-F., Lee, D., Mendoza, B., Nakajima, T., Robock, A., Stephens, G., Takemura, T., and Zhang, H.: Anthropogenic and Natural Radiative Forcing, in: Climate Change 2013: The Physical Science Basis. Contribution of Working Group I to the Fifth Assessment Report of the Intergovernmental Panel on Climate Change, edited by Stocker, T., Qin, D., Plattner, G.-K., Tignor, M., Allen, S., Boschung, J., Nauels, A., Xia, Y., Bex, V., and Midgley, P., Cambridge University Press, Cambridge, 2013.

Naftaly, U., Intrator, N., and Horn, D.: Optimal ensemble averaging of neural networks, Network: Computation in Neural Systems, 8, 283 – 296, https://doi.org/10.1088/0954-898X/8/3/004, 1997.

Nakai, T., Van der Molen, M., Gash, J., and Kodama, Y.: Correction of sonic anemometer angle of attack errors, Agricultural and Forest Meteorology, 136, 19–30, 2006.

Nemitz, E., Mannarella, I., Ibrom, A., Aurela, M., Burba, G. G., Dengel, S., Gielen, B., Grelle, A., Heinesch, B., Herbst, M., et al.: Standardisation of eddy-covariance flux measurements of methane and nitrous oxide, International agrophysics, 32, 517–549, 2018.

Neue, H., Wassmann, R., Lantin, R., Alberto, M. C., Aduna, J., and Javellana, A.: Factors affecting methane emission from rice fields, Atmospheric Environment, 30, 1751–1754, 1996.

Nygren, M. and Kellomäki, S.: Effect of shading on leaf structure and photosynthesis in young birches, Betula pendula Roth. and B. pubescens Ehrh., Forest Ecology and Management, 7, 119–132, 1983.

Ögren, E.: Convexity of the Photosynthetic Light-Response Curve in Relation to Intensity and Direction of Light during Growth., Plant physiology, 101, 1013–1019, 1993.

Olden, D. A. and Jackson, J. D. Y.: Illuminating the "black box": a ramdomization approach for understanding variable contributions in artificial neuronal networks., Ecological Modelling, 154, 135 – 150, 2002.

Paffen, B. and Roelofs, J.: Impact of carbon dioxide and ammonium on the growth of submerged Sphagnum cuspidatum, Aquatic Botany, 40, 61 – 71, 1991.

Papale, D. and Valentini, R.: A new assessment of European forests carbon exchanges by eddy fluxes and artificial neural network spatialization, Global Change Biology, 9, 525 – 535, https://doi.org/10.1046/j.1365-2486.2003.00609.x, 2003.

Parish, F., Sirin, A., Charman, D., Joosten, H., Minaeva, T., and Silvius, M.: Assessment on peatlands, biodiversity and climate change, Global Environment Centre, Kuala Lumpur, 2008.

Parmentier, F. J. W., Van Huissteden, J., Van Der Molen, M. K., Schaepman-Strub, G., Karsanaev, S. a., Maximov, T. C., and Dolman, a. J.: Spatial and temporal dynamics in eddy covariance observations of methane fluxes at a tundra site in northeastern Siberia, Journal of Geophysical Research: Biogeosciences, 116, 1 – 14, https://doi.org/10.1029/2010JG001637, 2011.

Patankar, R., Mortazavi, B., Oberbauer, S. F., and Starr, G.: Diurnal patterns of gas-exchange and metabolic pools in tundra plants during three phases of the arctic growing season, Ecology and Evolution, 3, 375–388, 2013.

Peltola, O., Mammarella, I., Haapanala, S., Burba, G., and Vesala, T.: Field intercomparison of four methane gas analyzers suitable for eddy covariance flux measurements, Biogeosciences, 10, 3749 – 3765, https://doi.org/10.5194/bg-10-3749-2013, 2013.

Peltola, O., Hensen, A., Helfter, C., Belelli Marchesini, L., Bosveld, F. C., van den Bulk, W. C. M., Elbers, J. A., Haapanala, S., Holst, J., Laurila, T., Lindroth, A., Nemitz, E., Röckmann, T., Vermeulen, A. T., and Mammarella, I.: Evaluating the performance of commonly used gas analysers for methane eddy covariance flux measurements: the InGOS inter-comparison field experiment, Biogeosciences, 11, 3163 – 3186, https://doi.org/10.5194/bg-11-3163-2014, 2014.

Perrone, M. P. and Cooper, L. N.: When networks disagree: ensemble methods for hybrid neural network, in: Neural Networks for Speech and Image Processing, edited by Mammone, R. J., pp. 126 – 142, Chapman Hall, London, 1993.

Pfadenhauer, J. and Klötzli, F.: Restoration Experiments in Middle European Wet Terrestrial Ecosystems: An Overview, Vegetatio, 126, 101–115, 1996.

Pfeiffer, E.-M.: Methanfreisetzung aus hydromorphen Böden verschiedener naturnaher und genutzter Feuchtgebiete (Marsch, Moor, Tundra, Reisanbau)., Hamburger Bodenkundliche Arbeiten, 37, 1997.

Pypker, T. G., Moore, P. a., Waddington, J. M., Hribljan, J. a., and Chimner, R. C.: Shifting environmental controls on CH4 fluxes in a sub-boreal peatland, Biogeosciences, 10, 7971 – 7981, https://doi.org/10.5194/bg-10-7971-2013, 2013.

Rinne, J., Riutta, T., Pihlatie, M., Aurela, M., Haapanala, S., Tuovinen, J. P., Tuittila, E. S., and Vesala, T.: Annual cycle of methane emission from a boreal fen measured by the eddy covariance technique, Tellus, Series B: Chemical and Physical Meteorology, 59, 449 – 457, https://doi.org/10.1111/j.1600-0889.2007.00261.x, 2007.

Rößger, N., Wille, C., Holl, D., Göckede, M., and Kutzbach, L.: Scaling and balancing carbon dioxide fluxes in a heterogeneous tundra ecosystem of the Lena River Delta, Biogeosciences, 16, 2591–2615, https://doi.org/10.5194/bg-16-2591-2019, 2019.

Saarnio, S., Winiwarter, W., and Leitão, J.: Methane release from wetlands and watercourses in Europe, Atmospheric Environment, 43, 1421 – 1429, https://doi.org/10.1016/j.atmosenv.2008.04.007, 2009.

Sarle, W. S.: Neural Networks and Statistical Models, in: Proceedings of the Nineteenth Annual SAS Users Group International Conference, April, 1994, pp. 1 – 13, https://doi.org/10.1.1.27.699, 1994.

Sarle, W. S.: Neural Network FAQ, periodic posting to the Usenet newsgroup comp.ai.neural-nets, ftp://ftp.sas.com/pub/neural/FAQ.html, 1997.

Schmidt, A., Wrzesinsky, T., and Klemm, O.: Gap Filling and Quality Assessment of CO2 and Water Vapour Fluxes above an Urban Area with Radial Basis Function Neural Networks, Boundary-Layer Meteorology, 126, 389 – 413, https://doi.org/10.1007/s10546-007-9249-7, 2008.

Schrier-Uijl, A. P., Kroon, P. S., Leffelaar, P. a., van Huissteden, J. C., Berendse, F., and Veenendaal, E. M.: Methane emissions in two drained peat agro-ecosystems with high and low agricultural intensity, Plant and Soil, 329, 509 – 520, https://doi.org/10.1007/s11104-009-0180-1, 2010.

Shoemaker, W. B., Anderson, F., Barr, J. G., Graham, S. L., and Botkin, D. B.: Carbon exchange between the atmosphere and subtropical forested cypress and pine wetlands, Biogeosciences, 12, 2285 – 2300, https://doi.org/10.5194/bg-12-2285-2015, 2015.

Shurpali, N. J., Hyvönen, N. P., Huttunen, J. T., Biasi, C., Nykänen, H., Pekkarinen, N., Martikainen, P. J., Hyvonen, N. P., and Nykanen, H.: Bare soil and reed canary grass ecosystem respiration in peat extraction sites in Eastern Finland, Tellus B, 60, 200 – 209, https://doi.org/doi:10.1111/j.1600-0889.2007.00325.x, 2008.

Sliva, J.: Renaturierung von industriell abgetorften Hochmooren am Beispiel der Kendlmühlilzen, Ph.D. thesis, Institut für Landespflege und Botanik München, 1997.

Smolders, A. J. P., Tomassen, H. B. M., Pijnappel, H. W., Lamers, L. P. M., and Roelofs, J. G. M.: Substrate-derived CO2 is important in the development of Sphagnum spp., New Phytologist, 152, 325 – 332, 2001.

Strack, M., Kellner, E., and Waddington, J.: Dynamics of biogenic gas bubbles in peat and their effects on peatland biogeochemistry, Global Biogeochemical Cycles, 19, 2005.

Suyker, A. E., Verma, S. B., Clement, R. J., and Billesbach, D. P.: Methane flux in a boreal fen: Season-long measurement by eddy correlation, Journal of Geophysical Research: Atmospheres, 101, 28 637 – 28 647, https://doi.org/10.1029/96JD02751, 1996.

Thornley, J. H. M.: Dynamic Model of Leaf Photosynthesis with Acclimation to Light and Nitrogen, Annals of Botany, 81, 421–430, 1998.

Tiemeyer, B., Albiac Borraz, E., Augustin, J., Bechtold, M., Beetz, S., Beyer, C., Drösler, M., Ebli, M., Eickenscheidt, T., Fiedler, S., Förster, C., Freibauer, A., Giebels, M., Glatzel, S., Heinichen, J., Hoffmann, M., Höper, H., Jurasinski, G., Leiber-Sauheitl, K., Peichl-Brak, M., Roßkopf, N., Sommer, M., and Zeitz, J.: High emissions of greenhouse gases from grasslands on peat and other organic soils, Global Change Biology, 22, 4134–4149, 2016.

Tuittila, E.-S., Komulainen, V.-M., Vasander, H., and Laine, J.: Restored cut-away peatland as a sink for atmospheric CO2, Oecologia, 120, 563–574, 1999.

Tuittila, E. S., Komulainen, V. M., Vasander, H., Nykanen, H., Martikainen, P. J., and Laine, J.: Methane dynamics of a restored cut-away peatland, Global Change Biology, 6, 569 – 581, https://doi.org/10.1046/j.1365-2486.2000.00341.x, 2000.

Tuzson, B., Hiller, R. V., Zeyer, K., Eugster, W., Neftel, a., Ammann, C., and Emmenegger, L.: Field intercomparison of two optical analyzers for CH_4 eddy covariance flux measurements, Atmospheric Measurement Techniques, 3, 1519 – 1531, https://doi.org/10.5194/amt-3-1519-2010, 2010.

Vanselow-Algan, M., Schmidt, S. R., Greven, M., Fiencke, C., Kutzbach, L., and Pfeiffer, E.-M.: High methane emissions dominated annual greenhouse gas balances 30 years after bog rewetting, Biogeosciences, 12, 4361 – 4371, https://doi.org/10.5194/bg-12-4361-2015, 2015.

Verma, S. B., Ullamn, F. G., Billesbach, D., Clement, R. J., and Kim, J.: Eddy correlation measurements of methane flux in a northern peatland ecosystem, Boundary-Layer Meteorology, 58, 289 – 304, 1992.

Vernay, A., Balandier, P., Guinard, L., Améglio, T., and Malagoli, P.: Photosynthesis capacity of Quercus petraea (Matt.) saplings is affected by Molinia caerulea (L.) under high irradiance, Forest Ecology and Management, 376, 107 – 117, 2016.

Vickers, D. and Mahrt, L.: Quality control and flux sampling problems for tower and aircraft data, Journal of Atmospheric and Oceanic Technology, 14, 512 – 526, https://doi.org/10.1175/1520-0426(1997)014<0512:QCAFSP>2.0.CO;2, 1997.

Vybornova, O.: Effect of re-wetting on greenhouse gas emissions from different microtopes in a cut-over bog in Northern Germany, Ph.D. thesis, Universität Hamburg, Hamburg, https://ediss.sub.uni-hamburg.de/volltexte/2017/8618/pdf/Dissertation.pdf, 2017.

Vybornova, O., van Asperen, H., Pfeiffer, E., and Kutzbach, L.: High N_2O and CO_2 emissions from bare peat dams reduce the climate mitigation potential of bog rewetting practices., Mires & Peat, 24, https://doi.org/doi: 10.19189/MaP.2017.SNPG.304, 2019.

Waddington, J. M., Warner, K. D., and Kennedy, G. W.: Cutover peatlands: A persistent source of atmospheric CO2, Global Biogeochemical Cycles, 16, 1–7, https://doi.org/10.1029/2001GB001398, 2002.

Whalen, S. C.: Biogeochemistry of methane exchange between natural wetlands and the atmosphere, Environmental Engineering Science, 22, 2005.

Wille, C., Kutzbach, L., Sachs, T., Wagner, D., and Pfeiffer, E.-M.: Methane emission from Siberian arctic polygonal tundra: eddy covariance measurements and modeling, Global Change Biology, 14, 1395 – 1408, https://doi.org/10.1111/j.1365-2486.2008.01586.x, 2008.

Wilson, D., Alm, J., Laine, J., Byrne, K. a., Farrell, E. P., and Tuittila, E. S.: Rewetting of cutaway peatlands: Are we re-creating hot spots of methane emissions?, Restoration Ecology, 17, 796 – 806, https://doi.org/10.1111/j.1526-100X.2008.00416.x, 2009.

Wilson, D., Blain, D., Couwenberg, J., Evans, C., Murdiyarso, D., Page, S., Renou-Wilson, F., Rieley, J., Sirin, A., Strack, M., et al.: Greenhouse gas emission factors associated with rewetting of organic soils, Mires and Peat, 17, 2016a.

Wilson, D., Farrell, C. A., Fallon, D., Moser, G., Müller, C., and Renou-Wilson, F.: Multiyear greenhouse gas balances at a rewetted temperate peatland, Global Change Biology, 22, 4080–4095, 2016b.

Wolpert, D. H.: Stacked generalization, Neural Networks, 5, 241 – 259, https://doi.org/10.1016/S0893-6080(05)80023-1, 1992.

Yu, Z., Loisel, J., Brosseau, D. P., Beilman, D. W., and Hunt, S. J.: Global peatland dynamics since the Last Glacial Maximum, Geophysical Research Letters, 37, n/a–n/a, l13402, 2010.

Zahniser, M. S., Nelson, D. D., Mcmanus, J. B., and Kebabian, P. L.: Measurement of trace gas fluxes using tunable diode laser spectroscopy, Philosohical Transactions: Physical Sciences and Engineering, 351, 371 – 382, 1995.

Zeltner, U.: Schutzgebiets- und Biotopverbundsystem Schleswig-Holstein- regionale Ebene - (Gebiete von überörtlicher Bedeutung für den Arten- und Biotopschutz); Fachbeitrag zur Landschaftsrahmenplanung; Spezieller Teil; Planungsraum I - Teilbereich Kreis Pinneberg, Landesamt für Natur und Umwelt des Landes Schleswig-Holstein, Flintbek, 2003.

Zheng, Y., Zhao, Z., Zhou, J.-J., and Zhou, H.: Evaluations of different leaf and canopy photosynthesis models: a case study with black locust (Robinia pseudoacacia) plantations on a loess plateau, Pakistan Journal of Botany, 44, 531–539, 2012.

Zhu, X., Zhuang, Q., Qin, Z., Glagolev, M., and Song, L.: Estimating wetland methane emissions from the northern high latitudes from 1990 to 2009 using artificial neural networks, Global Biogeochemical Cycles, 27, 592 – 604, https://doi.org/10.1002/gbc.20052, 2013.